Cape Peninsula University of Technology

Low cost pineapple peel biosorbent for the removal of aqueous cobalt from textile wastewater effluent

by

Zintle Ntshoko
203020758

Thesis submitted in fulfilment of the requirements for the degree

Master of Technology: Civil Engineering

in the Faculty of Engineering and Built Environment

at the Cape Peninsula University of Technology

Supervisor: Prof VG Fester
Co-supervisor(s): Dr OU Oputu/Prof R Haldenwang

Cape Town Campus
Date submitted:

Declaration

I, Zintle Ntshoko, hereby declare that this research dissertation is my own unaided work. It is being submitted for the MTech Degree at the Cape Peninsula University of Technology. It has not been submitted before for any degree or examination in any other University. Furthermore, it represents my own opinions and not necessarily those of the Cape Peninsula University of Technology.

28 February 2020

Signed **Date**

Abstract

The concept of waste and waste management is a Civil Engineering problem. Billions of Rands is spent each year to cater for industrial and municipal waste of a constantly increasing population. Traditional waste management practice prioritises landfilling as a primary and ultimate means of waste disposal. All capital-intensive projects end up transferring the original waste from one form to another or entombing the waste as is the case with landfilling. An alternative solution to the conventional practices in sustainable waste management approach, embraces the integration of renewable resources such as biomass use as an economically viable option. The advantage of such an integrated approach includes the elimination of waste transportation, landfilling, and ultimately the reduction of the ecological footprint.

In this study, a sustainable waste management strategy was explored by converting waste material into a potentially valuable product. Pineapple peels were applied for the biosorptive removal of cobalt (a class B carcinogen) from aqueous solution. Pineapple peels were collected from a communal residential villa and local vegetable retail outlet. Samples were dried, ground, sieved (150 µm) and subjected to chemical ($KMnO_4$ +H_2SO_4) and physical (carbonisation at 600°C in Nitrogen) treatments. The effect of physicochemical treatment and carbonisation on biosorption was thus investigated. In all, one pristine and two modified samples were obtained; raw pineapple peels (RPP), chemically treated pineapple peels (CTPP) and carbonised pineapple peels (CPP). Activated carbon (AC) served as an experimental control.

The bio-sorbents were characterized by Fourier transform infrared spectroscopy (FTIR), Brunauer Emmet Teller (BET) and scanning electron microscopy (SEM) to identify the functional groups in biosorbent and assess changes to surface area and morphology.

Biosorption experiments were conducted in batch and continuous mode with the residual cobalt determined by atomic absorption spectroscopy (AAS). For batch experiments, the optimum operating variables, biosorbent mass and initial pH, were found to be 0.05 g and pH 6, respectively. Maximum biosorption capacities of 8.958 mg/g, 16.731 mg/g, 22.314 mg/g and 6.337 mg/g were obtained for RPP, CTPP, CPP and AC, respectively. Carbonised samples displayed exothermic character while biosorption on non-carbonised samples was endothermic. Biosorption was rapid, reaching equilibrium in 60 minutes.

Batch kinetic data were in agreement with the pseudo-second-order model, while equilibrium data was better described by the Freundlich isotherm models ($R^2 \approx 0.99$) on the CPP and CTPP samples.

Column studies using CPP expectedly showed that breakpoint and saturation point was directly related to column mass and inversely related to solution flow rate and feed concentration. The maximum saturation capacity for CPP in column mode was 16.009 mg/g, achieved when the concentration of cobalt feed, flow rate, and the adsorbent bed was 25 ppm, 5 mL/min and 1 g, respectively. In general, column data were best fitted to the Yoon model, when compared to the Thomas and Bohart Adams models. Predicted maximum adsorption capacity by the Bohart Adams model did not agree with experimental data. Based on the data obtained, the biosorbent was successfully applied to treat industrial textile wastewater.

In conclusion, it was found that the biosorbent made from pineapple peels were suitable, especially when subjected to physical treatment for the biosorptive removal of cobalt ions from aqueous solution and gave better results in comparison to activated carbon used as control. As a novel addition to the existing body of literature, it was noted that the issue of residual colour observed when pineapple peels were used in their pristine form could be overcome by using carbonised pineapple peels. These peels which are vegetable wastes from retail shops is hereby proposed as a suitable candidate for a green approach to water treatment for cobalt contaminated water.

Acknowledgements

To Professor Fester, my heaven-sent supervisor, I am deeply and eternally grateful for who you are and all you have done. I honour you; may God bless you abundantly.

To Doctor Oputu, my heaven-sent supervisor, a massive thank you, for a life changing experience and continuously pouring out passion, knowledge and expertise for the success of this thesis. I am forever grateful for all your amazing help.

To Professor Halderdenwang, thank you for being such an inspiration and your encouraging words are heartfelt.

To the Flow Research Process Centre team; students and staff, thank you for all your assistance and encouragement in this thesis journey.

To my family, thank you that I could rely on your prayers and your heart for me.

To my loved ones, friends and community, your prayers, cheer and support have kept the flame in me alive even during load shedding.

To the Nedbank Eyethu Community Trust, thank you so much for your financial assistance.

To the National Research Foundation, I am very grateful for your financial assistance.

To my amazing God, I am deeply humbled by your plans, grace and faithfulness.

Dedication

My heart felt dedication goes to my eternal six; God, Holy Spirit, Jesus, Tato, Mamo and Bra.

Table of Contents

List of Figures

List of Tables

Glossary - Terms and Concepts

Biosorbate	: The liquid substance that has the ability to concentrate and be adsorbed.
Biosorbent	: The biomass substance whose surface area is used to adsorb another.
Biodegradable	: The ability of a substance to be decomposed by bacteria or other living organisms.
Biosorption	: The adhesion of atoms, ions or molecules between an adsorbate and adsorbent.
Biomass	: Organic material that comes from plants and animals.
Carbon footprint	: The amount of carbon dioxide released into the atmosphere as a result of the activities released into the atmosphere.
Equilibrium	: A point in an interaction between the reactant and product where there is no longer change with time when all the reactions have reached the same time.
Homogeneous process	: A process involving substances in one phase.
Heterogeneous process	: A process involving substances in different phases.

The concept of adsorption and biosorption are inter-related. Biosorption is adsorption is when a biomaterial is been used for the process. In this thesis, the prefix “ad” in such words as adsorption, adsorbate, and adsorbent was replaced with the prefix “bio” giving biosorption, biosorbent, and biosorbent, etc, respectively.

List of Abbreviations

AC	: Activated carbon
BET	: Brunauer -Emmet- Teller
CTPP	: Chemically treated pineapple peels
CPP	: Carbonised pineapple peels
FTIR	: Fourier transform infrared
FVW	: Fruit and vegetable waste
Min	: Minute
PP	: Pineapple peels
RPP	: Raw pineapple peels
SEM	: Scanning electron microscope

List of Symbols

BA	: Adam Bohart
As	: Arsenic
Bi	: Bismuth
Cd	: Cadmium
Ce	: Cerium
Cr	: Chromium
Co	: Cobalt
Cd	: Cadmium
Cu	: Copper
K	: Kelvin
K_1	: First order rate constant
K_2	: Second order rate constant
K_{BA}	: Constant of Adam Bohart
K_C	: Thermodynamics equilibrium constant
K_F	: Freundlich constant
K_L	: Langmuir constant
K_{TH}	: Thomas model constant
M	: mass
H	: Height in bed column

Ni	: Nickel
Pb	: Lead
Q	: Adsorption capacity of biosorbent
Qe	: Amount of metal adsorbed at equilibrium per unit weight of adsorbent (mg/g)
qm	: maximum biosorbent capacity (mg/g)
qt	: Amount of metal adsorbed at specified time (mg/g)
Sb	: Antimony
V	: Volume of mass in solution
Δ S º	: Standard entropy change (Kj/mol)
Δ Gº	: Standard Gibbs free energy (Kj/mol)
Δ Hº	: Standard enthalpy change (Kj/mol)

1 Introduction

1.1 Background

In South Africa, there is an abundant supply of fruit and vegetables produced by the agricultural industry. A large amount of waste is generated during various processes which include harvest, sorting, storage, and commercialisation. The waste discharged is both in the form of solid and liquid. The waste generation is rapid due to the perishable nature of the waste that makes it vulnerable to decay and decomposition (Cape, 2015).

Ayeleru et al. (2016) conducted a study of characterisation of fruit and vegetable at the Johannesburg market and reported that an average of 11 tons of fruit and vegetable waste is discarded at the landfill daily from the Johannesburg market. In the Western Cape, the Agriculture Industry is much larger than that of Johannesburg with a great amount of fruit and vegetable waste generated in both solid and liquid form. The decomposition of the waste produces organisms that are toxic and releases carbon dioxide (CO_2) which is a primary component of greenhouse gases. Priority on reclamation of food waste has been on fruit and waste characterisation for waste to energy conversion, which is a vital contribution to the bio-economy (Rao & Khan, 2017).

Heavy metal pollution from industrial wastewater discharge is a persistent problem due to the toxicity of the metals in the environment. Heavy metals have been reported to have a negative impact on human health (Bhatnagar et al, 2010). This study particularly looked into the presence of cobalt (Co), a non-volatile toxic heavy metal with an atomic number 27. Cobalt is found in natural and aquatic environment, humans, animals, and plants are adversely affected by the presence of an excess amount of cobalt. Studies indicate that human exposure to Co has a direct effect on the causes of bronchial asthma, cardiomyopathy, lung cancer and polycythaemia. Environmental regulations have permissible limits to the amount of cobalt released into the environment (James et al. 2006).

Conventional treatment technologies for the removal of heavy metals includes coagulation, oxidation, ion exchange, membrane separation and reverse osmosis. However these methods including commercial activated carbons are not economically viable (Ramachandra, 2014). Most of these methods require huge capital investment. Cost efficient technologies are therefore, needed to remove heavy metals from industrial wastewater.

Biosorption, the passive uptake of metals by biomass, has shown great potential in the removal of heavy metal. The advantages of biosorption include being economical, highly efficient, simplicity of the method and can be done both on the solid and liquid phase of the sorbent (Kanamadi, 2003). The method of biosorption has been explored through the utilisation of different biosorbents. Nadaroglu and Kalkan (2012) used industrial red mud waste for the adsorption of cobalt. The adsorbent was proven to be of great effect with maximum removal of 18.045 mg/g.

Due to the abundant supply of agricultural waste, their utilisation for biosorption is economical, environmental, and of human benefit. Further, advantages of agricultural waste include readily availability, accessibility, and high carbon content and porous nature. Diverse agricultural waste such as orange peels (Chu et al., 2011), rice husk (Boddu et al., 2008), potato peel waste (Mayer & Hillebrandt, 1997) have been explored as adsorbents to treat various types of water impurities. The results proved the efficiency of the biomass material due to the presence of multifunctional groups on the surface (Ahmad et al., 2016). A treated lemon peel was used for the adsorption of cobalt ions in batch studies with successive maximum adsorption of 22 mg/g (Bhatnagar et al., 2010).The adsorption capacity of the treated lemon peel reported is similar to that of the present study of a carbonised pineapple peel, achieving 22.314 mg/g adsorption capacity of cobalt ions.

A study by Ahmad et al. (2016) reported high efficiency in the removal of metals Cd (II) and Pb (II) through remediation using pineapple peel. The pineapple peel has been proven to be an economic biosorbent since 40% of the fruit is regarded as waste. The peel of the pineapple contains components such as celluloses, hemicelluloses, lignin, and pectin. These components contain a variety of functional groups such as hydroxyl and carboxyl groups (Mohammed, 2014).

1.2 Research problem

The efficiency of biosorbents produced from pineapple peels for removal of cobalt ions from textile wastewater has not been extensively validated in terms of the appropriate modification and the isotherm and kinetic models that is required for further scale-up to be used beneficially as a waste management strategy.

1.3 Research questions

How can the biosorbent be modified to achieve maximum adsorption of cobalt ions?
What would be the best-operating conditions for maximum adsorption?

Which are the isotherm and kinetic models that are best fitting to the experiment?

1.4 Aims and objectives

This study aimed to investigate the application of pristine and modified biomass prepared from pineapple peels for the biosorption of aqueous Co (II) ions in batch and column mode, to apply the best performing adsorbent to industrial wastewater treatment.

The objectives are as follows :

- To evaluate the effect of carbonisation on treatment efficiency through physical and chemical treatment of pineapple peels.
- To characterise the biosorbent with a scanning electron microscope (SEM), Fourier transform infrared (FTIR) and Brunauer Emmet Teller (BET).
- To investigate the effect of operating variables in biosorption.
- To establish the biosorption equilibrium and removal efficiency of cobalt ions.
- To evaluate performance in a column using model fluid and then treat industrial wastewater with the best performing biosorbent.

1.5 Significance of this research

This study explored a possibility in utilisation of fruit waste for the purpose of reclamation of industrial wastewater containing cobalt. Up to date there has been no literature found on using pineapple peel as a biosorbent on batch and column work for the remediation of cobalt. The application of the biosorbent serves as a sustainable integrated approach to industrial wastewater which was done to test the efficiency of the biosorbent in the real world.

1.6 Delineation of the study

The desorption of cobalt from used adsorbent was not covered in the study.
The effect of other transition and heavy metals on the biosorption capacity of pineapple peels for cobalt was not investigated in this study.
Kinetic models were limited to first, second order and intra-diffusion.
Equilibrium models were limited to Freundlich and Langmuir models.

Column data modelling was limited to Bohart-Adams, Thomas models and Yoon-Nelson.

1.7 Structure of the thesis

Chapter 2 Literature review

The literature review entails an overview of literature pertaining to sustainable waste management and the utilisation of biomass for the remediation of heavy metal. It also includes a review in literature based on the process of biosorption both in batch and continuous mode.

Chapter 3 Method

The method entails the research design and details of the materials, apparatus, and experimental procedure.

Chapter 4 Characterisation

The results on characterisation are presented and discussed.

Chapter 5 Batch studies

The results on batch studies are presented and discussed.

Chapter 6 Column studies

The results on column studies are presented and discussed.

Chapter 7 Conclusions and recommendations

Conclusions are drawn and recommendations are presented.

2 Literature review

2.1 Introduction

This chapter presents an overview of literature based on the sustainable waste management processes. The sustainable waste management processes include remediation and application of natural resources such as biomass. Application of biomass is reviewed in the context of water treatment, in particular, the removal of cobalt. Pertinent to the treatment of cobalt, the mechanism and parameters of biosorption in both batch and fixed bed studies are reviewed and discussed.

2.2 Integrated waste management

Integrated waste management (IWM) is a sustainable approach, which is a strategic, practical, and efficient way of managing waste. An IWM plan generally involves planning, implementation, and continuous evaluation of the adopted approach. Integrated waste managements (IWMs) are anchored on the pillars of sustainability, which include; environmental, economic, and social responsibility (City of Town,IWM policy.2000).The legislature on sustainability in South Africa was established in 2007, to ensure the protection of the ecosystem (air, water, and food) for the health and well-being of the present and future generations (Brutland, 1987). DEA (2012) established legislation that ensures that through continuous development and co-operation in environmental management the IWM structure is maintained.

Over the years, waste in South Africa has been managed using a linear approach. The linear approach simply moves the waste from the point of disposal to a landfill. The approach therefore only considers one aspect of the waste management hierarchy – landfilling. The overall waste management hierarchy in reducing order of appeal is as follows (Kosseva, 2009):

1. Avoid waste generation
2. Minimise waste
3. Reclaim discarded waste
4. Treatment of waste and sending for disposal in landfills

The IWM plan embraces all four levels of the waste management hierarchy. Unlike the linear approach which leads to huge amount of capital, transportation and maintenance cost, the IWM system provides an economical way of securing the environment from pollution and thus promotes better health and a cleaner ecological system.

The success of an IWM system is dependent on a holistic approach with continuous application, and evaluation. In South Africa, it has been identified that even though there is a system under way and efforts towards practise, there is still a lack in the framework, assessment strategies and innovative solutions in order to transform the waste generated into material of secondary use. Assessment strategies include waste quantities and data required to navigate and create innovative successful IWM (Dlamini et al., 2019). With the implementation strategies, the focus on the ecological system needs to be inclusive of all components of the ecosystem. The strategies in the framework should seek the development and recovery of renewable resources in an economical way.

Grandin and Pletschke (2015) established a model that integrates a framework for the implementation of biomass across the ecosystem. The model seeks to implement IWM for waste, energy, and water. There is still a scarcity of utilisation of biomass for the treatment of water. On this proposed model (Figure 2-1) water has been included for the bioremediation of household, commercial, and industrial wastewater including waste to energy conversion. To ensure the successes of an IWM, developed countries, such as the United Kingdom apply a Life Cycle Assessment (LCA) system for waste management. This strategy applies the principle of “cradle to grave”, and presents a comprehensive report on the impact of providing a product or service (Barton et al.,1996). It becomes pertinent for the countries seeking to develop IWM systems to work out the life cycle of products so that the various waste management hierarchal levels can be incorporated during product design and development.

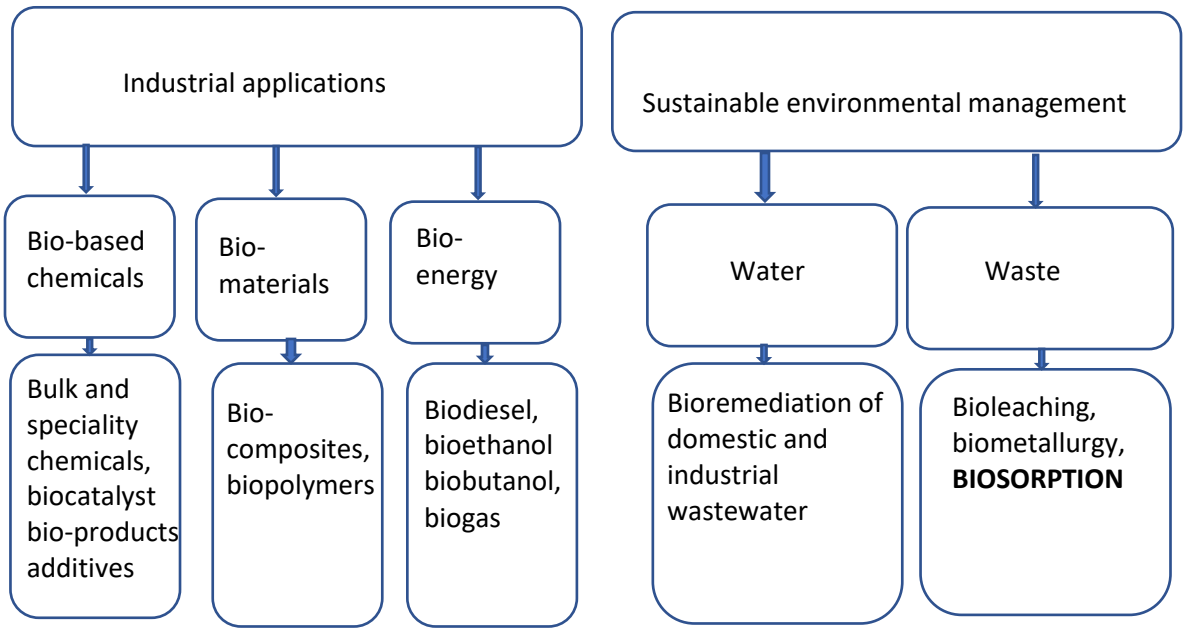

Figure 2-1 Sustainable integrated model (Khan et al. 2014)

There is a growing number of research into the recovery of waste, and in particular, the concept of converting waste to energy (Maheshwariet al., 1981; Garba et al.,1995 ; Sagagi et al., 2009). A study by Dlamini et al. (2018) argued that there is still a lack of assessment strategies, planning and regulatory framework providing waste quantities and data required to navigate innovative solutions of waste transformation. In their study, they looked into recovery of waste to energy in South Africa. Khan et al. (2014) established a model Figure 2-1 that not only focuses on waste to energy recovery, as numerous study have done but also extended to cover waste for water remediation. The concept of biosorption, a sustainable environmental management strategy for water treatment is been applied in this study.

2.3 Classification of biodegradable waste

Biodegradable waste is waste that decomposes biologically and is broken down by microorganisms. Biodegradable waste has a calorific value and consist of food or kitchen (including fruit and vegetable), garden, wood, and paper waste (Joshi & Ahmed, 2016).

Fruit and vegetable waste (FVW) is generated during harvest, sorting, packaging, storage, and commercialisation (Joshi & Ahmed, 2016). FVW is high in biodegradability and classified as perishable waste therefore vulnerable to decay. When disposed at the landfill, they discharge

gases that contribute to the carbon footprint, gives off odour, and produces leachate (Barton et al.1996).

Biomass has been studied and shown to contain organic molecules and biological polymers that consist of hemicellulose, lipids, protein, sugars, starches and hydrocarbons that are also rich in fibre (Rao & Khan, 2017).These contain valuable chemicals and functional groups which are particularly advantageous in waste to energy conversion and in waste water treatment. These chemicals are composed of cellulose, lipids, protein, hemicellulose, amino, amido, carboxyl groups, polysaccharides and phosphate groups (Singh et al., 2018).

Characterisation of biodegradable waste is done in order to determine the potential of the waste for treatment and reclamation (Ayeleru et al., 2016). Classification of biodegradable waste is done according to characteristics, composition, degree of biodegradability, physical and chemical form, moisture content, chemical reactivity ,volatile content, leachability and toxicity (Barton et al.,1996).

In Johannesburg, South Africa, a fruit and waste characterisation study was done at the Johannesburg fruit and vegetable market (Ayeleru et al., 2016). Fruit and vegetable waste were coded according to colour as follows;

1. Red waste category (49%) comprises of red apples, blood oranges, cherries, cranberries, red grapes, red pear, pomegranate, raspberries, watermelon, beetroot, red peppers radish, red onion, red potato, rhubarb and tomato.

2.Blue fruit (24%) category comprises of blue and black berries, black current, concord grapes, dried plums, elder berries, grape fruit, purple fig, purple figs, black olive, purple asparagus, purple cabbage, purple carrot, eggplant, purple peppers and potato.

3.Yellow fruits (22%) category comprises of yellow apples, nectarine, apricot, cantaloupe, yellow figs, grapefruit, lemons, mangoes, oranges, papayas, peaches, yellow pear, pineapple, tangerines, yellow beetroot, yellow peppers, pumpkin, squash, sweet corn and sweet potato.

4. Green fruits (5 %) comprises of Avocado, green apple, green grapes, honey dew, kiwi fruit, lime and green peas, artichoke, arugula, asparagus, broccoli, brussed sprouts, celery, leafy greens, leeks, green onion, okra, peas, green peppers, spinach, watercress and zucchini.

From the study it was identified that there is a variety of potential that can be utilised in IWM system that needs to be explored.

In the Western Cape, South Africa a general waste characterisation study gave the following results (Cape, 2015) :

1. Biodegradables (45%) comprises of agriculture organics (28%), municipal organics (6%), sewage sludge (4%), animal waste (2%), forestry residues (1%) and paper (4%).
2. Non-degradable waste (46%) comprises of construction waste (22%), plastic (3%), metal (7%), paper (4%), glass (2%), and commercial/industrial (11%)
3. Non-recyclables (9%)

A review study compiled waste generated over South Africa and presented data on the amount of fruit waste produced annually (Grandin & Pletschke, 2015). Table 2-1 presents results obtained from the literature reviewed, which showed a ready availability of biomass for possible application in an integrated waste management system whether in waste to energy, water treatment and biofuel. An average of 149,573.50 tons of fruit and vegetable wastes (FVW) were produced over two years in South Africa. Comparatively, in India 5.6 million tons of FVW is discarded annually. In Tunisia 180 tons of fruit and waste is discarded monthly. In Barcelona 90 ton per day is discarded (Barton et al. 1996).These studies show the amount of potential waste that is not utilised.

From his study of characterisation of waste material Arina and Orupe (2012) recommended source separation system and a source of treatment in order to apply the biomass. One of the main approaches of utilisation of biomass, is through treatment of water in the most efficient and low-cost way. Researchers are emerging in finding the most efficient viable ways of treating water that is cost effective and sustainable (Bhatnagar et al., 2015).

Table 2-1: Waste characterisation study (Grandin & Pletschke, 2015)

Fruit	**Total production in tonnes (2011/2012)**	**Volume processed in tonnes (2011/2012)**
Citrus	2 102 618	441 899
Grapes	1 839 030	1649 (processed) 151 628 (dried) 1 413 533 (pressed)
Apples	790 636	244 469 (processed) 1110 (dried)
Bananas	371 385	Not indicated
Pears	346 642	120 811 (processed) 9872 (dried)
Peaches	190 531	125 706 (processed) 8994 (dried)
Pineapples	**108 697**	**81 753**
Watermelons and melons	93 277	-
Avocados	87 895	-
Apricots	66 762	48 792 (processed) 8725 (dried)
Mangoes8	65 439	~50 000
Plums	60 925	1712
Guavas	23 699	20 896
Papayas	12 565	-
Litchis	7782	-
Strawberries	5543	2724
Other berries	5073	3914
Prunes	3426	-
Figs	1925	448
Pomegranates9	1324	883
Cherries10	775	83
Granadillas	484	-
Quinces	208	-

2.4 Application of biodegradable waste

Biomass can be sourced from one of the following sources: synthetic, agricultural, natural, biomass and Industrial (Singh et al., 2018). Biodegradable waste can be utilised in the following ways: Energy production, composting and water remediation.

Biodegradable waste for energy production

Anaerobic digestion of organic waste is a thriving mechanism for alternative energy production (Zhen et al., 2016). Through anaerobic digestion (AD), bacteria decompose organic matter in the absence of oxygen. The ultimate gas production is determined by chemical composition of the substrate and parameters of the biodegradation process, (Kythreotou, 2014). The rate of AD is influenced by the feedstock type and characteristics. High methane producing biomass are often recommended for the primary substrate. Pre-treatment of feedstock is a fundamental stage that helps with improving the biodegradation rate and eliminating contaminants through physical, chemical, and chemical reduction (Khalid et al., 2017). Biodegradation depends on the availability of the moisture content, carbon, and nutrients on the feedstock. It has been proven that fats have a greater potential for producing high amount of biogas and volatiles (Clifford et al., 1986).

The biodegradation process has four stages that occur simultaneously namely; hydrolysis, acidification, acetogenesis and methanogens (Sundaram et al., 2001).

Biodegradable waste for composting

Composting is an aerobic biological process that happens in the presence of oxygen (Sharma and Garg, 2018).The product of compost is a fully fermented material, humus used as feed on plant soil. Through the aerobic process micro-organisms break down simple sugars and organic food under moderate temperature (Joshi & Ahmed, 2016).The microorganisms facilitating the biological process thrive under these factors (Sharma & Garg, 2018):

Table 2-2 Factors influencing composting (Sharma & Garg, 2018)

Factor influencing composting	***Conditions***
Moisture content	40 – 60 %
Carbon to nitrogen ratio	10:1
Temperature	32 to 60
Oxygen	Continuous

Composting can be done both mechanically and physically. There are four methods of composting: Windrow process, forced aeration, pulverised and mechanical composting system (Joshi & Ahmed, 2016).

Biodegradable waste for water remediation

Adsorption is a process where a biosorbent naturally binds heavy metal through ion exchange on active site of the adsorbent/adsorbate. Khan et al. (2013) defined it as a mechanism where chemical groups found in the surface of the adsorbate are bound with metal ions. The process involves the exchange of ions, physical adsorption, chemisorption, and complexation. This process happens through dispersion, diffusion, and binding between the biosorbent and adsorbate.

Table 2-3 presents conventional approaches of metal removal in wastewater that have been practised (Singh et al., 2018) .

Table 2-3: Water treatment techniques (Bharat & Manchanda, 2017)

Filtration techniques	**Polymer and nanotechnology**	**Electrical techniques**	**Disinfection techniques**	**Adsorbent material**
Membrane technique	Nano particles	Electro dialysis	Sonification	Zeolites
Micro technique	Nano tubes	Floatation	UV Radiation Solar energy	Activated carbon
Ultra-technique	Nano composite	Electrochemical	Solar energy	Ferric hydroxide
Nano technique	Thin films	Electro coagulation	Photo catalysis	Ceramic

2.5 Environmental pollution

The environment consists of three aspects namely; air, water and soil, which all form part of the ecological unit. Any threat-giving organisms within the environment are known as contaminants (Babalola, 2018). Contaminants are either ionic, inorganic or pathogenic and are grouped up as illustrated in Table 2-4.

Table 2-4: Environmental contaminants (Babalola, 2018)

Anions	***Inorganic pollutants***	***Pathogens***
Nitrates	Acids	Bacteria
Phosphates	Salts	Viruses
Sulphates	Metals	Protozoa
Radioactive substances		

Metals are defined as an element with metallic bonds that form cations. The combination of more than one metal produces an alloy. The nature of an alloy may be either ferrous or non-ferrous depending on the presence of iron. Ferrous metals are those with the presence of iron and includes, alloy steel, carbon steel, cast iron and wrought iron. Non-ferrous metals do not have iron and include aluminium, copper, zinc and tin (Babalola, 2018).

The presence of metals in the atmosphere is toxic and poses a threat to the environment and living organisms. Metals are emitted in industries that work with textile, leather, tannery, electroplating, galvanising pigment, dyes, metallurgy and paint (Salleh et al. 2011; Babalola, 2018).

Previous studies have typified metals as; toxic, strategic, precious and radio nuclides metals. There are 91 metals out of 118 elements present on the periodic table (Kanamadi, 2003).

Heavy metals are composed of high density with a specific gravity ranging between 4 and 7 g/cm^3. These metals are antimony, arsenic, bismuth, cadmium, cerium, chromium, cobalt, lead, manganese, mercury, nickel, terrullium, thallium, uranium, tin, vanadium and zinc (Babalola, 2018). Metals enter the atmosphere through diffusion either in a passive manner and respiration (Kanamadi, 2003).

Upon investigating the removal of heavy metal ions (copper, zinc, nickel, and cobalt) the hazard of heavy metals to the public health and the urgent need of reducing concentration on drinking, agricultural, and wastewater was highlighted (Ghomri et al., 2013).

Table 2-5 resents the effects from accumulation of heavy metals on human health. These impacts are due to the increase in the industrial wastewater and is subject to the fast industrial and residential development rate. A study by Nadaroglu & Kalkan (2012) demonstrated that the water treatment can be done not only to prevent the effects of heavy metals (such as degradability on biological systems, human physiology and human health) but also to manage the industrial waste disposed.

Table 2-5 The effect of heavy metals on human health (Arief et al., 2008)

Heavy metal	***Effect on health***
Cr (VI)	Carcinogenic, Headache, nausea, diarrhoea, vomiting, epigastria
Cr (III)	Allergies and cancer
Co (II)	Bronchitis, lung cancer, low blood pressure and diarrhoea
Zn(II)	Depression, lethargy, neurologic signs
Cu (II)	Liver damage, Wilson deases, insomnia
Cd (II)	Kidney failure, rennal disorder, Itai-Itai, hepatic damage, cancer hypertension
Pb (II)	Encephalopathy, seizures & mental retardation
Ni (II)	Dermatitis, nausea, chronic asthma, coughing, bronchial haemorrhage, gastrointestinal distress.

2.6 Biosorption process

Biosorption is the passive uptake of heavy metals by biomass that has shown great potential as an emerging technology for the purpose of treating water at relatively low cost (Arief et al., 2008). Key advantage of biomass in treatment of water is the efficiency, ready availability and low cost (Kanamadi, 2003).

Biosorption is known as a physical and chemical mechanism that binds negative and positive ions together for the passive uptake of heavy metal by biomass from water. Biosorption happens between three spheres; biosorbent, solvent and metal (Ramachandra, 2014).The mechanism is between biosorbent, surface binding charges and facilitating the biosorption from the biosorbate, the substance biosorbed on the surface until an equilibrium is reached. The quality of the biosorbent determines the quantity of adsorption (Singh et al., 2018).

Mechanism of biosorption

The mechanism of biosorption occurs on the surface of a biosorbent through chemical and physical exchange. The negative ions from the functional groups (such as celluloses, hemicelluloses, lignin, lipids, water, protein, sugars and starch) of a biomass interacts with the positive cations (the metal in solution). In order to understand the underlying mechanism on the biomass surface, the physical and chemical features of the biosorbent are crucial and present a necessary guide in any attempt to enhance a biosorption process (Arief et al., 2008). Figure 2-2 illustrates the process of biosorption.

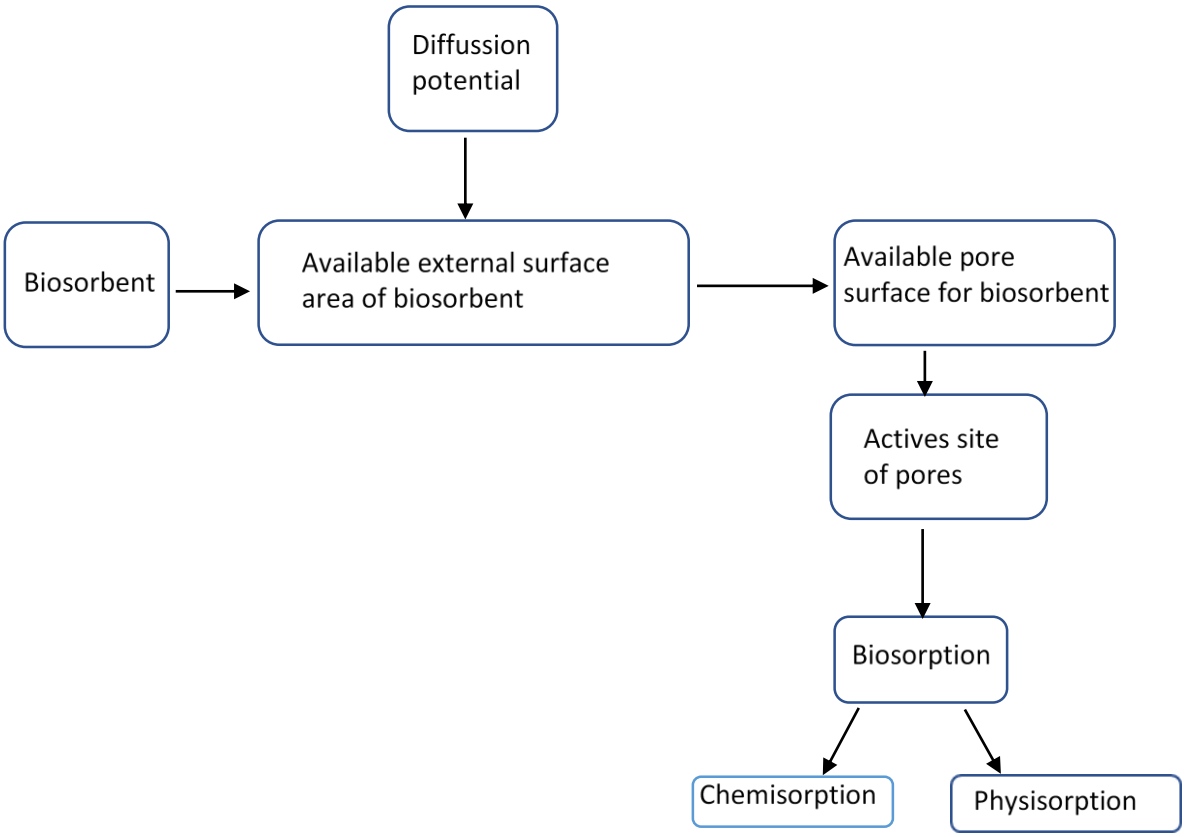

Figure 2-2 Biosorption process (Singh et al., 2018)

Modification of biosorbents

The purpose of modifying biosorbents is to enhance their surface characteristics. Treatment enforces the exchange between the metal ions and further removes any remaining metals in the water. Chemical treatment has been proven to have more effect on the increase biosorption capacity and surface area than a pristine biosorbent (Changmai et al., 2018). The treatment process showed an increase in the biosorption capacity due to the availability of active sites. In a study conducted by Amin et al. (2017) using date leaves and orange peels as adsorbent in batch mode comparing both the treated and non-treated showed a 20 to 30 percent increase in removal

capabilities of treated biosorbent. Figure 2-3 illustrates a typical rationale behind chemical treatment using sulphuric acid (H_2SO_4) and potassium permanganate ($KMnO_4$).

The results showed an enhancement in the overall biosorption through treatment of the pineapple peel (Ahmad et al., 2016). Due to the presence of functional groups of hydroxyl, epoxy and carboxylic groups the binding capabilities of the peel for Cd (II) and Pb (II) after oxidative treatment was maximised and inhibiting groups were eliminated.

Figure 2-3 Illustrations of chemical treatment in pristine pineapple peels (Ahmad et al., 2016)

2.7 Cobalt and the biosorption process

2.7.1 Properties, advantages and disadvantages of cobalt

Cobalt is a heavy metal with an atomic number 27. It is sourced from natural spheres such as the earth, atmosphere, ocean and air. Cobalt has both advantages and disadvantages to humans and living organisms. Cobalt is utilised in industries such as the battery, electronics, jet alloy, metallurgical , mining and phone industries (Islam et al., 2018). With the increase in production from these industrial sectors resulting in extensive usage of cobalt and excess generation of cobalt related waste. These wastes end up been discharged directly into the atmosphere and water streams such as oceans, rivers and dams into the food chains. Due to the non-biodegradable nature of cobalt it poses a threat to the environment (Amin et al., 2017; Islam et al., 2018).

Under limited contact, cobalt exposure is not harmful. However, prolonged exposure at concentrations beyond permissible limit poses threat to living organism. In humans the side effects are asthma, bronchitis, bone ailments, lung cancer and diarrhoea (Changmai et al., 2018). Cobalt remediation in natural environment has been approached through conventional water treatment technologies such as chemical precipitation, electro dialysis, ion exchange, lime coagulation, solvent extraction, reverse osmosis and ultra-filtration (Kanamadi, 2003).

2.7.2 Biosorption of cobalt

Biosorption is known to be a cost effective and simple process of treating water. Several adsorbents have been explored for the sorption of aqueous cobalt ions such as activated carbon, al-oxides, biopolymers, carbonaceous materials, mn-oxides, clay minerals, miscellaneous adsorbents and zeolites (Islam et al., 2018). Amongst adsorbents investigated low cost adsorbent have been found to be the most sustainable, also abundantly available, easily accessible and efficient in adsorption (Tofan et al., 2013).

Red mud has been successfully utilised for the removal of cobalt on a contaminated river with a concentration of 12.307 mg/g .The removal quantity was that of 7.051 mg/g which constitutes 57.29 % (Nadaroglu & Kalkan, 2012).

Tofan et al. (2013) explored natural hemp fibres for the removal of cobalt in aqueous solution in batch and column mode. In batch experiments a removal of 13.66 mg/g cobalt was adsorbed and 15.44 mg/g in column mode. Upon completion of study, it was recommended that adsorbent be applied to industrial wastewater and scale up purposes. The study also recommended low cost modifiers. Currently researchers are looking into economical natural material such as agricultural waste for the adsorption of cobalt. Agricultural waste is vastly available and low on costs.

Table 2-6 presents economical agricultural biosorbent tested for the biosorption of cobalt from a review of organic. The fruit nutshell and spirulina showed best biosorption capacities of 98.95 and 95.9 mg/g respectively (Andal et al., 2003 ; Peres et al.,2018).

Table 2-6: Cobalt adsorption with agricultural waste (Bhatnagar et al., 2015)(A review); Islam et al., 2018; Changmai et al., 2018; Peres et al., 2018)

Adsorbent	***qmax (mg/g)***
Almond green	11.53
Area shell biomass	45.5
Black carrot residues	5.35
Crab shell	20.47
Coir pith	12.82
Fruit nutshell	98
Lemon peel adsorbent	22.00
Marine green algae	46.10
QSC Chemically treated Raw husk	33.00
Spirulina	95.9
Water lemon ring	23.2

2.8 Pineapple waste as a biosorbent

In a study by Ahmad et al. (2016) on biosorption with pineapple peel, it was stated that the composition of a pineapple peel skin to the edible part which is a ratio of 40:60 percent. The skin of the pineapple is rich in cellulose, hemi-cellulose, lignin and pectin. This was confirmed by the study of Mohammed et al. (2014) who concurred that 58 % carbohydrates found in pineapples constitute of hemicellulose and cellulose.

A large number of pineapples are processed daily. Between 2011 and 2012 an amount of 108 697 and 81 753 tonnes of pineapples were processed daily in South Africa (Grandin & Pletschke, 2015). Even after a traceable number of agro-adsorbents pineapple waste has not yet been explored as a biosorbent for certain metals (Bhatnagar et al., 2015). The reduction of organic waste, pineapple peels have proven to be a promising sustainable adsorbent in the removal of dye, Safranin-O with 93.24% removal from initial concentration of 120 mg/L in 80 minutes contact time.

2.9 Biosorption study experiments

Factors affecting biosorption

The quality of adsorption is affected by factors such as pH, concentration, kinetics and temperature (Abdi & Kazemi Omran, 2015).

2.9.1.1 The degree of pH

The degree of pH has the most significant effect on adsorption due to the fact that the surface charge is directly proportional to the degree of ionisation of the metal solution and therefore has a great influence and impact on the adsorption. It was observed that an increase on pH gives rise to an increase in adsorption capacity (Changmai et al., 2018). In removal of Safranin-O at 50 ppm concentration with pineapple peels optimum removal capacity was found between pH 6-8 (Mohammed et al., 2014). Similar results were found with those of Yusuf et al. (2015) where the set pH range was between 2 and 12 in the study of kinetics on removal of Safranin-O with pineapples.Optimum removal was achieved at pH of 6.

This phenomenon was confirmed by Abbas et al. (2014) who stated that the increase is due to electrostatic attraction between the metal ions and functional groups in the adsorbate and adsorbent respectively. The alkaline zone of the adsorbate had a decrease in adsorption capacity due to excess hydrogen ions competing for active sites whilst the more acidic zone was under precipitation after reaching a plateau at pH 6 (Yusuf et al., 2015).

2.9.1.2 Concentration

The initial concentration is crucial due the fact that it is a pre-requirement for the facilitation of the mass transfer between the biosorbent and the adsorbate. With the increase of the metal ions there is increase in adsorption capacity, this is due to the availability of metal ions for adsorption (Tomul et al., 2017). After an optimum adsorption has been reached, a point of exhaustion was reached which is due to the depletion of active sites and slows down the rate of adsorption (Kumar & Barakat, 2013).

The dosage of the biosorbent has a significant role in the uptake of metal capacity. Metal ions in the adsorbate occupy available sites of the adsorbent (Nadaroglu & Kalkan, 2012).The dosage capabilities are dependent on the quality of the adsorbent; this was discovered on the adsorption of cobalt using carrot and tomato. Due to the porous nature of the tomato, better adsorptive capabilities were achieved on smaller dosage due to more available active sites (Changmai et al., 2018). In the study by Mohammed et al. (2014) more adsorption site were available with the increase of dosage. This does not always happen, in some cases there is aggregation due to excess mass for the adsorbate and leads to less available surface area and thus a decrease in adsorption per unit mass due to diffusional path (Meseldzija et al., 2019).

The effect of mass is determined by the following equation :

$$\%\ adsorption = \frac{C_i - C_e}{C_i}\ x100 \qquad \textbf{Equation 2-1}$$

Where C_i is the initial concentration and C_e is the concentration at equilibrium.

Modelling of experimental data

2.9.1.3 Kinetic study

Kinetic study determines the rate and control of time in the adsorption process. The purpose of kinetics is to describe the mechanism within the process of adsorption in relation to time. The time where the biosorbent can no longer adsorb and reaches a plateau (Islam et al., 2018).

Biosorption capacity has been observed to increase with the increase in contact time till the surface area sites has been filtrated and equilibrium is reached (Changmai et al., 2018).

Kinetics regulates the rate of biosorption and determines the equilibrium time of the adsorption process. In a study by Abbas et al.(2014) in a kinetic and equilibrium study of cobalt adsorption on apricot stone activated carbon equilibrium was reached at 90 min In the study conducted by Ahmad et al.(2016) in biosorption of Cd (II) and Pb (II) equilibrium was reached at 30 min.

In order to describe the kinetic studies, models are used and applied and plotted on linear scale. The suitability and fit of model is determined by the linear regression. Models pertaining to kinetics studies are:

- Pseudo first order

The first model was founded by Lagregren formulated to describes the rate of adsorption in the liquid to solid phase in relation to capacity adsorbed (Changmai et al., 2018).

It is expressed as follows:

$$\text{Log } (qe - qt) = \log (qe) - \frac{k1}{2.303t} \qquad \textbf{Equation 2-2}$$

Where Qe is the amount of metal ions adsorbed per biosorbent unit mass at equilibrium measured in (mg/g) ,qt is the amount of biosorbent adsorbed at a specified time (t).K_1 is the pseudo first order rate, A linear plot of $\frac{-t}{qt}$ against time is plotted.

- Pseudo second order

The Pseudo-second order kinetics determines the rate-controlling step and analyses the chemical reaction and mechanism of mass transfer over the entire process of adsorption (Changmai et al., 2018). The initial part in the linear plot shows the external to internal fusion of particles, whilst there second particle of the linear shows the internal fusion of particles (Ahmad et al., 2018).

The formula is expressed as follows:

$$\frac{t}{tq} = \frac{t}{k2\,qe^2} + \frac{1}{qet} \qquad \textbf{Equation 2-3}$$

Where t is specified time and qt is the amount of biosorbent adsorbed Qe is the amount of metal ions adsorbed per biosorbent unit mass at equilibrium measured in (mg/g), qt is the amount of biosorbent adsorbed at a specified time (t).k_2 is the pseudo second order rate constant.

The initial part in the linear plot shows the external to internal fusion of particles, whilst the second part of the linear plot shows the internal fusion of particles (Ahmad et al., 2016).

- Intra particle diffusion

The intra particle diffusion model is the most efficiently used to study the diffusion mechanism in the biosorption process.

It is expressed as follows :

$$Qt = 1 + kp$$ **Equation 2-4**

Where kp is the intra particle diffusion constant.

2.9.1.4 Adsorption isotherm

The adsorption isotherm analysis is an illustration of the relationship between the adsorbate and adsorbent**.** The relationship is described in a numeric form and is expressed in mg/g (Changmai et al., 2018). Isotherms play an crucial role in the designing of adsorption systems (Yusuf et al., 2015).

When plotted the isotherm has been studied to portray four shapes identified as L,S,H and C, as illustrated in (Abbas et al., 2014).The shape of the adsorption identifies and determines the manner of adsorption and characteristics of the nature of the adsorbent.

In the study on adsorption of cobalt using apricot stone, an L shape was achieved due to minimal adsorption at the early stage of adsorption. As the cobalt concentration increased so did the adsorption rate (Abbas et al., 2014).

The adsorption isotherms have various models, the mainly used are namely the Langmuir and Freundlich (Mohammed et al., 2014).

The Langmuir model

The Langmuir model is based on the fact that adsorption is achieved on monolayers in homogeneous surface that is composed of single layer of adsorbent (Mohammed et al., 2014).

The formula is expressed as follows :

$$\frac{C_e}{q_e} = \frac{1}{q_m K} + \frac{C_e}{q_m}$$ **Equation 2-5**

Where Ce (mg/L) is the concentration at equilibrium, qe (mg/g) is the quantity adsorbed at equilibrium, qm (mg/g) is the maximum quantity adsorbed and K is the Langmuir constant.

The Freundlich model

The Freundlich model operates differently from that of Langmuir model, it is based on the fact that adsorption occurs on multi layered in heterogeneous surfaces (Mohammed et al., 2014).
In Freundlich's model adsorption is based on a chemical reaction, where an exchange between ions and electrons take place in between the adsorbent and the adsorbate (Abba et al., 2014).
The formula is expressed as follows :

$$\ln(q_e) = \ln(K_f) + \ln(C_e)$$ **Equation 2-6**

Where ln (qe) is ln of quantity adsorbed, ln (Kf) is ln of the Freundlich constant and ln (Ce) is ln of the concentration in equilibrium. From the isotherm parameters and plots of the model values were determined.

2.9.1.5 Thermodynamic studies

Thermodynamics is the study in relation to energy mechanism in operation during biosorption. Physical and chemical reactions differ in terms of releasing or taking in energy. The physical and chemical is endothermic and exothermic, respectively. Thermodynamics has 4 parameters namely;

Enthalpy (ΔH_0), entropy (ΔS_0) and Gibb's free energy (ΔG_0)

$$K_c = \frac{CA_e}{C_e}$$ **Equation 2-7**

$$\Delta G^{\circ} = -RTln(K_C)$$ **Equation 2-8**

$$\ln(K_c) = \frac{\Delta S}{R} - \frac{\Delta H}{RT}$$ **Equation 2-9**

$$\log(K_c) = \frac{\Delta S}{2.303R} - \frac{\Delta H}{2.303RT}$$ **Equation 2-10**

Kc is the distribution coefficient, CAe is the solid-phase concentration at equilibrium (mg/L), and Ce is the concentration at equilibrium. T (K) is the temperature (K) and R molar gas constant of 8.314 J $mol^{-1}K^{-1}$. ΔH0, ΔS0 and ΔG0 are obtained from the slope and intercept .Negative value of ΔG° and ΔH indicate a spontaneous and exothermic reaction (Ahmad et al., 2016).

Characterisation of biosorbents

2.9.1.6 Scanning Electron Microscope (SEM)

Scanning electron microscope (SEM) is used to define the characteristics of a biosorbent.
Amhad (2015) in his study of adsorption of heavy metals using a pineapple peel, analysed the surface morphology of the pristine PP and a CTPP one. The study compared the PP with the CTPP.
Through chemical treatment it was clear that inhibiting groups were eliminated, this were said to be soluble oligosaccharides. The picture shown on SEM was that with many pores and highly caves. After biosorption, the image depicted a total change from an irregular surface with no pores. This is in agreement with Mohammed et al. (2014) who also studied the biosorption of pineapple peels. After adsorption Mohammed observed a different in pore size as they had filled and multi-layered the surface.

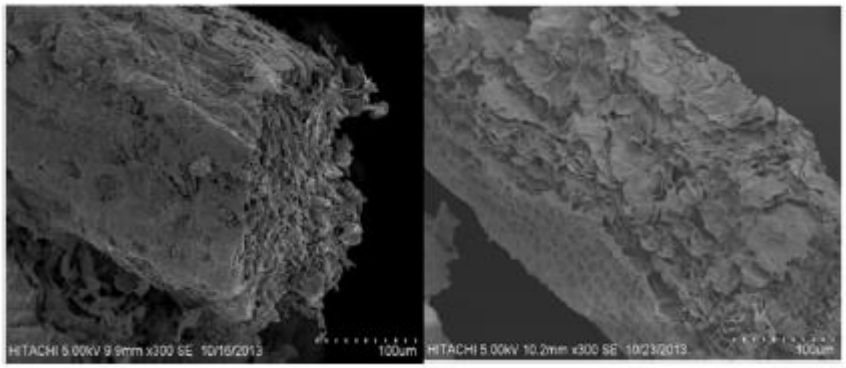

Figure 2-4 SEM image of PP before and after biosorption (Mohammed et al., 2014)

2.9.1.7 Fourier transform infra-red spectrometer (FTIR)

The purpose of the Fourier transforms infra-red spectrometer (FTIR) is to identify and quantify the different functional groups on the surface of the adsorbent. The functional groups identified by the FTIR spectrum are charged by the adsorbate ions (Li et al., 2008). The length of each band determines the functional group of the adsorbents. Bands within the region of 3400 – 3700 indicate the presence of free hydrogen bands O-H. Region between 2900 indicate and 3400 indicate stretching in hydroxyl and aliphatic groups. Bands in the range 2870 and 2900 indicate the existence of alkyl groups, C-H stretching. Bands on the regions of 1745 and 1642 indicate the presence of C = O bands which are the antisymmetric bridge stretching of aldehydes, ketones and ester groups (Ahmad et al. 2016; Bedia et al. 2018).

Amhad (2015) on characterisation of pineapple peels on FTIR achieved new peaks after chemical treatment and adsorption. He reasoned that these are due to C-H stretching. Mohammed et al. (2014) observed similar findings where on pristine pineapple the peak at 1825 was extended to a sharper peak of 2920. Figure 2-5 presents the FTIR spectrum of a pineapple peel before and after biosorption.

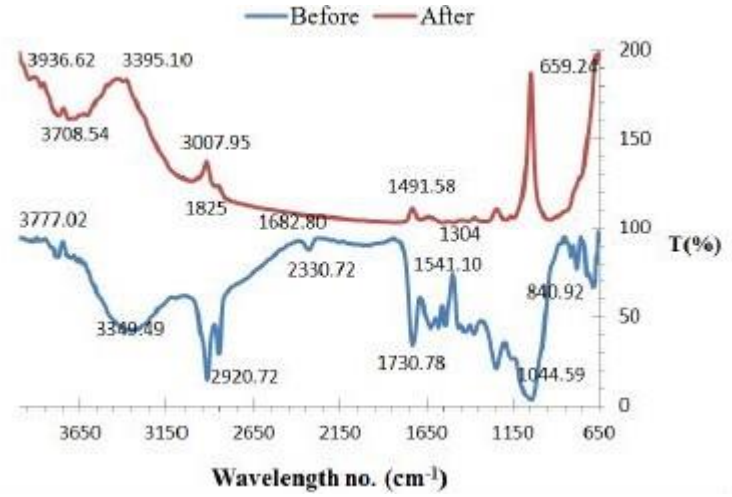

Figure 2-5 FTIR of pineapple peel (Mohammet., 2014)

2.9.1.8 BET Surface area

The Brunauer, Emmet and Teller (BET) is used to measure the surface morphology in terms of pore area, volume and size distribution. BET is traditionally measured as surface adsorption of nitrogen on a firstly degassed surface. The surface area measurements are important since adsorption (and indeed biosorption) is a surface phenomenon. Figure 2-6 shows the shapes of the five types of isotherms obtainable from a BET assay, which gives an idea of the character of the adsorbing surface. Type 1 Isotherm depicts a microporous nature of the biosorbent with an initial increased rate of adsorption followed by a plateau, this phenomenon is depicted by a concave shape. Type 2 Isotherm depicts a microporous nature with multilayer biosorption, the rate of biosorption in respect to concentration is depicted by a concave shape. Type 3 depicts a convex type with a rare shape. Type 4 shows a hysteresis loop with capillary condensation happening in mesoporous nature of adsorbent. Type 5 depict porous and weak interaction between the adsorbate and adsorbent. Type 6 shows a non-porous multi-layer step adsorption which is graphically presented by steps (Khalfaoui, 2003).

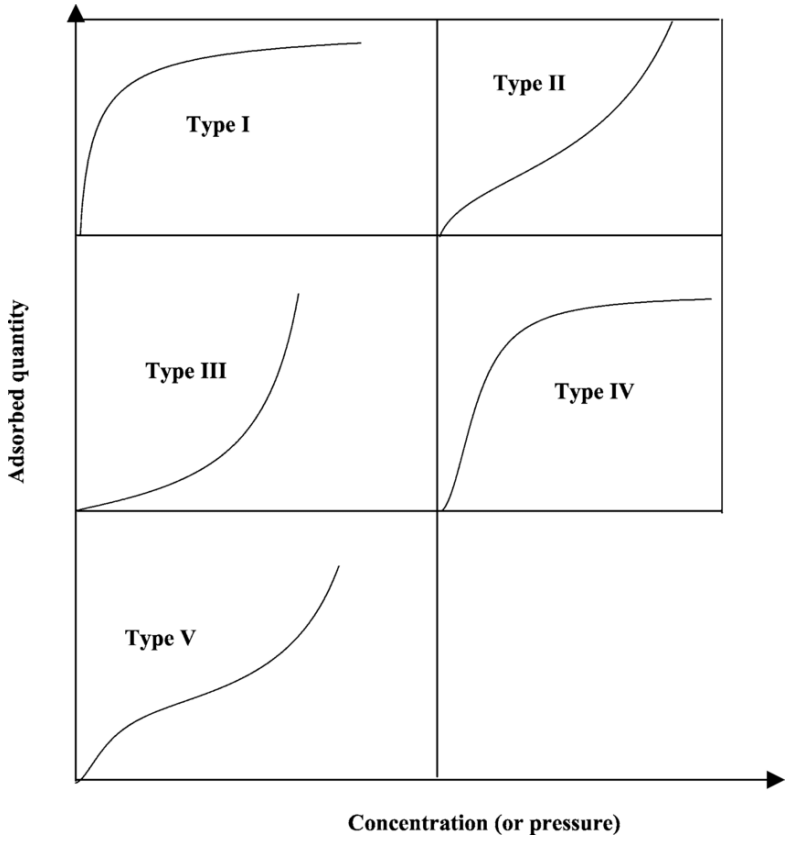

Figure 2-6 BET isotherm types (Khalfaoui, 2003)

2.10 Fixed bed column studies

The biosorption process in fixed bed is performed in a column with the biosorbent packed to a specified height and the adsorbate is continuously passed through. The adsorbent binds ions on the surface of the adsorbate as it passes through (Patel, 2019). Fix bed column has been evaluated to be more advantageous due to effectiveness and ease on the process treatment, mode operation and industrial scale up. Fix bed adsorption has the advantage of achieving high maximum removal capacity due to the simplicity of the process and the ability of scaling it up , (de Franco et al.2017). Adsorption in fixed bed column studies is performed in continues mode which makes it much simpler than batch mode experiment in biosorption. The adsorbent in a fixed bed column provides a greater extent of surface area which results to greater adsorption. From the fixed column results industrial application can be determined, (Andrea et al., 2017).

The purpose of the fixed bed is to quantify adsorption parameters required to determine the scale suitable for industrial application, (Karunarathne & Amarasinghe, 2013). The fixed bed parameters are evaluated using breakthrough curves and the results are described by the mathematical models by Bohart –Adam, Thomas and Yoon (Trgo et al., 2011).

The adsorption results obtained from column fixed bed are illustrated by a breakthrough curve where the initial point of change on the graph is marked as the breaking point (tb) and the point where adsorption has reached a plateau is marked as the saturation time (ts). The process and response of the column adsorption is expressed by the shape of the breakthrough curve.

The shaped is affected by the concentration, adsorption rate, changes on breakthrough area and mass transfer. The increase of the concentration results in the availability of active site for increased adsorption. This is indicated by the steepness of the s-curve whilst on initial concentration the breakthrough curve is spread over the whole area (Tofan et al.,2013).

Adsorption in fixed bed column studies is performed in continues mode which makes it much simpler than batch mode experiment in biosorption.

A study by Lakshmipathy et al. (2015) agricultural waste was reviewed indicated a lack of studies on continuous bed studies, his finding was that many literatures has focused on batch studies of adsorption using biomass.

Parameters affecting biosorption on fixed bed are those of bed height, concentration and flow rate. Table 2-7 presents studies of biosorption capacity in the removal of Co (II) with biomass performed in batch and column mode. A few studies has been carried out in column mode whilst more studies are carried in batch mode. The results show the need to upscale to column mode Overall the column study showed greater adsorbent capacity. In batch studies the bone char showed a high adsorption capacity (108 mg/g).

Table 2-7 Column and batch studies on Co(II) adsorption (Tofan et al., 2013)(A review)

Biosorbent	Batch (mg/g)	Column
Alga spirogyra hyalina	12.821	
Almond green haul	45.50	
Black carrot residue	5.35	
Brown Alga Sargassum		27.6
Brown seaweed	20,63	50
Bone char	108,7	
Cells of Saccharomyces Cervisae	0,68	1,56
Fresh water algae	12,821	
Citrus reticula Ligno		
Cellulostic fibre		
Coal fly ash	0.401	
Marine green algae		46.1
Rose waste biomass	27.15	

Fixed bed modelling

The fixed bed parameters are evaluated using breakthrough curves and the results are described by the mathematical models of Bohart–Adams, Thomas and Yoon–Nelson (Trgo et al. 2011).Illustrated on Figure 2-7 are two zones of operation ; the initial mass transfer zone and fresh adsorbent zone which leads to the saturation point.

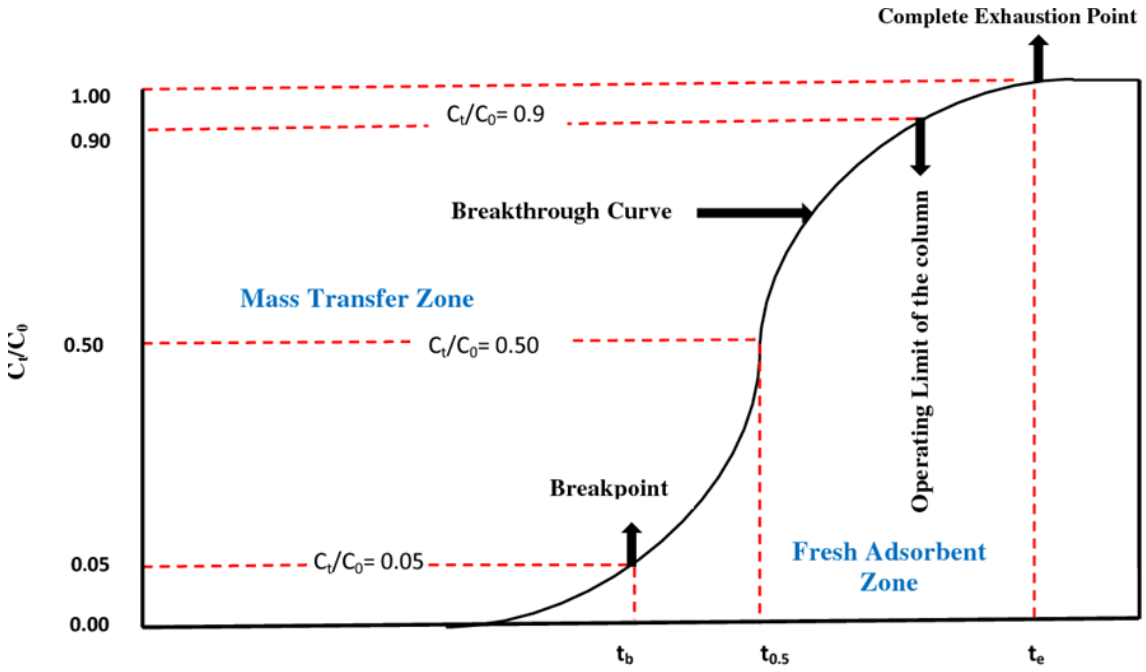

Figure 2-7 : Break through curve in fixed bed column illustration (Chowdhury et al., 2013)

Bohart – Adam model

On studying the behaviour of charcoal in respect to chlorine, Bohart & Adams (1920) initiated an equation for fixed bed adsorption. From the study, it was discovered that the rate of the reaction is proportional to the fraction of the adsorbate retained by the adsorbent. The adsorbate reaction is considered monolayer.

Bohart Adams is used for the description of the initial part of the curve within the operating limit of the column(Tiwari et al., 2009). The mathematical equation of the model is written as:

$$Ln\frac{Ct}{Ci} = K_{BA}\, C_i t\, (K_{BA}\, q_{BA}\, H)/V$$ **Equation 11**

Where Ct is concentration at time t, Ci is the initial concentration, K_{BA} is the constant of Adam-Bohart. H represents bed depth in metres and ν is the linear flow velocity (flow per unit area).

The main purpose of the Bohart-Adam is to determine the size of the fixed bed column for industrial set up. Two parameters are essential for design purpose the K_{BA} and q_{BA}, which can be determined from the plot ln Co/Ct against t. Change in slope, has a direct effect on the intercept (Singh & Mehta, 2015).

Certain patterns have been identified on the column parameters. On bed mass, the removal capacity increased with increase in bed height. On adsorbate concentration, the breakthrough curve was observed to be steeper with increase in concentration. Increase in flow rate results in decrease in adsorption and increase on K_{BA} (Mahmoud, 2016).

Thomas model

The function of the Thomas model is to determine the performance of the column pertaining to its breakthrough curve. The model is largely influenced by the Second order kinetics of Langmuir, (Singh, 2015). The formula is written as :

$$Ln\left(\frac{Ci}{Ct} - 1\right) = \frac{K_{TH} q_{TH} m}{Q} - \frac{K_{TH} C_i V}{Q}$$ **Equation 12**

The flow rate constant K_{TH} and q_{TH} are determined from the plot of $Ln\left(\frac{Ci}{Ct} - 1\right)$ against V (volume).

K_{TH} is the Thomas model constant

$$q_{TH} = \frac{Slope\ of\ equation\ x\ Q}{K_{TH} x\ m}$$

Q is the flow (m^3/min).

m is the mass of bed in (g).

The value of K_{TH} decreases with the increase on bed height.

Time required for 50% adsorbate breakpoint time.

Yoon-Nelson model

Yoon and Nelson (1984) during their study about application of gas adsorption kinetics discovered a much simpler method that looks at the relationship of the linearized form and assumes that the rate of adsorption rate decreases with the decrease in concentration.

K_{YN} is can be determined at a specific bed height, flow rate and initial concentration.

K_{YN} is the rate constant per minute. In a study by Singh and Mehta (2015) the K_{YN} constant increase with an in increase in concentration. In 200 and 500 ppm the K_{YN} value was 0.023 and 0.006. In Han et al. (2009) the K_{YN} value decreased with the increase in mass. Contrary to the results of Nwabane (2012) where the K_{YN} value increase with bed height as follows ; 7.96, 3.56 and 2.167 the adsorption capacity increased as follows; 3.51, 4.94 and 5.99 mg/g. In study by de Franco (2017), the Yoon-model predicted the highest adsorption of 11.18 mg/g.

K_{YN} can be determined at a specific bed height, flow rate, and initial concentration.

$$\ln \frac{Ct}{Ci - Ct} = K_{YN}\, t - K_{YN}\, \tau \qquad \textbf{Equation 13}$$

Where Ct is concentration at time t, Ci is the initial concentration, K_{YN} is the Yoon rate constant. τ is intercept over the gradient.

2.11 Overview and conclusion

The literature reviewed showed that there is significant research pertaining to waste, waste management and integrated waste management system. A study by Dlamini et al. (2019) pointed out a lack of framework with regards to implementation and assessment strategies in South Africa pertaining to transformation of waste material. Grandin and Pletschke (2015) established a model that indicates a framework for the utilisation of biomass for conversion to energy and utilisation in wastewater however most waste charactisation is for the purpose of waste to energy. From a review study on biosorption of cobalt it was shown that in utilisation of fruit waste a large portion of the fruit discarded has not been experimented for the remediation of cobalt. Even further, the small fraction of waste covered shows that very little has been done to extend this process to industrial application. This is shown by the ratio of studies performed in batch to those in column studies. Therefore, candidacy for a suitable biomass is still subject to scientific investigation, which would necessarily depend on local available resources and the effectiveness of the biomass in the remediation of cobalt from textile wastewater.

3 Methodology

3.1 Introduction

This chapter presents the details of the materials, apparatus and experimental procedure used for this study. The experimental set up and procedure entailed collection and pre-treatment of biomaterials, characterisation of the adsorbent material, and preparation of reagent standards as well as the batch and column biosorption.

3.2 Research design

The quantitative research design was used. Experiments were conducted in the laboratory, testing the biosorbent material through biosorption procedures namely batch and continuous mode. The original sample, dried pineapple (peels) was dived into 3 samples with the addition of activated carbon as a standard for comparison as follows:

- Original (pristine) raw biosorbent (RPP)
- Chemically treated biosorbent (CTPP)
- Carbonised pineapple peel (CPP)
- Activated carbon (AC)

3.3 Materials and method

Sourcing and treating of pineapple peels

Fruit waste generated at a local vegetable and fruit retail outlet was characterised and quantified. Pineapple waste (peels) was found readily available. The peels were collected and thoroughly washed with distilled water and oven dried at 60ºC for 60 hours in a Scientific oven. The dried peels were physical treated by grinding of the pineapple peels in a miller and sieved through 150 µm sieve sizes. Figure 3-1 presents one third of the RPP of Figure 3-1 a) used as pristine raw, Figure 3-1 one chemically treated (CTPP) with $KMnO_4$ and H_2SO_4 and the last third was carbonised (CPP) in Figure 3-1 d) at 600°C in nitrogen in order to determine the effect of the treatment.

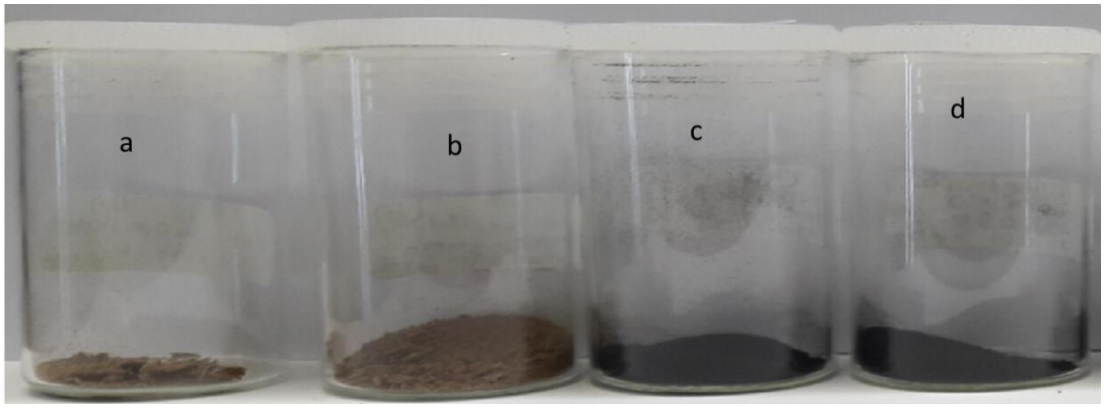

Figure 3-1 Prepared biosorbents (a) RPP (b) CTPP (c) CPP (d) AC

Cleaning of containers

All containers used; beakers, conical flasks, measuring cylinders, mortar, and pestle were thoroughly washed with detergents and tap water. After rinsing all containers thoroughly with distilled water, it was then soaked in HNO_3 for 48 hours then rinsed with distilled water and dried.

Reagents

One litre 1000 ppm cobalt solution was prepared from a mass of 7.96 g cobalt chloride hexahydrate 7.96 g ($CoCl_2.6H_2O$: mm 237.93 g/mol) obtained from Sigma Aldrich, South Africa and dissolving it in 1 litre of water. The solution was transferred to a 2 litre volumetric flask and filled up to the mark with distilled water to prepare a 200 ppm solution. From the 200 ppm the 100,

50, 25 and 10 ppm concentration was prepared. A mass of 0.3 g of biosorbent was placed in 8 beakers and two reserved as blanks. Then 30 ml of the 200 ppm solution was poured into each of the beakers. The beakers were placed on a shaker for 90 minutes. The biosorbent was removed after 90 minutes from the solution by filtering through Whatman filter size 110 mm and then dried.

3.4 Modification of RPP

Chemical treatment

Chemical treatment was done in accordance to the method of Ahmad et al. (2016) where 45.6 grams of RPP was treated with 380 ml of $KMnO_4$ and subsequently treated with 380 ml of 0.1 M H_2SO_4. Treated sample was then washed with MilliQ water until was solution was neutral to litmus paper. Treated samples were oven dried at 60 ºC until for 24 hours.

Physical treatment – carbonisation

The carbonisation of the RPP was conducted in a Pyrotherm tube furnace (Alser Teknik Seramik PTF series, Turkey), at 600 ºC under nitrogen at 10 L/min flow rate. The RPP was loaded into a steel tube inside the furnace and was subjected to thermal treatment in the absence of oxygen for 120 minutes. After heating it was allowed to cool for 12 hours.

Characterisation

3.4.1.1 Scanning Electron Microscope (SEM)

The scanning electron microscopy (SEM) was conducted using an Auriga SEM at the University of the Western Cape. RPP, CTPP, CPP, and AC samples were coated with a thin layer of gold-palladium (Au-Pd) using a Q150 T Turbo pumped sputter coater to enhance conductivity of the samples. An Edward vacuum pump was used to pump out charging artefacts formed by build-up electrons. The micrographs were taken at 5000 magnification.

3.4.1.2 Fourier transform infra-red spectrometer (FTIR)

The Fourier Transform infrared (FTIR) was conducted at the Cape University of Technology. was used to determine the chemical structure and the functional groups of the adsorbent RPP, CTPP, CPP and AC sample.

3.4.1.3 BET

The Brunauer-emmet-teller (BET) experiment was conducted at University of Cape Town, Analytical laboratory in the Department of Chemical Engineering. The instrument used was a Tristar II (BET & BJH). The BET was used to measure surface morphology, which are the pore area, size distribution, and volume through adsorption of nitrogen. The biosorbent samples were degassed at 200ºC with size of < 150 μm under vacuum on a Micromeritics Vacprep 061.The sample was analysed on a Micromeritics Tristar II 3020.The gassing was done in order to remove pores of the sample including the water and carbon dioxide. The BET equations were applied to determine the distribution, micropore, and mesopore volumes.

3.5 Batch studies

The effect of mass, pH, time, temperature and cobalt ion concentration were done in batch mode. Typically, a weighed amount of biosorbent was contacted with a known concentration of cobalt ions in a given volume at a specified pH for a set time. The adsorbed sampled was filtered and analysed for residual cobalt ions. The percentage and quantity biosorbed were calculated according to:

$$\% \; adsorption = \frac{C_i - C_e}{C_i} \; x100$$

Equation 2-1

Effect of biosorbent mass

The effect of dosage was determined through variation of different masses of the biosorbent. An amount of either 0.05, 0.10, 0.20, 0.30, 0. 40 or 0.50 grams was added to 30 ml cobalt chloride solution in a 50ml tube and shaken for 24 hours in a water bath. The effluent was filtered through a Whattman filter and collected in a 50 ml tube as shown in Figure 3-2 and sent to an Atomic Adsorption (AA) for analysis. The percentage adsorbed was plotted against the different masses.

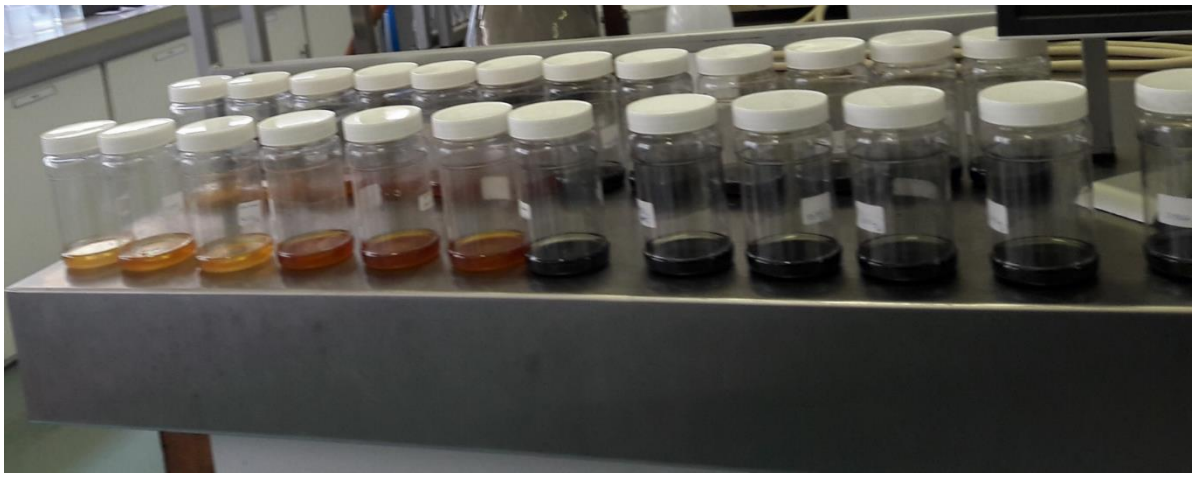

Figure 3-2 Samples prepared to evaluate the effect of mass

Effect of pH

The effect of the pH on the adsorption process was determined by varying initial pH within the range of 2 to 9 A volume of 30 ml of 50 ppm cobalt chloride solution was placed in contact with 0.05 g of biosorbent for 90 minutes. The pH was adjusted with 0.1 molar hydrochloric acid and sodium hydroxide.The biosorption behaviour of the cobalt ions in different pH was depicted on graph where percentage adsorbed was plotted against pH.

Effect of time

The effect of time on the adsorption process was determined by varying contact time in batch mode from 0.5,1, 3, 5, 10, 20, 30, 45, 60 and 90 minutes. Optimised biosorbent dosage and cobalt solution of 0.5g and 50mg/L respectively, were placed in 180 plastic jars to 30 ml volume and placed in a shaker then filtered out of the biosorbent. The remaining solution was sent to the AA for analysis. The results obtained were used to determine the effect of time, on the biosorption process.

Effect of temperature

The effect of temperature on the adsorption process was studied in the range of 10, 20, 30 and 40 ºC using 0.5 g of biosorbent in 50 ppm cobalt solution. The water bath was pre-set to the required temperature study the sample was subjected to 90 minutes contact time. From the results obtained thermodynamic parameters namely enthalpy (ΔH°), entropy (ΔS°) and Gibb's free energy (ΔG°) were determined.

Effect of metal concentration

The effect of initial concentration was determined by varying cobalt chloride solutions within the range of 1, 5, 20, 50, 100 and 200 mg/L using 0.5 g of each biosorbent. The samples were placed in a shaker for 90 minutes and filtered. The results obtained were used to evaluate equilibrium models.

Modelling of batch biosorption data

3.5.1.1 Adsorption isotherm

Adsorption isotherms were used to illustrate the relationship between the concentration obtained at equilibrium and the amount adsorbed at equilibrium. The Langmuir and Freundlich models were applied to compare the performance of the biosorbents. The data applied was obtained from effect of concentration studies. The Langmuir theorem assumes that the adsorption occurs in a monolayer whilst the Freundlich assumes adsorption takes place in multi-layered surface where non-uniformity and adsorption is expected to increase with the increase in concentration

$$\text{Log } (qe - qt) = \log (qe) - \frac{k1}{2.303t} \qquad \text{Equation 2-2}$$

3.5.1.2 Kinetic modelling

Kinetic studies were done to determine the adsorption rate and mechanism of contact. Equilibrium time was varied in the range of 1, 3, 5,10, 20, 30, 40, 45, 60 and 90 minutes adsorption time in an orbital shaker at 60 rpm. An adsorbent of 0.05 g was added with 30 ml of cobalt chloride solutions of 50 ppm.

From the results obtained, the models applied were that of the first order and second order kinetic equations as described ;

$$\frac{t}{tq} = \frac{t}{k2\,qe^2} + \frac{1}{qet} \qquad \text{Equation 2-3}$$

3.5.1.3 Thermodynamics

Thermodynamics parameters namely, Gibbs free energy change (ΔG^o), enthalpy change (ΔH^o) and entropy change (ΔS^o) of the biosorption process were applied to further determine the effect of temperature on the adsorption of cobalt ion.

3.6 Fix bed column studies (modelling)

The best performing biosorbent from RPP, CTPP and CPP as well as AC evaluated in the batch study was selected for a ontinuous flow fixed be column study.

Fixed bed column studies were performed in a plastic column with a diameter of 1.7 cm and height of 19 cm. The column was packed with filter paper cut to 1.7 cm diameter and with cotton and CPP biosorbent.

Figure 3-3 Fixed bed column apparatus

The CPP was used for varying masses of 0.5, 1.0 and 1.5 g, flow rates of 1, 3 and 5 ml/sec, and concentrations of 10, 25 and 50 ppm were used in fixed bed mode. After the optimisation of parameters, the optimal conditions were applied to industrial wastewater with CPP.

The experiment was conducted at room temperature and a pH of 6.

From the equilibrium data obtained a breakthrough curve was derived to analyse and describe the performance of the adsorption process in the fixed bed column. Four response factors were applied namely:

The breakpoint time of adsorbent (TB), Fractional bed utilization (FBU), Saturation time (TS) and volume of effluent treated per gram (VS). TB is the time taken to reach 5% of inlet concentration determined as.ST is the time taken for effluent to reach 95% of the inlet concentration. Fixed bed models were used to analyse the column data obtained. The model used were that of Bohart-Adams model, Thomas model and Yoon-Nelson.

3.7 Conclusion

This chapter described the sourcing of material, equipment used and processes of treatment. The characterisation of the pineapple peel biosorbent was described. The procedure for the evaluation of the performance of the various biosorbents prepared in batch and column studies was also presented. Laboratory images of some key processes described are presented in Appendix D

4 Characterisation

4.1 Introduction

This chapter presents the results for the characterisation of RPP, CTPP, CPP and AC adsorbents using Scanning Electron Microscopy (SEM), Fourier transform infrared spectroscopy (FTIR) and Brunauer-Emmet-Teller (BET) analysis. RPP, CTPP, CPP, and AC samples of 0.1 g were subjected to adsorption of cobalt metal ion, 200 ppm at pH 5 and subsequently characterised.

The 200 ppm concentration was selected based on the outcome of preliminary results that showed no increase in adsorption capacity beyond this point. Elemental composition obtained via SEM-EDS are also presented and discussed.

Figure 4-1 presents the effect of chemical modification and physical treatment in RPP, CTPP, CPP and AC after contact with Co(II). Poor quality of water was found on the non-carbonised samples.

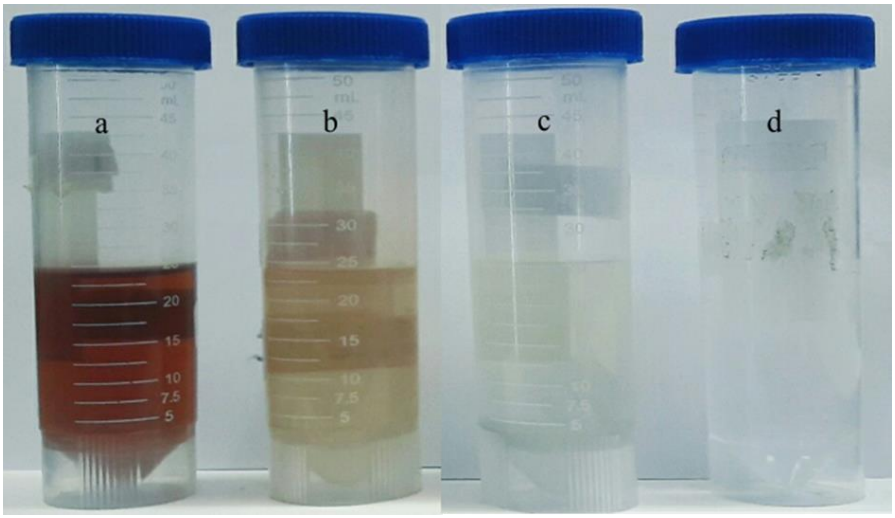

Figure 4-1 Impact of various biosorbents on aqueous system (a) RPP b) CTPP c) CPP d) AC

4.2 Scanning Electron Microscopy (SEM)

The surface morphology of RPP, CTPP, CPP, and AC biosorbents was characterised by scanning electronic microscopy (SEM). SEM characterisation was done for all the adsorbent samples before and after biosorption. The micrographs captured on Figure 4-2 to Figure 4-2 are obtained at a magnification of 5 K.

Figure 4-2 1(a) and 1(b) depict the structure of the RPP sample before and after biosorption respectively, showing the uneven texture, exhibiting thick threads and irregular shape for both. After adsorption with cobalt ion, there was no distinct difference in form and no quantified cobalt adsorption according to the EDS spectra as shown in Table 4-1. The morphology of the CTPP in Figure 4-2 2(a) and 2 (b) shows smaller fragments due to increased surface area. There was no noticeable difference in sample CTPP after biosorption.

The surface of the CPP shown in Figure 4-3 1 (a) and 1(b) appears to be decorated with smaller particles in comparison to the smooth texture of the RPP as well as the CTPP. The AC samples shown in Figure 4-3 2 (a) and 2 (b) are decorated with finer ‘dust like’ particles. There is no effect of biosorption or traces of Co (II). According to the EDS, the CPP exhibited maximum adsorption of Co (II) from all the biosorbents prepared as well as in comparison to the AC. This work shows that biosorption takes place without the need for chemical treatment as described by (Ahmad et al., 2016).

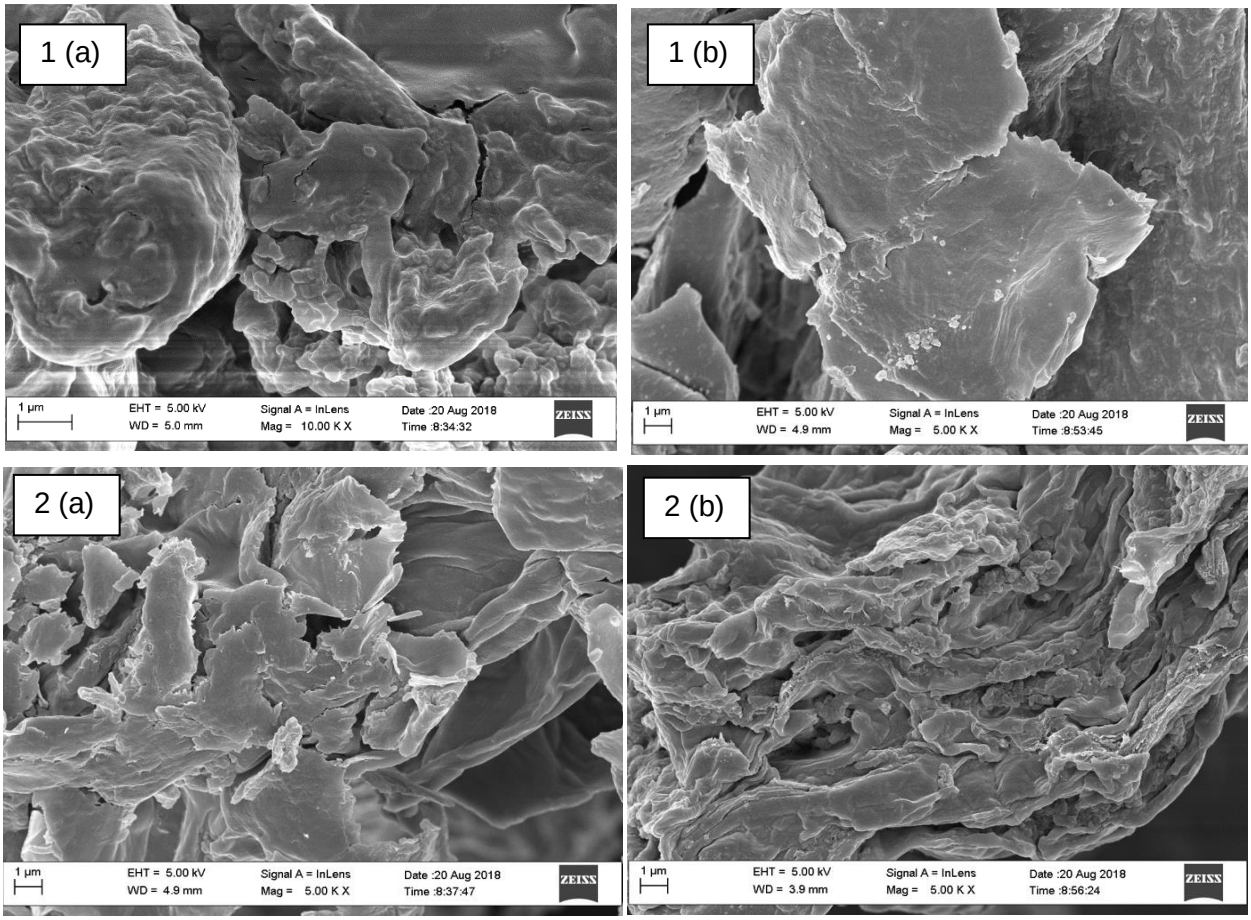

Figure 4-2 SEM micrographs of 1) RPP 2) CTPP (a) before adsorption (b) after contact with cobalt

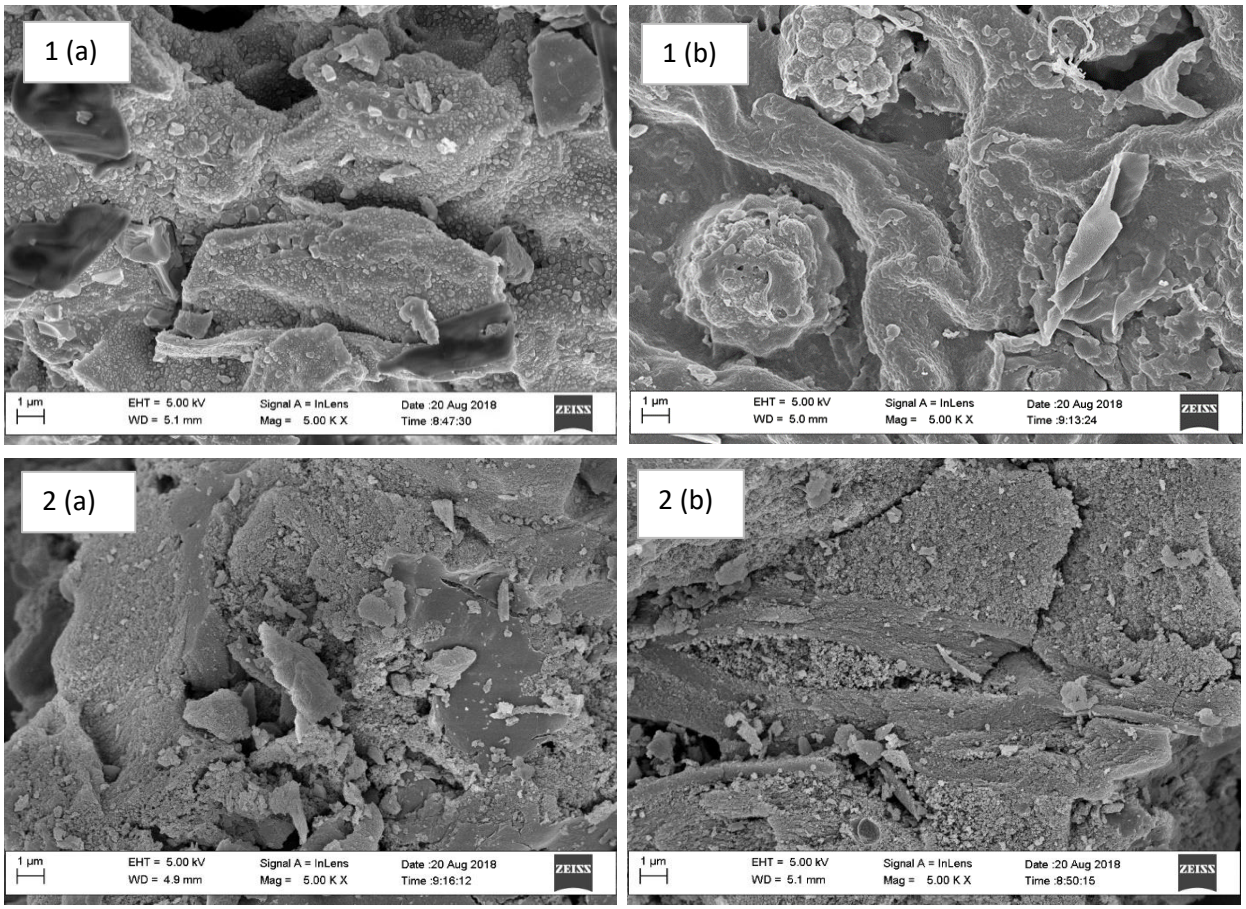

Figure 4-3 SEM micrographs of 1) CPP 2) AC (a) before adsorption (b) after contact with cobalt

4.3 Energy Dispersive X-ray Spectroscopy (EDS) Summary of biosorbents

EDS in conjunction with SEM was used to determine the elemental composition of the biosorbent samples before and after cobalt biosorption. A typical EDS spectrum is shown in Figure 4-4 while a summary of EDS results is presented in Table 4.1.

In general, EDS results showed high percentage of C and O as would be expected from an organic matrix. The O content of the carbonised sample was significantly lower than the raw or chemically treated sample. The presence of oxygen on the activated carbon may be attributed to water present in the activated carbon. It was also observed that the chemically treated sample did not show any trace of the element potassium (K).

Before biosorption, the biomasses did not show any cobalt ion in their elemental composition. However, EDS results for CTPP and CPP after contact with cobalt solution showed the presence of cobalt ions on the surface of the biomass. This gives proof of biosorptive removal of the metal ion from aqueous solution only for the CTPP and CPP. This work confirmed that chemical treatment is required to activate the pineapple peel as biosorbent as was shown in the case of (Reference to original paper) cadmium and lead removal using PP. This work showed however that carbonisation of RPP can improve biosorption by 3-fold. Carbonisation is a much simpler process where no chemicals are needed.

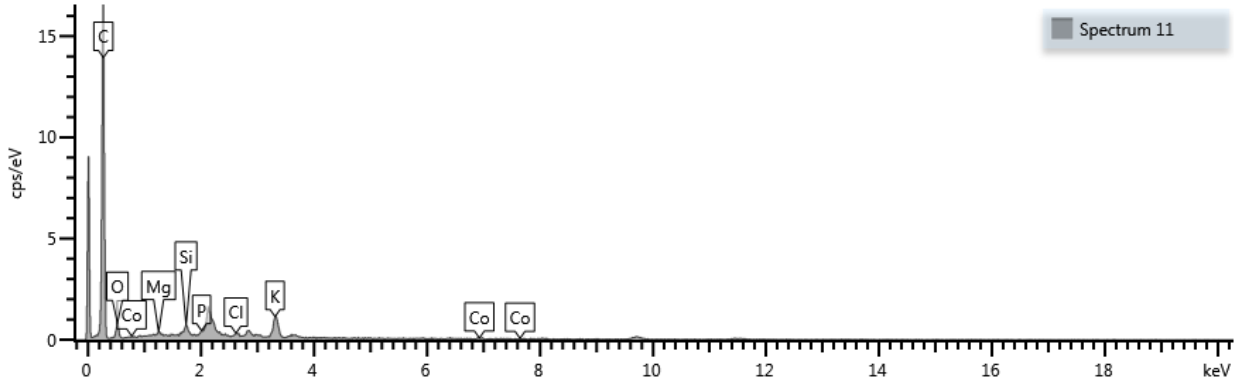

Figure 4-4 EDS spectrum

Table 4-1Table 4-1 : Energy Dispersive X-ray Spectroscopy (EDS) data of pristine and used biosorbents

	Sample	*C*	*Ca*	*Cl*	*Co*	*K*	*Mg*	*Mn*	*P*	*O*
1a	RPP	56,32	-	0,31	-	1,76		-	-	41,61
1b	RPP after absorption	60,19	-	-	-	0,16				39,51
2a	CTPP	65,99	-	-	-					33,05
2b	CTPP after adsorption	61,38	-	-	**0,06**					38,31
3a	CPP	83,41	0,56	-	-	2,26				13,65
3b	CPP after adsorption	89,01	0,23	-	**0,2**	1,25	0,15			8,79
4a	AC	79,04	-	-	-				1,54	19,42
4b	AC after adsorption	83,46	-	-	-					16,54

4.4 FTIR

FTIR was used to characterise the chemical structure of the biosorbent by identifying the functional groups present therein. The FTIR spectra of biosorbent RPP, CTPP, CTPP and CT before and after adsorption are presented from Figure 4-5 to Figure 4-6.

Presented on Figure 4-5 1(a) and 1 (b) is the morphology of RPP before and after adsorption.

A range of bands of functional groups was identified on the surface. The broad band at 3307 can be attributed to stretching in OH. The bands represent the presence of free OH groups and stretching in hydroxyl groups. Between 1400 and 400 cm^{-1} a sharp peak of 1033 was observed. This indicate the presence of stretching in pyranose and skeletal ring. This is in agreement with the findings of a study by Ahmad et al. (2016) who studied the FTIR spectra of a pineapple peel for the adsorption Cd(II) and Pb (II). His results were compared to those of this study. A broad band of 1037 cm^{-1} was identified and was said to be due to the lignin structure of the pineapple.

In the morphology of the pineapple, peel there is no distinct change before and after adsorption as shown in Figure 4-5. However, it was identified that the characteristic of the morphology of the

adsorbed RPP slightly differs to that of the chemically treated pineapple peel therefore the impact of chemical treatment was shown.

The FTIR spectrum for CTPP showed a significant reduction of the characteristic pineapple pyranose peaks in RPP after oxidation and a complete elimination of these peaks in CPP upon carbonisation. There was no significant or observable difference in the FTIR spectrum of CTPP and CPP before and after application for the sorption of Co (II). The FTIR spectrum for AC showed the presence of water (1600 cm^{-1}).

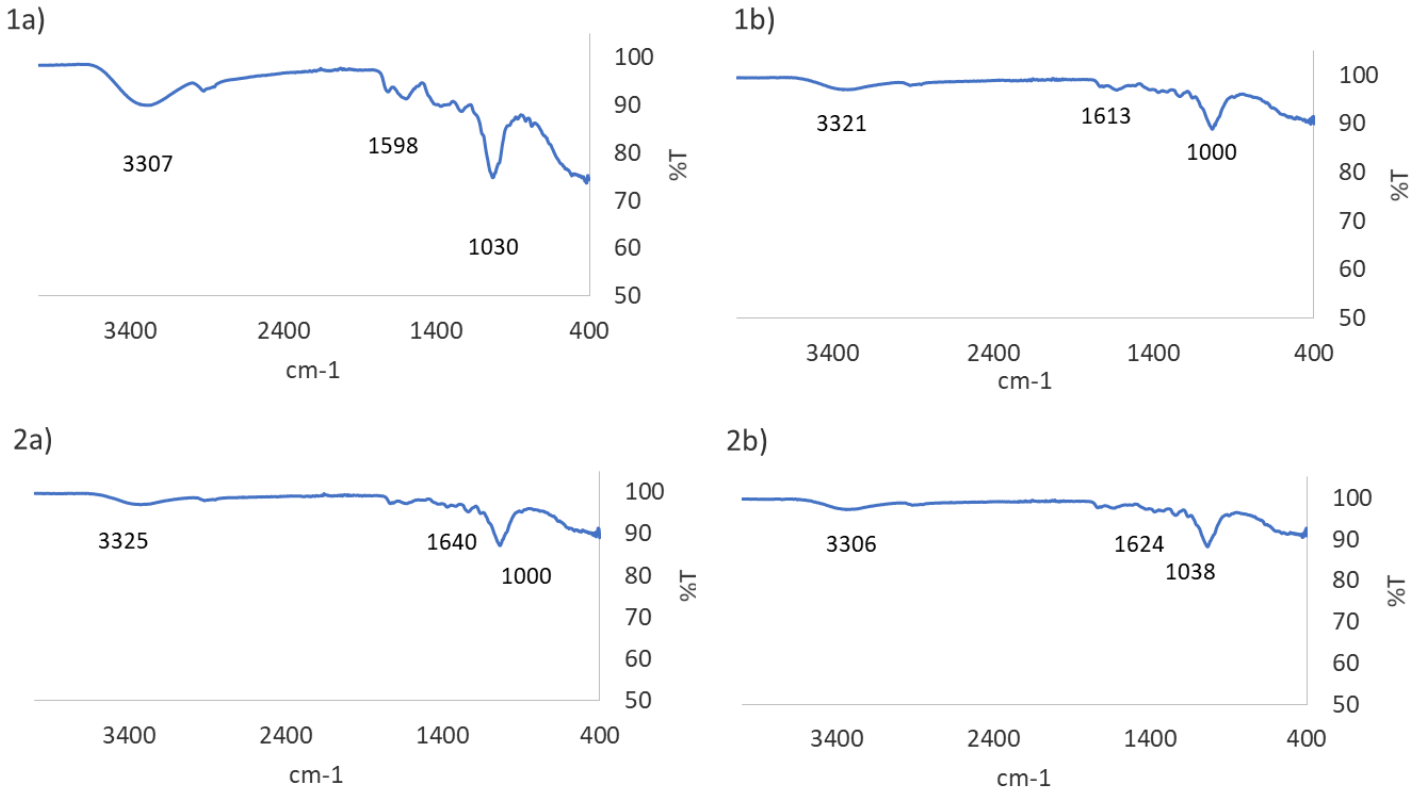

Figure 4-5 FTIR spectrum of 1) RPP and 2) CTPP. (a) before and (b) after contact with cobalt

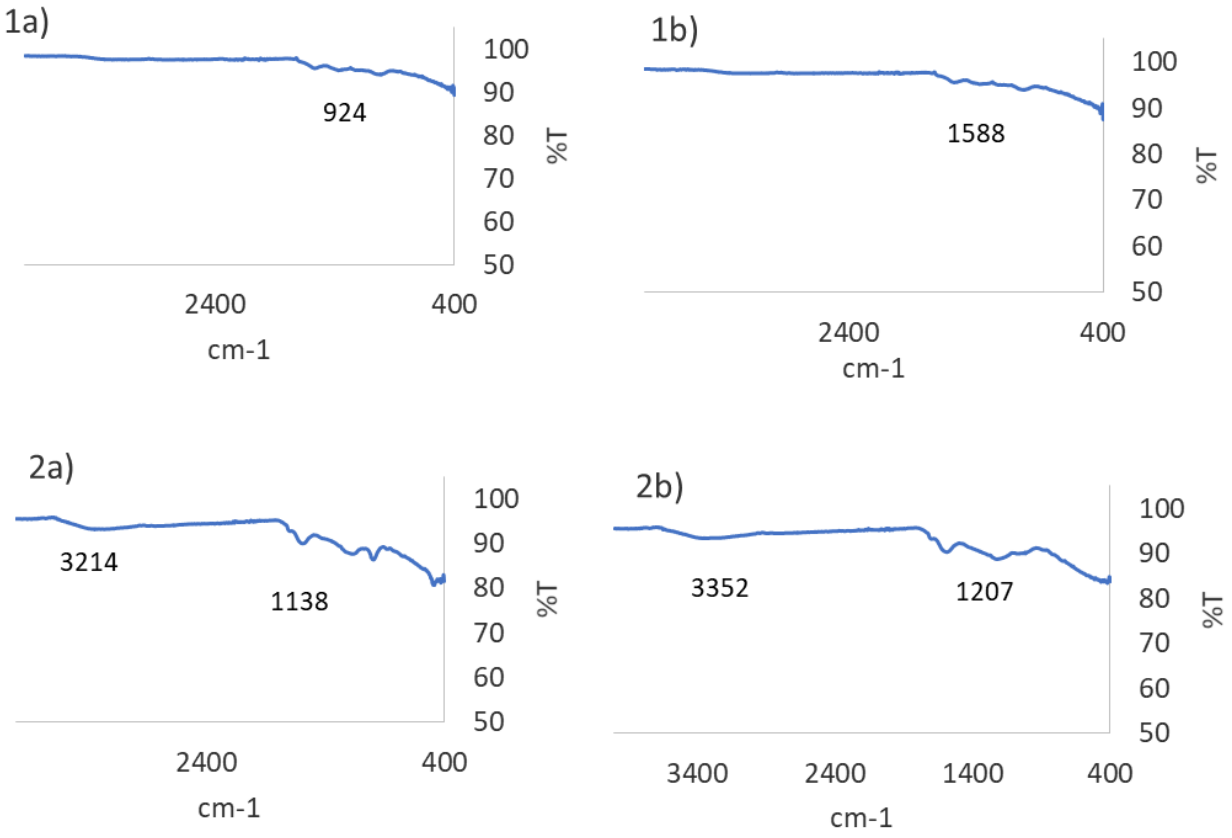

Figure 4-6 FTIR spectrum of 1) CPP and 2) AC (a) before and (b) after contact with cobalt

4.5 BET

BET was used to measure the surface morphology in terms of the surface area, pore size and volume. A summary of the characterisation of RPP, CTPP, CP and AC is presented in Table 4-2. Characterisation results could not be obtained for RPP because the biomass was not stable at 200 ºC, which was the temperature of the degassing before surface area measurements. CTPP had the largest surface area, pore size and pore volume of 1.2319, 470.248 m^2/g and 0.000290 cm^3. The CPP and AC had a pore size 69.558 m^2/g and 43.198 m^2/g. On a study pertaining

Table 4-2: Summary of BET parameters for RPP, CTPP, CPP and AC

Sample	***Surface area m^2/g***	***Pore size (m^2/g)***	***Pore volume cm^3/g***
RPP	-	-	-
CTPP	1,2319	470.248	0.000290
CPP	0.2255	69.558	0.00019
AC	1,002.89	43.198	0.687086

4.6 Conclusion

SEM images of RPP, CTPP, CPP and AC showed varying degree of porosity and particle distribution. No clear correlation could be drawn from SEM images and treatment protocols applied to RPP. EDS results identified the presence of Co (II) on the surface of CTPP and CPP after biosorption. The absence of Co (II) on RPP and AC may well be due to their low uptake capacities FTIR results of RPP showed the presence of water peaks as well as characteristics of pyranose and lignin peaks. Chemical and physical treatment brought about a significant and complete elimination of RPP characteristic peaks of CTPP and CPP, respectively. There was no observable difference in FTIR spectrum when CTPP, CPP and AC were applied for biosorption of Co (II). Best results for surface area, pore size and pore volume were obtained for CTPP. Based on BET results it may be hypothesised that CTPP would yield better biosorption capacities, but the batch showed that the CPP removed 3 times the amount of Co (II) than that of CTPP.

5 Batch studies

5.1 Introduction

In this chapter, the results of the biosorption capabilities of the biosorbents applied in batch mode are presented.

Experimental parameters optimised are (1) the initial pH and (2) dosage of biosorbent of the cobalt ion solution. The effect of starting cobalt ion concentration contact time and temperature was investigated, and the data obtained was used for equilibrium isotherms, kinetic and thermodynamic modelling, respectively.

Optimisation of variables

Effect of pH

The pH of the solution is the most critical parameter as it controls the overall reaction and mechanism of the ions involved in the biosorption process. Presented in Figure 5-1 is the effect of pH determined by varying pH between the ranges of 2 to 9 for all biosorbents. To adjust the pH to the required value, sodium hydroxide (NaOH) and hydrochloric acid (HCl) was used.

Beyond pH 7, there is precipitation of cobalt ions as cobalt hydroxide. Illustrated in Figure 5-1 is an initial gradual increase of biosorption metal uptake until a plateau is reached for RPP, CTPP, and CPP and a peak at 6.5 for carbonised and activated carbon. This is in line with results obtained for the biosorption of copper by citrus peels and saw dust where pH 6.5 was reported as optimum by Khan et al. (2013). At low pH, cobalt ions compete with hydrogen ions for active sites on the biosorbents and hence cobalt removal is low. As pH increases, the hydrogen ions reduce and so does their competitive effect. Biosorption expectedly increases. A study by Changmai et al.(2018) reasoned that the pH is directly proportional to the surface charge and cobalt is cationic in nature therefore cobalt adsorbed overall increases with the increase in pH.

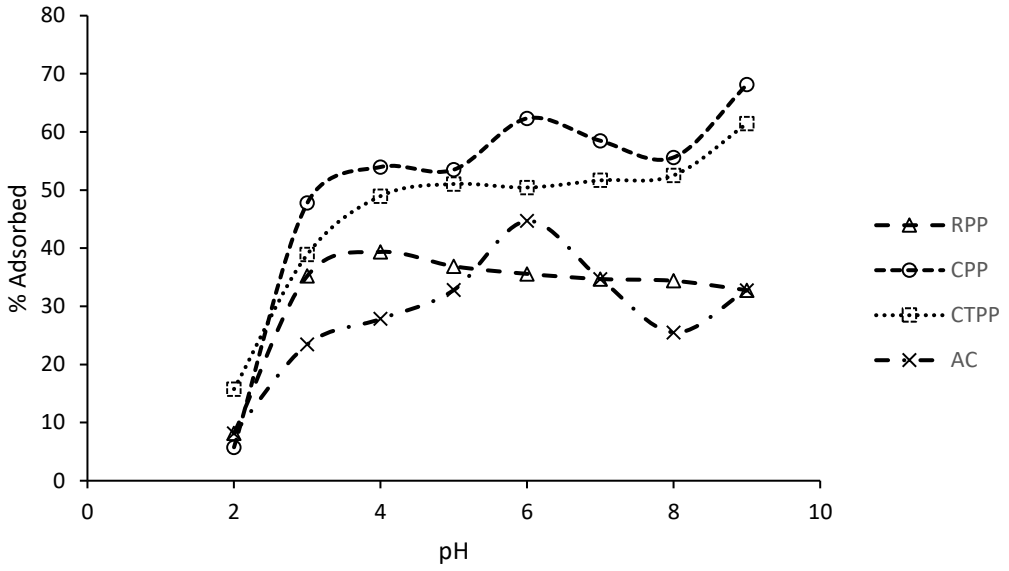

Figure 5-1 Effect of Ph on the biosorption character of RPP,CTPP,CPP and AC.

Effect of adsorbent dose

Mass is an influential parameter in determining the adsorption percentage and quantity adsorbed in sorption experiments. Figure 5-2 presents the experimental data of RPP used with varying mass.

The effect of mass was varied from 0.05 , 0.1 , 0.2 , 0.3 , 0.4 and 0.5 g in 30 mL Co (II) concentration of 50 ppm at pre-set pH of 6. The maximum adsorption was observed for lower masses; 96.96 % at 0.1 g and 85.70 % at 0.05 g. On the basis of these results 0.05 g mass was used on subsequent experiments. This is despite the fact that 0.1 g gives a higher percentage removal. It was rationalised that it was better to use two portions of 0.05 g as compared to 0.1 g in a single exercise. It was observed that with a further increase of mass beyond 0.1 g there was a decrease of percentage Co (II) removed. This could be attributed to the agglomeration of particles resulting in surface area decrease and the fact that the mass and quantity adsorbed is not directly proportional (Changmai et al., 2018).

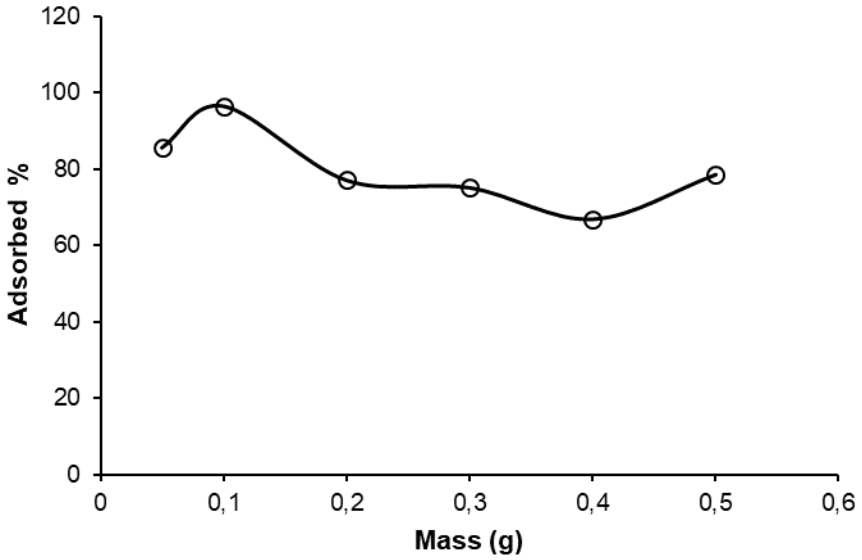

Figure 5-2: Pineapple peels mass as a function of percentage cobalt adsorbance

Effect of concentration and modelling of data

The effect of concentration on the biosorbent character RPP, CTPP, CPP and AC was investigated for Co (II) concentration: 1, 5, 10, 25, 50, 100, and 200 mg/L as described in section 3.5. Results depicted as qe vs concentration (mg/L) are presented in Figure 5-3 where qe refers to the quantity of cobalt ions adsorbed Co (II) in mg/g biosorbed from solution by the biosorbents and is a concentration driven variable. The value of qe for all biosorbents rises as the concentration of Co (II) ions increases. For RPP and AC, the qe peaks at a concentration of 50 mg/L Co (II) and starts to decrease. The plot of qe vs Ce for CTPP only plateaus at 100 mg/L while the qe vs Ce plot for CPP rapidly reaches a maxima at 25 mg/L after which the slope of the curve reduces markedly, without reaching a plateau.

It may be referred from these results that CPP was more effective at removing Co (II) from all treated solutions when compared to RPP, AC and CTPP. The plot also showed that a higher concentration gradient was required to drive CTPP to saturation when compared to CPP (CTPP only reached saturation at 100 mg/L on a much lower gradients curve).

The maximum qe obtained from the plots for RPP, CTPP, CPP and AC were 8.958, 16.731, 22.314, and 6.337 mg/g respectively. The region of the first inflexion of the curve for CPP was taken as the qe_{max} since a saturation point was not reached during experimentation.

The results obtained clearly highlight the importance of treatment, whether chemical or physical on the biosorption character sorption capacity of biomass. This improved in biosorption capacity via chemical and physical treatment has been demonstrated in several studies.

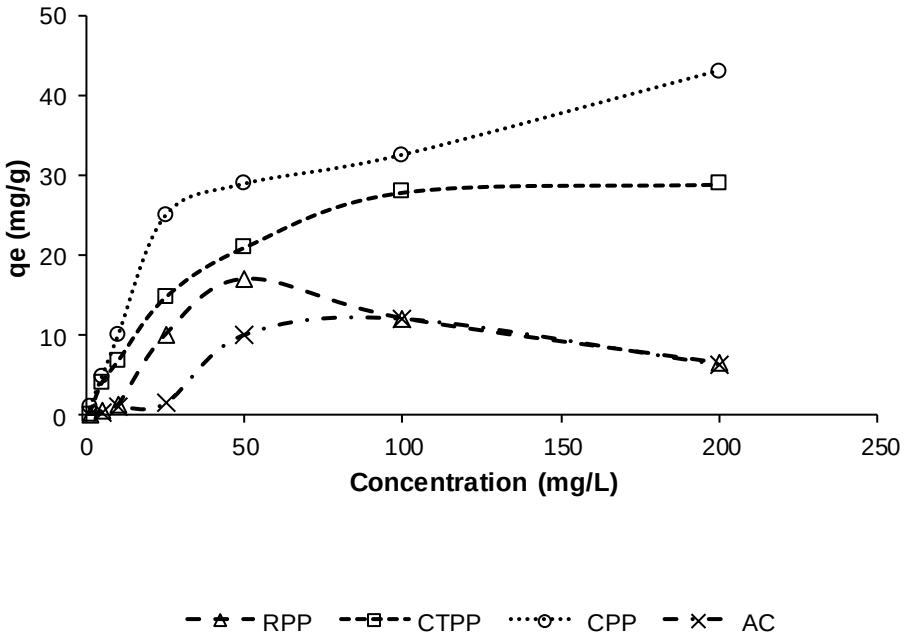

Figure 5-3 Adsorption isotherm for cobalt ions in RPP, CTPP, CPP and AC adsorbent samples

Effect of temperature

The effect of temperature influencing the biosorption of cobalt ions was tested on a pre-set water bath with temperatures of 10 , 20 , 30 , and 40ºC. The effluent from 50 ppm cobalt solution adsorbed with 0.05 g of each sample of bio sorbent, RPP, CTPP, CTCPP and AC. The aim of the thermodynamics study was to determine the influence of the different variations of the biosorbent at the different temperatures on the adsorption rates and capacity. Presented in Figure 5-4 are the experimental illustrations of the variations of pineapple peel adsorbents in a water bath set at temperatures from 10 to 40°C. From the experimental results, it was shown that the different biosorbents reacted differently in different temperatures. The RPP and AC performance seem to decrease with increasing temperature with minimum biosorption at the maximum temperature. For the CTPP a maximum was obtained at 30°C with the lowest value obtained at the highest temperature. Maximum biosorption capacities of 22.069 mg/L on CTPP and 20.44 mg/L on CPP were achieved at 30 and 40°C. The CPP sorbent was the only one showing possible benefits of increasing the temperature as the adsorption capacity doubled from 10°C to 40°C. Hayrunnisa and Kalkan (2012) observed similar trends, achieving maximum adsorption at 30°C. From their observations it was reasoned that the increase of biosorption capacity was due to the permeable nature of the adsorbed that permits the mobility of the cobalt ions in high temperatures.

Ghomri et al. (2013) further described that metal distribution is known as endothermic process and therefore biosorption is deemed favourable in high temperatures. On the contrary study by Bhatnagar et al. (2010) of biosorption of Co (II) using lemon peels showed the biosorption process as exothermic with a decrease of adsorption capacity with the increase in temperature, highest adsorption capacity of 22 mg/g was obtained at 25ºC.

It is clear from literature as well as the results obtained for the experiments conducted that more work is needed to derive more conclusive evidence of the benefits of operations at higher temperatures.

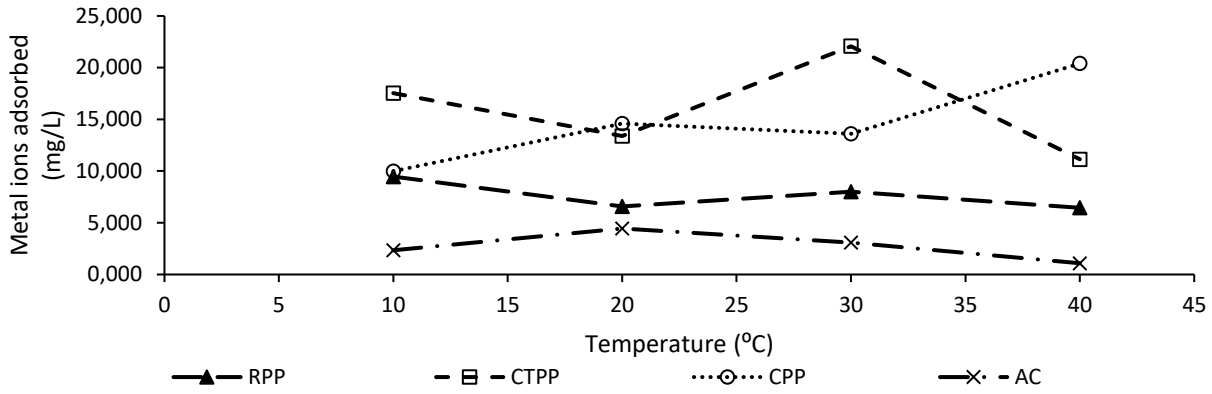

Figure 5-4: Effect of temperature in biosorption of Co (ii) onto RPP, CTPP, CPP and AC.

Thermodynamics parameters

Thermodynamics parameters namely, Gibbs free energy change (ΔGº), enthalpy change (ΔHº) and entropy change (ΔSº) of the biosorption process were applied to further determine the effect of temperature on the adsorption of cobalt ion. The equations were used to determine the parameters:

$$K_c = \frac{CA_e}{C_e}$$ Equation 2-7

$$\Delta G^{\circ} = -RTln(K_C)$$ Equation 2-8

$$\ln(K_c) = \frac{\Delta S}{R} - \frac{\Delta H}{RT}$$ Equation 2-9

$$\log(K_c) = \frac{\Delta S}{2.303R} - \frac{\Delta H}{2.303RT}$$ Equation 2-10

Kc is the equilibrium constant, CAe is the solid-phase concentration at equilibrium (mg/L), and Ce is the concentration at equilibrium. T (K) is the temperature (K) and R molar gas constant of 8.314 J mol¬-¹K-¹.

Figure 5-5 presents Thermodynamic parameters with ln Kc against 1/T. From the slope and intercept obtained the values of ∆H and ∆S were obtained. Table 5-1 presents van't Hoffs plot with the values of (ΔG^o), (ΔH^o) and (ΔS^o) of the biosorption process.

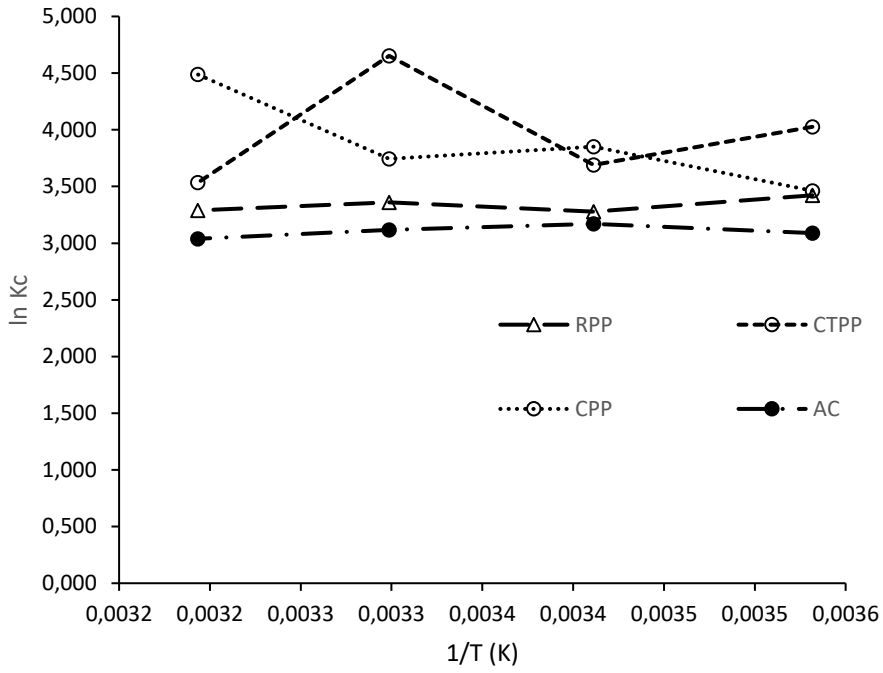

Figure 5-5: Thermodynamics parameters for the adsorption of Cobalt (II) ions on pineapple RPP, CTPP, CPP and AC

Table 5-1: van't Hoff plot for cobalt ion adsorption by pineapple peels.

	∆*G*◦ *(kJ/mol)*				∆H^o	∆*S*	R^2
Biosorbent	**10°**	**20°**	**30°**	**40°**	**(kJ/mol-¹)**	**(kJ/mol-¹)**	**(kJ/mol¹)**
RPP	-8,056	-7,989	-8,465	8,561	0,289	2,3649	0,3922
CTPP	-9,478	-8,993	-11,727	-9,200	0,412	2,5094	0,0147
CPP	-8,150	-9,383	-9,434	-11,000	-2,612	12,66	0,7698
AC	-7,274	-7,726	-7,858	-7,911	0,173	2,5212	0,2125

From the results shown the two carbonised biosorbents showed a negative value of ∆H which indicates that cobalt biosorption on biosorbent is exothermic and therefore indicates that biosorption capacity increases with a decrease in temperature as illustrated in Figure 4.3.2 . The uniform negative values of G show a spontaneous reaction.

Positive values of ∆H indicate an endothermic nature in cobalt biosorption and an increase in biosorption with the increase in temperature. The RPP, CTPP and AC indicated an endothermic nature which corresponds with that of a study by Hayrunnisa and Kalkan (2012) where ∆H and ∆S were 0.145 and -15.07 at 293 K, -15.33 at 298 K and -15.59 at 303 K.

The effect of time

The effect of time is a vital parameter of particle transfer for biosorption as ionic diffusion rates through biomass pores is crucial in determining time taken to reach equilibrium. The effect of time was studied by varying biomass contact time as follows; 0.5,1,3 ,5,10, 20, 30, 45, 60, 90, 120, 180 and 210 minutes at 50 ppm as presented in Figure 5-6. A detailed description of the method is given in Section 3.5.3. Equilibrium was reached at similar times for each different adsorbent. A similar trend was observed on the RPP, CTPP, CCT, CT and AC sample of an increase in the adsorption over time. This was confirmed with the experiment conducted by Changmai et al. (2018).This is due to the availability of a surface area that attract the metals in the initial stage of adsorption. As the equilibrium is reached the active sites are depleted. The overall average equilibrium time reached was 60 minutes. Similar to Khan et al. (2013) in the investigation of biosorption of copper with *citrus sinensis* peels for the purification of drinking water where a variety of concentrations were explored and found that the equilibrium was reached at 60 minutes.

From the basis of the time achieved subsequent experimental parameters were determined.

Samples analysed within the first 30 seconds of contact showed a percentage Co (II) removal of 45%, 21% and 15% for RPP, CTPP, CPP and AC, respectively. This indicated that metal sorption from solution was instantaneous. For RPP and AC, the percentage removal reduced steadily over time as desorption processes become more dominant. Final percentage removed upon equilibration was 26% and 10%, respectively. Conversely, for the treated samples, percentage removal continued to increase reaching a maximum at 41% and 64% for CTPP and CPP respectively. As seen with the results for RPP and AC, desorption of originally sorped metals metal is inevitable which could be observed after 90 minutes. Therefore, 90 minutes was selected as optimal contact time for further experiments.

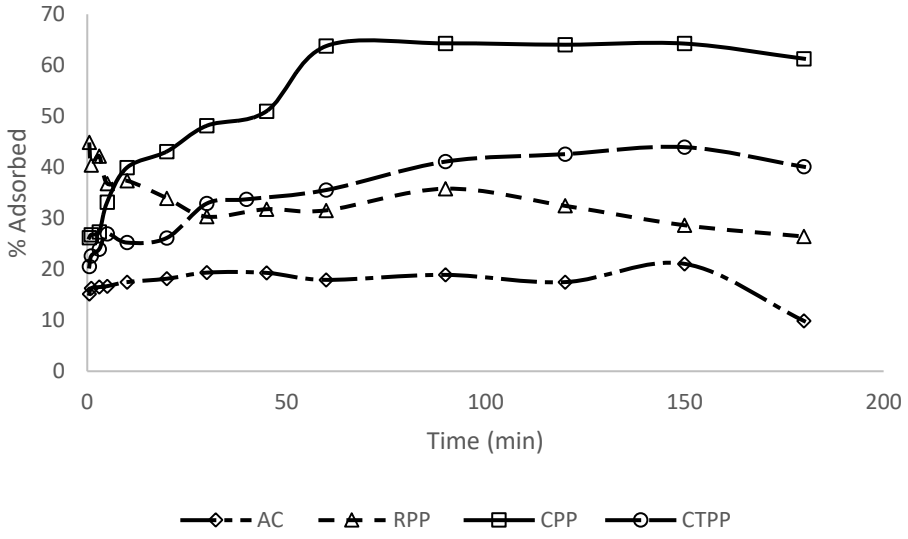

Figure 5-6: Effect of time on different treatments (a) RPP (b) CPP (c) AC (d) CTPP

5.2 Modelling

Isotherm models

The isotherm models are used to explain and describe the biosorption characteristics and performance of the biosorbent. The Langmuir and Freundlich models were used to analyse and illustrate the equilibrium data. The two models are compared, where overall the Langmuir models showed better performance by fitting more suitable on regression. Table 5-2 presents are a summary of biosorption isotherm parameters for cobalt adsorption. The CTPP and CPP gave the best results of 0.9790 and 0.9628 on the Langmuir. According to the experimental results the Langmuir model showed a favourable fitting than that of Freundlich with the highest correlation coefficient of 0.97 achieved with the CCP adsorbent. In a study by Amhad et al. (2013) of where heavy metal adsorption with pineapples peels, the Langmuir model had achieved an accurate correlation coefficient fit in comparison to Freundlich model. From the isotherm model plot the constants of qm and b on Langmuir and n on Freundlich model were derived.

The Langmuir model predictions were slightly higher than the experimental value.

The highest biosorption capacity obtainable on experiment was 22,314 mg/g on CPP.

Table 5-2: Langmuir biosorption isotherm parameters for the adsorption of cobalt ions on RPP, CTPP, CPP and CTCPP.

Biosorbent	r^2	q_m	q_{mb}	b	q_{max}
RPP	0,7605	4,9	0,178	0,036327	8,958
CTPP	0,5986	22,124	0,499	0,022555	16,731
CPP	0,9628	20,877	3,995	0,191359	22,314
AC	0,3886				14,73

Table 5-3 : Freundlich model isotherm parameters for the adsorption of cobalt ions on RPP, CTPP, CPP and CTCPP.

Biosorbent	r^2	*Log* k_f	n	k_f	m
RPP	0,7296	-0,799	1,220107	0,15885467	0,8196
CTPP	0,6773	-0,0496	1,467782	0,89207219	0,6813
CPP	0,449	0,6181	3,183699	4,150496	0,3141
AC		0			

Kinetic modelling

Biosorption kinetics were performed in order to understand the mechanism of biosorption of Co (II) ions in pineapple peels in aqueous solution, accordance to the contact time of the adsorbate on the biosorbent. The study of kinetics entails an application of mathematical models namely; the pseudo first, second order models and intra particle diffusion. In order to explain the mechanism of biosorption there must be a good establishment of kinetic data. The model is efficient in the analysis mechanism of mass transfer and chemical reaction. The pseudo first order is limited to within the first few minutes and was applied only to kinetic data obtained with the first few minutes and was applied only to kinetic data obtained with the first 30 minutes for all samples. The pseudo second order model is based is based on the assumption that the adsorption rate is proportional to the square of the number of unoccupied sites. The intra-particle diffusion described the internal diffusion within the particles in from surface to the pores.

The rate constants were calculated from the linear graph of the slope and intercept. Figure 5-8 to Figure 5-9 illustrates the pseudo first and second model kinetics as well as intra-particle diffusion on RPP, CTPP, CPP, and AC.

Pseudo-second order was perceived as the best suitable fit with a regression of 0,984, 0.999, 0.992 and 0.998 for RPP, CTPP, CPP, and AC, respectively. The results obtained agree with those of Bhatnagar et al. (2015) who also found in the study of adsorption of cobalt with lemon peels the pseudo second order fit best.

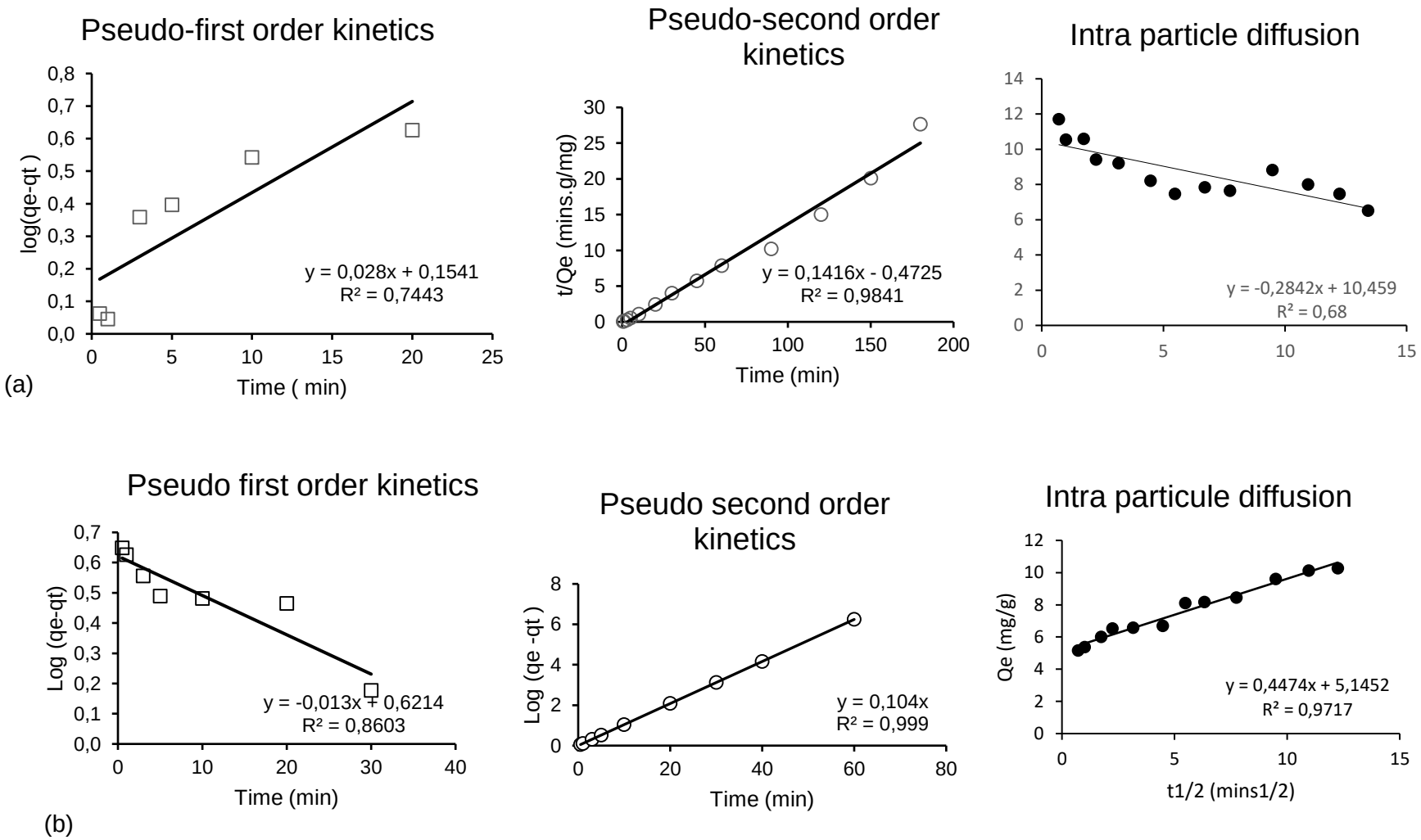

Figure 5-8 Kinetic modelling – pseudo first order, pseudo second order and intra particle diffusion for (a) RPP and (b) CTPP

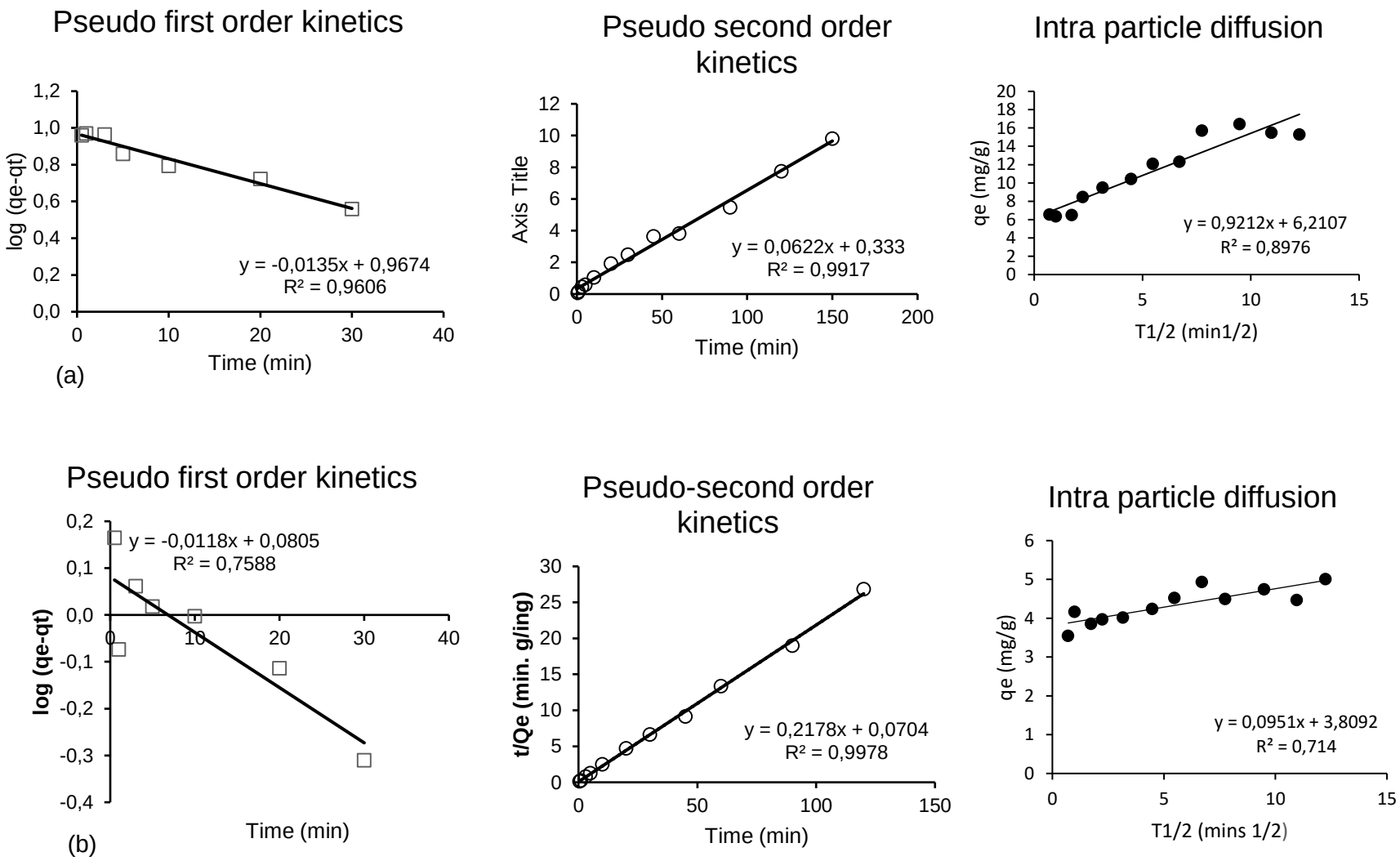

Figure 5-9 Kinetic modelling pseudo first order, pseudo second order and intra particle diffusion for (a) CPP and (b) AC

Conclusion

Maximum biosorption was achieved on the lowest masses of biosorbent of 0.05 g and 0.1 g. With increase in mass there was a decrease in the percentage removed due to agglomeration of particles resulting in less surface area. Optimum biosorption was obtained between pH 5 and 6. At low pH cobalt ions completed in occupying available sites in biosorbent surface area and thus resulted in low adsorption. Initially with the increase in pH there was an increase in biosorption, however after pH 6 there was precipitation.

In biosorption isotherms, Langmuir was found fitting best for the kinetic study the data was model best with a pseudo second order fit. The highest adsorption between the biosorbent was that of the CPP with 22.314 mg/g better than that of the RPP with 8.958 mg/g. From the results obtained carbonisation was found effective in biosorption. From the basis of the results the CPP was thus used for the column studies which are presented in the next chapter. Data sets for batch studies and kinetic modelling are presented in Appendix A and Appendix B, respectively.

6 Column studies

6.1 Introduction

Fixed bed studies were conducted using CPP, which was selected for column work, based on its performance in batch studies. The effect of mass (bed height), flow rate, and cobalt metal solution concentration on the CPP performance in a fixed bed column system were evaluated using prepared cobalt nitrate solutions. The CPP was then also applied to cobalt-containing real industrial wastewater in the same column system.

To analyse the performance of the biosorption process in the fixed bed column, four-response factors were evaluated namely; the breakpoint time of the biosorbent (tb), fractional bed utilisation (FBU), saturation time (ts) and the volume of effluent treated per gram CPP (Vs) for three bed heights, three flow rates and three concentrations.

To describe the biosorption performance in the fixed-bed column, three mathematical models were evaluated namely the Bohart-Adams model, the Thomas model and the Yoon-Nelson model. The models were applied to industrial wastewater to determine which model fits best.

6.2 Optimisation of column parameters

This section presents the effect of mass, flowrate, and concentration on the quantity adsorbed at breakpoint (qb), the quantity at saturation (qs) and ts, tb, Vs and FBU. The column parameters were evaluated, and the response factors are summarised in Table 6-1, which highlights the optimum conditions for maximum uptake at saturation by the biosorbent.

Table 6-1: **Cobalt adsorption experimental performance summary**

Biosorbent	***Experimental conditions***			***Response factors***					
Sample	Ci (mg/L)	W (g)	Q (ml/min)	tb (min)	ts (min)	Vs (ml/g)	qb (mg/g)	qs (mg/g)	FBU
0,5 g	42,17	0,503	3	4	31	5,20	0,255	1,973	0,129
1 g	40,05	1,006	3	10	52	17,44	1,209	6,285	0,192
1,5 g	40,62	1,503	3	21	75	37,58	3,846	13,737	0,280
1ml/min	41,57	1,005	1	40	170	170,85	1,671	7,102	0,235
3ml/min	43,9	1,004	3	27	117	39,16	3,570	15,471	0,231
5ml/min	40,05	1,006	5	7	55	11,07	1,410	11,080	0,127
10 ppm	10,15	1,001	5	20	150	30,03	1,016	7,620	0,133
25 ppm	24,41	1,009	5	15	130	26,23	1,847	16,009	0,115
50 ppm	40,05	1,006	5	8	42	8,45	1,612	8,461	0,190
Wastewater	16,34	1,009	5	20	100	20,18	1,649	8,244	0,200

Effect of mass

Presented in Figure 6-1 are breakthrough curves of three masses ; 0.5, 1.0 and 1.5 g used to determine the effect of mass at a pH of 5, a concentration of 40 ppm and a flow rate of 3 ml/min. A significant pattern is distinguished on the breakthrough curves showing that the breakpoint time increase with increasing mass. Similarly, the saturation time increase with increasing mass. For the mass of biosorbent of 0.5 g, the break time and saturation time was 4 and 31 minutes, respectively. For 1.0 g, the breakpoint and saturation time was achieved at 10 and 52 minutes, respectively, and for 1.5 g, the breakpoint and saturation time were achieved at 21 and 75 minutes, respectively. The quantity of cobalt adsorbed at saturation point (qs) also increased with increasing mass of biosorbent. This work is in agreement with that of Anon (2012) who reported adsorption performance of a packed bed column using oil palm fibre for the removal of lead (II). They reported that with lower masses saturation is faster and further argued that an increase of

adsorption capacity is due to an increase in binding sites with larger adsorbent surface area and greater contact time.

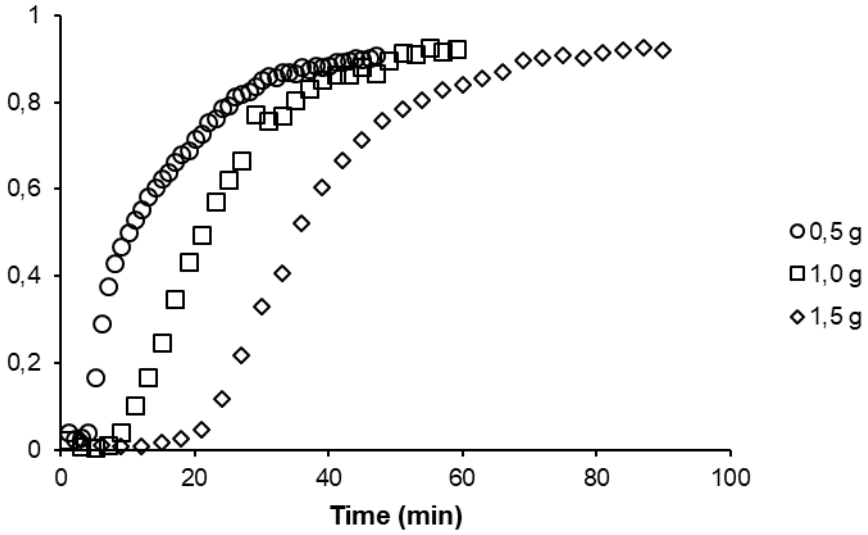

Figure 6-1 : Effect of mass on adsorption of Co (II) onto CPP

Effect of flow rate

Presented in Figure 6-2 are the breakthrough curves of flow rates of 1, 3 and 5 ml/min on 1.0 g of CPP. The breakthrough curve illustrates that the breakpoint and the saturation time decrease with increasing flow rate. The breakpoint time at 1, 3 and 5 ml was achieved at 40, 27 and 7 minutes, respectively and saturation time at 170, 117 and 55 minutes, respectively. The findings are in good agreement with those of de Franco et.al (2017) who also concluded that sharper breakthrough curves were observed with a slower flow rate as the modification of flow rate had a great influence on breakthrough and saturation time in the removal of Fe^{3+} in fixed-bed column studies. Sabourian et al. (2016) also reported that the breakthrough time is shorter for higher flow rates due to the effluent passing too quickly, which allowed for less contact time with the biosorbent.

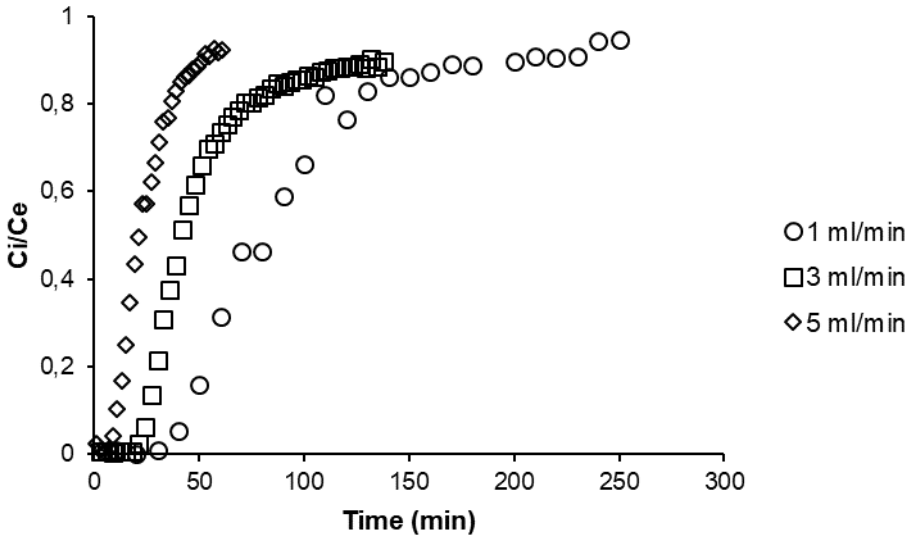

Figure 6-2: Effect of flow rate on adsorption of Co (II) onto CPP

Effect of concentration

Figure 6-3 showed the breakthrough curves for Co (II) solutions at concentrations of 10, 25 and 50 ppm. The breaking points were at 20, 15 and 8 minutes, respectively and saturation points at 150,130 and 42 minutes for concentrations of 10, 25 and 50 ppm, respectively. The breakthrough curves depict that the higher the concentration, the faster the breaking point time and maximum biosorption attainable, contrary to lower concentrations. The finding was in agreement with those of Sulaymon et al. (2009) who reasoned that with higher concentrations the steepness of the breakthrough is due to the equilibrium obtained faster. The study by de Franco et al. (2017) confirmed that the steepness is due to the available sites been occupied faster, and that the increase of the concentration is directly proportional to the FBU.

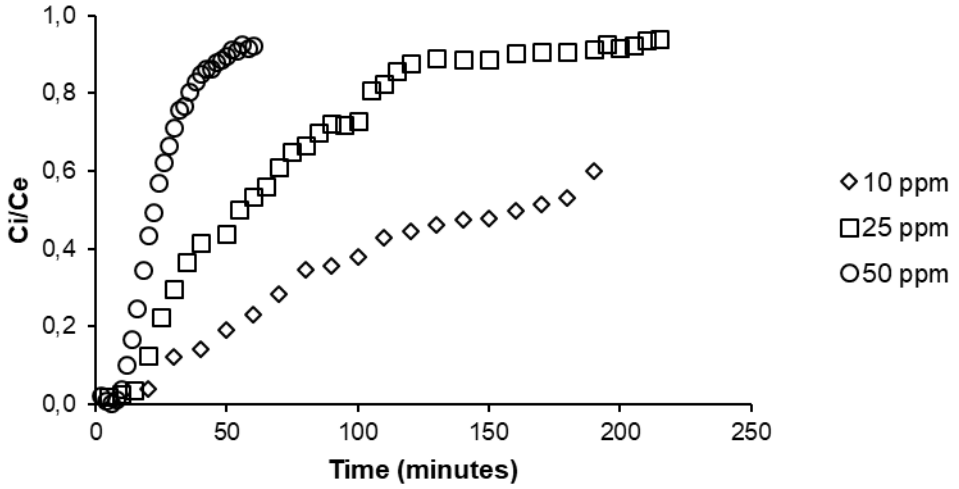

Figure 6-3 : Effect of concentration on adsorption of Co (II) onto CPP

6.3 Fixed bed kinetic modelling

Developed fixed bed models were used to determine and describe the breakthrough and saturation curves using non-linear regression. The models used were Bohart-Adams, Thomas, and Yoon-Nelson. The linearised data from the breakthrough curves are presented in Figure 6-4 From these plots, the bed height performance coefficients are determined. The model performance is evaluated using the regression coefficient R^2. The Bohart-Adam coefficient is expressed by K_{BA} (min/mg) and the quantity biosorbed is expressed by q_{BA} (mg/g). The Thomas model coefficient is expressed as K_{TH} and the quantity adsorbed as $qe_{TH..}$The Yoon-Nelson model was used in a linear plot to describe the performance of the different mass on fixed model. From the linear plot Ct/ (Co – Ct) versus volume, the value of k_{YN} was obtained as shown in Equation 2-1.

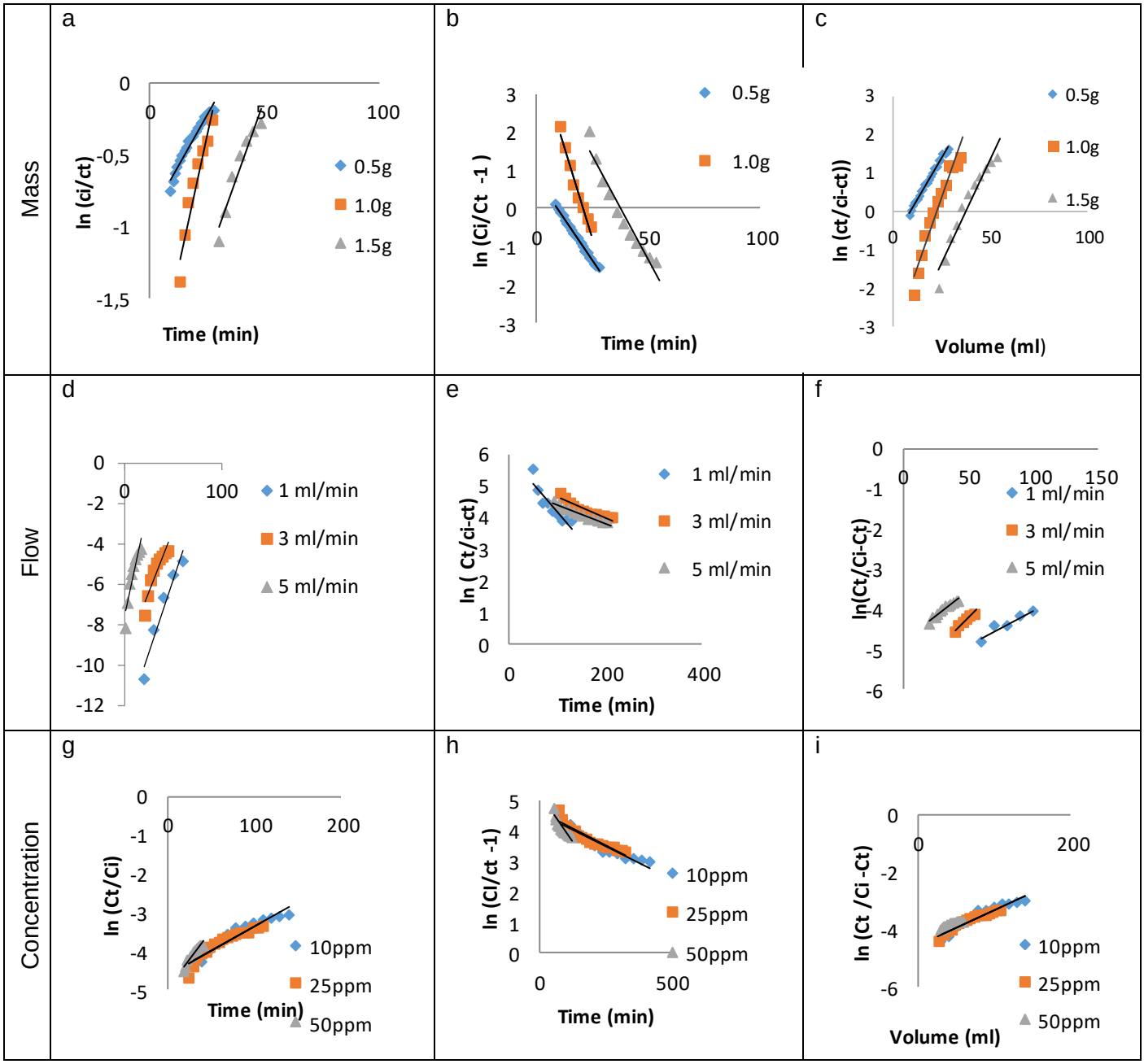

a) Bohart-Adam **b) Thomas** **c) Yoon-Nelson**

Figure 6-4: Modelling the effect of mass a) Bohart- Adams (b) Thomas (c) Yoon-Nelson
Modelling the effect of flow d) Bohart-Adam (e) Thomas (f) Yoon-Nelson
Modelling the effect of concentration g) Bohart- Adam (h) Thomas (i) Yoon-Nelson

Modelling of data for effect of mass on column biosorption

The regression coefficients for all three models are presented in Table 6-2 for modelling the effect of mass in the column system. The highest regression coefficient was found for the low mass (0.5g) in comparison with the higher masses. Regression coefficients of 0.961, 0.996 and 0.995 for Bohart-Adams, Thomas and Yoon-Nelson, respectively were obtained on 0.5g.

In comparison of the models the Yoon-Nelson regression coefficients showed better compliance. The regression showed to fit perfectly well with regression of 0.996, 0.9485 and 0.9446 with 0.5, 1.0 and 1.5 g, respectively. This confirmed the findings of de Franco (2017) who overall found the model the best performing. The basis of which the model was founded was confirmed, which was formulated to eliminate any errors from the Thomas model. The correlations obtained from the plots in Figure 6-5 are presented in Table 6-2 and used to determine the adsorption coefficients for each of the models.

For the Bohart-Adam model coefficient, K_{BA} determined from equation in Table 6-2. K_{BA} for mass 0.5, 1.0, and 1.5 g was 0.676, 1.967, and 1.132 x 10^{-3} l/min.mg, respectively and the quantity biosorbed, N_o, was 660793, 913517, and 389698 mg/l, respectively.

Presented in Figure 6-4 b, e and h are the linear plots of Thomas model from where the constant K_{TH} (Thomas model) obtained was 10.46, 5.38 and 13.53 ml/mg .min in mass variation . The quantity adsorbed obtained was 0.76, 3.32, and 1.02 mg/g, for the three tested masses .This was in agreement with the findings of Chowdhury et al., (2013) who confirmed that with the increase in mass the K_{TH} and q_{TH} value increased.

The adsorption coefficient for the Yoon-Nelson model constant, K_{YN} for mass obtained were as follows; 0.0873, 0.1449 and 0.0921 l/min. In a study by Singh, Sehgal and Mehta (2015) the value of K_{YN} decreased with the increase of mass, with K_{YN} value ranging from 0.062, 0.025 and 0.018 l/min on 7.5,15 and 22.5 mg/g, respectively. The trend was contrary to Chowdhury et al., (2013) finding where the k_{YN} value increased with the increase in mass. In bed height of 3 and 4 cm the k_{YN} increased from 0.023 to 0.043.

Table 6-2: Summary of regression coefficients for models for mass variation

Mass (g)	Bohart - Adams equation	R^2	Thomas model equation	R^2	Yoon-Nelson equation	R^2
0.5	y = 0.0285x -0.9305	0.961	y= -0.0882x + 0.8466	0.996	y= 0.0873x - 0.8325	0.995
1.0	y = 0.0788x -2.5106	0.931	y= -0.043x + 3.5905	0.815	y= 0.1419x - 3.3797	0.953
1.5	y = 0.046x - 2.392	0.932	y= -0.1099x + 4.1464	0.945	y = 0.0921x -3.1223	0.953

Modelling of data for effect of flow rate on column biosorption

Presented in Table 6-3 are the regression coefficients for flow rates of 1, 3 and 5 ml/min. The linearised plots are shown in Figure 6-4d to Figure 6-4f. The best regression fit was for higher flow rates with 0.9616, 0.9926 and 0.9764, respectively on 1, 3 and 5ml/min flow rate, respectively.

The model with best fitting regression was that of Thomas with a regression of 0.9315, 0.9491 and 0.9926, respectively.

Table 6-3 Summary of regression coefficients for models for flow variation

Flow ml/s	Bohart-Adams equation	R^2	Thomas equation	R^2	Yoon-Nelson equation	R^2
1	y = 0.0291x – 3.318	0.7876	y = -0.0384x + 3.172	0.9315	y= 0.0576x -4.833	0.8766
3	y = 0.008x – 0.8096	0.9144	y = -0.017x + 2.1064	0.9491	y= 0.0904x-4.2667	0.8659
5	y = -0.0263 - 1.1651	0.9616	y = -0.0179x + 1.894	0.9926	y = 0.0739x -1.4304	0.9764

The Bohart-Adams coefficient (k_{BA}) obtained was 0.463, 0.459 and 0.734, respectively. The quantity adsorbed was 54486.4, 129840 and 304830 mg/l.

The Thomas coefficient (K_{TH}) obtained was 0.9237, 1.1617 and 2.2347 on 1, 3 and 5 ml/s. The quantity adsorbed was 24.3876, 4.10176 and 2.6255 mg/g. The findings were contrary with those of Nwabanne (2012) where adsorption capacity increased with increase in flow rate as follows; 3.928, 4.983 and 6.39 mg/g on flow rate of 5, 7.5 and 10 ml/min.

The Yoon-Nelson coefficient achieved was 0.0576, 0.0904 and 0.0739.

Modelling of data for effect of concentration on column biosorption

Presented in Table 6-4 is the summary of linear regression correlations plot of concentrations of cobalt at 10, 25, and 50 ppm. The best-fit regression achieved was on higher concentrations as follows; 0.9091 ,0.9803 and 0.9563 in 50 ppm for Bohart-Adams, Thomas and Yoon-Nelson model, respectively.

As with the mass regression coefficient the Yoon-Nelson model achieved best fit with 0.9628, 0.9325 and 0.9563 shown in Table 6-4.

Table 6-4: Summary of regression co-efficient for models for concentration variation

Conc ppm	Bohart - Adams equation	R^2	Thomas model equation	R^2	Yoon-Nelson equation	R^2
10	0.0047x – 1.5589	0.8626	y = 0.0016x – 3.8482	0.8701	y = 0.0108x -1.873	0.9628
25	0.0112x – 1.2881	0.939	y = 0.0113x -1.9102	0.0.9462	y = 0.0294x -1.7481	0.9325
50	0.0294x – 1.2917	0.9091	y = -0.0335x +2.2159	0.9803	y = 0.0524x – 0.480	0.9563

The Bohart-Adams coefficient were 0.463, 0.459 and 0.734 min/mg with No of 54486.4 ,129840 and 340830 mg/g respectively. In Chowdhury et al., (2013) study The k_{BA} decreased with the increased in concentration. The k_{BA} obtained was 1.80, 1.29 and 1.20 $x^{10\text{-}4}$ l/mg.min in concentration of 50, 70 and 100 mg/L.

The Thomas coefficient (K_{TH}) achieved was 0.7881, 2.3146 and 4.1822 ml/min/mg and the quantity adsorbed was 24.3876, 4.1017 and 2.6255 mg/g. This was confirmed by Han (2009) whose results showed that the higher the concentration the lesser the kTH value but higher the qe. At 30 and 50 ppm the k value was 75, 7 and 69.4 with q_{TH} of 135 and 141 mg/g, respectively.

The Yoon-Nelson constant (K_{YN}) increased with the increase in concentration from 0.0108, 0.0294 and 0.0524 for the concentration of 10, 25 and 50 ppm, respectively. This was in agreement with Chowdhury et al., (2013) whose K_{YN} increased from 0.016 ,0.017 ,0.024 with concentration of 50,70 and 100 mg/l, consecutively. This was in agreement with results from Chowdhury et al., (2013) whose K_{YN} value increased from 0.016 ,0.017 and 0.024 l/min in concentrations of 50 ,70 and 100 mg/l respectively.

Presented in Table 6-5 is a summary of the Bohart-Adams, Thomas and Yoon-Nelson model parameters evaluated for the same experimental conditions. The experimental adsorption capacity of the cobalt is compared with the one achieved from the models.

It was observed that both the adsorption capacity of the actual experiment and the Thomas adsorption capacity of cobalt increases with the increase in mass. The Thomas prediction was lower than the actual experiment. The Thomas adsorption capacity was that of 0.7637, 3.3165 and 1.0196 whilst the actual experiment obtained was 1.973, 6.285 and 13.737 mg/g. This is due to the increase of available surface area available for biosorption. Overall the maximum quantity of Thomas predicted was 24.3876 and 16.009 mg/g of the experimental, respectively.

With the increase in concentration, a decrease on the quantity adsorbed was observed for Thomas model prediction. The adsorption quantity adsorbed was 24.3876, 4.1017 and 2.625 mg/g. The actual experiment was 7.62, 16.009 and 8.461 on 10, 25 and 50 mg/g respectively.

On a study by Saudi, Reyhanne and Fazaeli (2013) where the focus was on adsorption of Pb (ii) by using nano structured y-alumina upon evaluation of Bohart-Adams model it was also found that the adsorption capacity increased with the increase rate and concentration.

The constant of Bohart and Thomas both increased with the increase in flow rate. Bohart constant increased form 0.70, 0.182 and 0.657 on 1, 3 and 5 ml/min respectively. The Thomas constant increased from 0.9237,1.16173 and 2.2347 mg/g.

Overall the optimum constant obtained on Bohart, Thomas and Yoon were 1.967 (mass - 1.0g), 13,527 (mass - 1.5g) and 0.1419 (mass - 1.0g) respectively.

Table 6-5 Summary of mathematical modelling adsorption performance

Experimental conditions			***Bohart model***			***Thomas model***			***Yoon-Nelson model***		***Experimental***
Co	W	Qexp	K_{BA} 10^{-3}	No	R^2	K_{TH}	q_{TH}	R^2	K_{YN}	R^2	qs
(mg/l)	(g)	(Ml/min)	(ml/min.mg)	(mg/l)		ml/min.mg	mg/g		l/mg		mg/g
42.17	0.503	3	0.676	660793	0.9614	10.4576	0.7637	0.9961	0.0873	0.9959	3.288
40.05	1.006	3	1.967	913517	0.9313	5.3807	3.3165	0.8151	0.1419	0.9529	10.475
40.62	1.503	3	1.132	389698	0.9319	13.5278	1.0196	0.9446	0.0921	0.9526	22.894
41.57	1.005	1	0.700	67470	0.7876	0.9237	3.416	0.9491	0.0576	0.8766	7.102
43.9	1.004	3	0.182	55645	0.9144	1.16173	5.4177	0.9926	0.0904	0.8659	15.471
40.05	1.006	5	0.657	304892	0.9616	2.2347	4.2124	0.8766	0.0739	0.9764	11.080
10.15	1.001	5	0.463	54486	0.8626	0.7882	24.3876	0.8701	0.0108	0.9628	7.620
24.41	1.009	5	0.459	129840	0.9390	2.3146	4.1017	0.9462	0.0294	0.9325	16.009
40.05	1.006	5	0.734	340830	0.9091	4.1822	2.6255	0.9803	0.0524	0.9563	8.4610

6.4 Application of biosorbent in textile industrial wastewater

Fixed bed column study was conducted using 1g of CPP on industrial wastewater with Co (II) at a concentration of 16 mg/L and flow rate of 3 ml/min. **Figure 6-5** shows the breakthrough curve obtained for the wastewater. The breakpoint and saturation point were at 20 and 100 minutes, respectively. The quantity adsorbed at breakpoint and saturation point was 1.649 and 8.244 mg/g respectively.

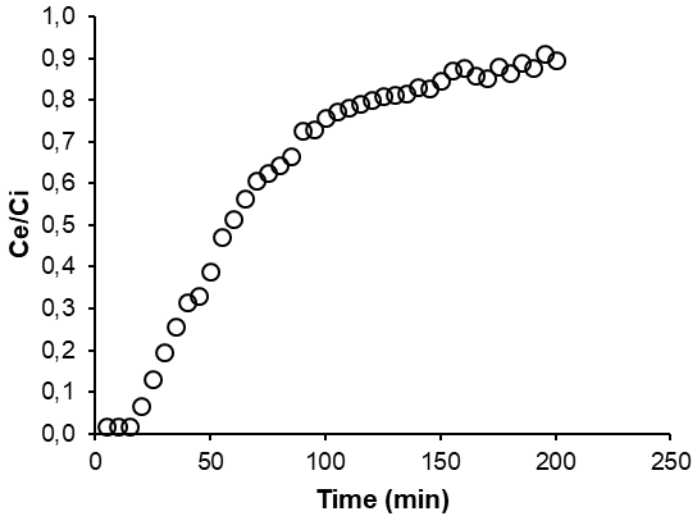

Figure 6-5 Adsorption of Co (II) from wastewater.

Modelling on industrial wastewater

Developed mathematical models based on modelling data from Section 6.3were fitted in the textile industrial wastewater to determine which model best predicts the fixed bed experimental data. The models used were Bohart-Adams, Thomas and Yoon-Nelson. The wastewater conditions were 3 ml/min,16 ppm and 1 g for flow rate concentration and mass, respectively. The model parameters applied were 3 ml/min, 25 ppm and 1 g. been closest to those of the wastewater. The model's results are plotted with the wastewater results and presented in Figure 6-6. In comparison with the models of Bohart-Adams and Yoon-Nelson. The Thomas model showed a better fit with the wastewater experimental results. The findings are in agreement with those of Andrea et al.. (2017).

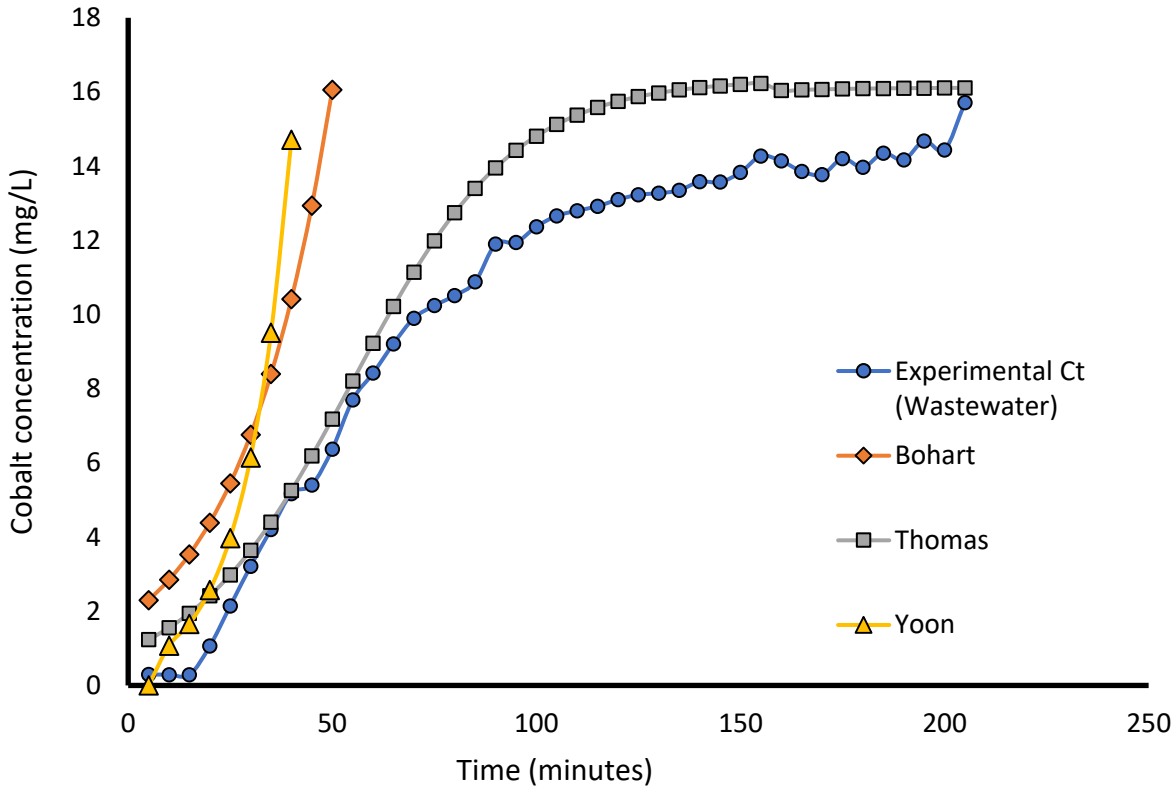

Figure 6-6 Breakthrough curves of cobalt adsorption onto carbonised pineapple peels in fixed bed column

6.5 Conclusion

The maximum biosorption obtained from all the experiments conducted was 16.00 mg/g taken from the 25 ppm concentration.

The results of the column studies showed that the performance of the biosorbent is influenced by the parameters evaluated; mass used, flow rate applied and cobalt ion concentration.

The effect of mass was determined in 0.5, 1.0 and 1.5g, respectively. The biosorption capacity increased with the increase in mass. Maximum adsorption was obtained at 1.5g was 13.737.

The effect of flow rate was tested in 1, 3 and 5ml/min, respectively. Maximum adsorption was obtained at 3 ml/min with 15.471 ml/min. The adsorption capacity initially increased then dropped at 5ml/min.

The effect of concentration was varied at 10, 25 and 50 ppm, respectively. Maximum biosorption was achieved at 25 ppm with 16.009 mg/g. An initial increase in biosorption capacity was observed on initial concentration followed by a sudden decrease.

Developed fixed bed model of Bohart-Adams, Thomas and Yoon-Nelson model applied were compared. The data obtained was linearised and the regression indicated the suitability of the model on the data. This proved that it was aimed to improve the mathematical errors.

The performance of the fixed bed column on the models was favoured by the Yoon-Nelson model. The Thomas model had predicted a maximum adsorption of 24.3876 however the actual experimental quantity biosorbed was 16.009 mg/g.

The biosorbent was successfully applied on industrial wastewater with a maximum removal of 8.244 mg/g from an initial concentration of 16.34 mg/g.

Data on the column studies are presented in Appendix C, while the modelling data is presented as a separate excel file along with this document.

7 Conclusions and recommendations

7.1 Introduction

The aim of this work was to investigate the application of pristine and modified biomass prepared from pineapple peels for the biosorption of Co (II) in batch and column mode. The best performing biosorbent was found and the biosorbent was subsequently applied to industrial wastewater in continuous mode.

This chapter presents the outcome and the conclusions of the experimental work and recommendations for future research work.

7.2 Summary of results

Pineapple peels were chemically treated with H_2SO_4 and KM_NO_4 to give chemically modified pineapple peels (CTPP). Raw pine apple peels were physically treated by carbonising in nitrogen at 600 ºC to give carbonised pineapple peels (CPP). Biosorbents were characterised using SEM, FTIR and BET. The efficiency of chemical treatment and carbonisation was evaluated by subjecting biomaterial to comparative biosorption experiments. The biosorption capacities at equilibrium were; 8.959 mg/g, 16.731 mg/g, 22.314 mg/g, and 6.337 mg/g for RPP, CTPP, CPP and AC, respectively.

For batch experiments, the operating variables were investigated and the best operating condition for biosorbent mass and pH was 0.05 g and pH 6, respectively. Adsorption data was analysed and quantified through isotherms and found that equilibrium data was better described by the Freundlich isotherm model ($R^2 \approx 0.99$). From kinetic studies, adsorption was found rapid, reaching maxima at 60 minutes, and finally equilibrating at 90 minutes. Batch kinetic data were in agreement with the pseudo-second order model. In thermodynamics the entropy change, standard enthalpy changes and standard free energy was determined. Carbonised samples displayed exothermic character while adsorption on non-carbonised samples was endothermic. Carbonised biomass (CPP) was applied to column studies based on its comparative behaviour in batch experiments. Column biosorption data was subjected to mathematical modelling with Yoo-Nelson model give the best fit.

7.3 Conclusion

In conclusion it was found that biomass prepared from pineapple peels were suitable for the biosorptive removal of cobalt ions from aqueous solution and gave better results in comparison to the commercial activated carbon used for control. It was found that carbonisation gave better results in adsorption capacity and also the colour of the treated water after adsorption was much cleaner and clearer with the CPP sample. Based on the data obtained the biomass was successfully applied to the industrial textile water with Co (II) concentration of 16.34 mg/g.
Upon the basis of the results of the pineapple peels, which are vegetable wastes from retail shops, it may be concluded that pineapple peels can be regarded as a useful biosorbent for removal of Co (II) and thus proposed as a suitable candidate for a green approach to water treatment in industries. Results shown prove that upscaling is possible for industrial use in continuous system.

7.4 Recommendations for further research

A number of studies have been pursued to determine the efficacy of heavy metal removal by biosorbents and it has been argued that the next step should be in planning and installing on site industrial size columns. The research work to be done towards this recommendation would require a pilot plant study which includes costing and implementation to determine industrial feasibility of the process.

Pertaining to waste management, it is recommended that waste separation should be done on site in order to obtain suitable biomass that may be applied for remediation of metal contaminated water. These biomaterial waste may then be transported to treatment sites and subsequently to the pilot plants/industries.

It is also recommended that two additional modifications of the RPP to be pursued which are combining both the chemical treatment and carbonisation. One sample should first be chemically treated and then carbonised. The second sample should be first carbonised and then chemically treated in order to determine the order which will give better results.

8 References

Abbas, M, Kaddour, S. & Trari, M. 2014. Journal of Industrial and Engineering Chemistry Kinetic and equilibrium studies of cobalt adsorption on apricot stone activated carbon. *Journal of Industrial and Engineering Chemistry*, 20(3): 745–751. http://dx.doi.org/10.1016/j.jiec.2013.06.030.

Abbas, M., Kaddour, S. & Trari, M. 2014. Kinetic and equilibrium studies of cobalt adsorption on apricot stone activated carbon. *Journal of Industrial and Engineering Chemistry*, 20(3): 745–751. http://dx.doi.org/10.1016/j.jiec.2013.06.030.

Ahmad, A., Khatoon, A., Mohd-Setapar, S.H., Kumar, R. & Rafatullah, M. 2016. Chemically oxidized pineapple fruit peel for the biosorption of heavy metals from aqueous solutions. *Desalination and Water Treatment*, 57(14): 6432–6442.

Amin, M.T., Alazba, A.A. & Shafiq, M. 2017. Batch and fixed-bed column studies for the biosorption of Cu(II) and Pb(II) by raw and treated date palm leaves and orange peel. *Global Nest Journal*, 19(3): 464–478.

Andrea, M., Franco, E. De, Carvalho, C.B. De, Bonetto, M.M., Soares, R.D.P. & F, L.A. 2017. Removal of amoxicillin from water by adsorption onto activated carbon in batch process and fi xed bed column : Kinetics , isotherms , experimental design and breakthrough curves modelling. , 161.

Anon. 2012. Adsorption Performance of Packed Bed Column for the removal of Lead (ii) using oil Palm Fibre. , 2(5): 106–115.

Anon. Yoon -Nelson model.

Arief, V.O., Trilestari, K., Sunarso, J., Indraswati, N. & Ismadji, S. 2008. Recent progress on biosorption of heavy metals from liquids using low cost biosorbents: Characterization, biosorption parameters and mechanism studies. *Clean - Soil, Air, Water*, 36(12): 937–962.

Arina, D. & Orupe, A. 2012. Characteristics of mechanically sorted municipal wastes and their suitability for production of refuse derived fuel. *Environmental and Climate Technologies*, 8(1): 18–23.

Ayeleru, O.O., Ntuli, F. & Mbohwa, C. 2016. Of fruits and vegetables wastes in the City of Johannesburg. *Lecture Notes in Engineering and Computer Science*, 2226: 659–663.

Barton, J.R., Dalley, D. & Patel, V.S. 1996. Life cycle assessment for waste management. *Waste Management*, 16(1–3): 35–50.

Bedia, J., Peñas-Garzón, M., Gómez-Avilés, A., Rodriguez, J. & Belver, C. 2018. A Review on the Synthesis and Characterization of Biomass-Derived Carbons for Adsorption of Emerging Contaminants from Water. *C*, 4(4): 63.

Bharat, S. & Manchanda, D. 2017. Efficient bio adsorbents for removal of heavy metals from water : A review. , 5(4): 1691–1694.

Bhatnagar, A., Minocha, A.K. & Sillanpää, M. 2010. Adsorptive removal of cobalt from aqueous solution by utilizing lemon peel as biosorbent. *Biochemical Engineering Journal*, 48(2): 181–186.

Bhatnagar, A., Sillanpää, M. & Witek-Krowiak, A. 2015. Agricultural waste peels as versatile biomass for water purification - A review. *Chemical Engineering Journal*, 270: 244–271. http://dx.doi.org/10.1016/j.cej.2015.01.135.

Boddu, V.M., Abburi, K., Talbott, J.L., Smith, E.D. & Haasch, R. 2008. Removal of arsenic (III) and arsenic (V) from aqueous medium using chitosan-coated biosorbent. , 42: 633–642.

Cape, G. 2015. Market Intelligence Report: RE. , (November 2012): 1–11.

Changmai, M., Banerjee, P., Nahar, K. & Purkait, M.K. 2018. A novel adsorbent from carrot, tomato and polyethylene terephthalate waste as a potential adsorbent for Co (II) from aqueous solution: Kinetic and equilibrium studies. *Journal of Environmental Chemical Engineering*, 6(1): 246–257. https://doi.org/10.1016/j.jece.2017.12.009.

Chowdhury, Z.Z., Zain, S.M., Rashid, A.K., Ra, R. & Khalid, K. 2013. Breakthrough Curve Analysis for Column Dynamics Sorption of Mn (II) Ions from Wastewater by Using Mangostana garcinia Peel-Based Granular-Activated Carbon. , 2013(Ii).

Chu, K.H., Feng, X., Kim, E.Y. & Hung, Y.-T. 2011. Biosorption Parameter Estimation with Genetic Algorithm. *Water*, 3(1): 177–195.

Dlamini, S., Simatele, M.D. & Serge Kubanza, N. 2019. Municipal solid waste management in South Africa: from waste to energy recovery through waste-to-energy technologies in Johannesburg. *Local Environment*, 24(3): 249–257.

de Franco, M.A.E., de Carvalho, C.B., Bonetto, M.M., Soares, R. de P. & Féris, L.A. 2017. Removal of amoxicillin from water by adsorption onto activated carbon in batch process and fixed bed column: Kinetics, isotherms, experimental design and breakthrough curves modelling. *Journal of Cleaner Production*, 161: 947–956.

G.N. Tiwari, Vimal Dimri & Chel, A. 2009. Parametric study of an active and passive solar distillation. , (September 2015).

Ghomri, F., Lahsini, A., Laajeb, A. & Addaou, A. 2013. The removal of metal ions (copper , zinc , nickel and cobalt) by natural bentonite. : 37–54.

Grandin, K.A. & Pletschke, B. 2015. Fruit waste streams in South Africa and their potential role in developing a bio-economy. , 111(5): 1–11.

Han, R., Zhang, J., Han, P., Wang, Y., Zhao, Z. & Tang, M. 2009. Study of equilibrium , kinetic and thermodynamic parameters about methylene blue adsorption onto natural zeolite. , 145: 496–504.

Islam, M.A., Morton, D.W., Johnson, B.B., Pramanik, B.K., Mainali, B. & Angove, M.J. 2018. Opportunities and constraints of using the innovative adsorbents for the removal of cobalt(II) from wastewater: A review. *Environmental Nanotechnology, Monitoring and Management*, 10(July): 435–456. https://doi.org/10.1016/j.enmm.2018.10.003.

Joshi, R. & Ahmed, S. 2016. Status and challenges of municipal solid waste management in India : A review. *Cogent Environmental Science*, 28(1): 1–18. http://dx.doi.org/10.1080/23311843.2016.1139434.

Kanamadi, R.D. 2003. Biosorption of Heavy Metals. , 7(4).

Karunarathne, H.D.S.S. & Amarasinghe, B.M.W.P.K. 2013. Fixed Bed Adsorption Column Studies for the Removal of Aqueous Phenol from Activated Carbon Prepared from Sugarcane Bagasse. , 34: 83–90.

Khan, S., Farooqi, A., Danish, M.I. & Zeb, A. 2013. Biosorption of copper (II) from aqeous

solution using citrus sinnesis peel and wood sawdust . , 16(August): 297–306.

Kosseva, M.R. 2009. *Processing of food wastes*. 1st ed. Elsevier Inc. http://dx.doi.org/10.1016/S1043-4526(09)58003-5.

M. A., M. 2014. Batch Removal of Hazardous Safranin-O in Wastewater Using Pineapple Peels as an Agricultural Waste Based Adsorbent. *International Journal of Environmental Monitoring and Analysis*, 2(3): 128.

Mahmoud, M.A. 2016. Kinetics studies of uranium sorption by powdered corn cob in batch and fixed bed system. *Journal of Advanced Research*, 7(1): 79–87. http://dx.doi.org/10.1016/j.jare.2015.02.004.

Mayer, F. & Hillebrandt, J.O. 1997. Potato pulp: Microbiological characterization, physical modification, and application of this agricultural waste product. *Applied Microbiology and Biotechnology*, 48(4): 435–440.

Meseldzija, S., Petrovic, J., Onjia, A., Volkov-Husovic, T., Nesic, A. & Vukelic, N. 2019. Utilization of agro-industrial waste for removal of copper ions from aqueous solutions and mining-wastewater. *Journal of Industrial and Engineering Chemistry*, 75: 246–252. https://doi.org/10.1016/j.jiec.2019.03.031.

Nadaroglu, H. & Kalkan, E. 2012. Removal of cobalt (II) ions from aqueous solution by using alternative adsorbent industrial red mud waste material. , 7(9): 1386–1394.

Patel, H. 2019. Fixed - bed column adsorption study : a comprehensive review. *Applied Water Science*, 9(3): 1–17. https://doi.org/10.1007/s13201-019-0927-7.

Peres, E.C., Cunha, J.M., Dortzbacher, G.F., Pavan, F.A., Lima, É.C., Foletto, E.L. & Dotto, G.L. 2018. Treatment of leachates containing cobalt by adsorption on Spirulina sp. and activated charcoal. *Journal of Environmental Chemical Engineering*, 6(1): 677–685. https://doi.org/10.1016/j.jece.2017.12.060.

Perring, M.A. 1974. Fruit Analysis. *Acta Horticulturae*, (45): 39–42.

Ramachandra, T. V. 2014. Biosorption of chromium (VI) from aqueous solutions by the husk of Bengal. , 8(May): 8–11.

Rao, R.A.K. & Khan, U. 2017. Adsorption of Ni(II) on alkali treated pineapple residue (Ananas comosus L.): Batch and column studies. *Groundwater for Sustainable Development*, 5(June): 244–252. http://dx.doi.org/10.1016/j.gsd.2017.08.002.

Sabourian, V., Ebrahimi, A., Naseri, F., Irani, M. & Rahimi, A. 2016. Fabrication of chitosan/silica nanofibrous adsorbent functionalized with amine groups for the removal of Ni(ii), Cu(ii) and Pb(ii) from aqueous solutions: Batch and column studies. *RSC Advances*, 6(46): 40354–40365.

Salleh, M.A.M., Mahmoud, D.K., Karim, W.A.W.A. & Idris, A. 2011. Cationic and anionic dye adsorption by agricultural solid wastes: A comprehensive review. *Desalination*, 280(1–3): 1–13.

Sharma, K. & Garg, V.K. 2018. Learn more about Composting Process Solid-State Fermentation for Vermi- composting.

Singh, N.B., Nagpal, G., Agrawal, S. & Rachna. 2018. Water purification by using Adsorbents: A Review. *Environmental Technology and Innovation*, 11: 187–240. https://doi.org/10.1016/j.eti.2018.05.006.

Singh, S.K. & Mehta, D. 2015. Fixed Bed Column Study and Adsorption Modelling on the Adsorption of Malachite Green dye from wastewater using Acid Activated Sawdust Fixed Bed Column Study and Adsorption Modelling on the Adsorption of Malachite Green dye from wastewater using Acid Activated Sawdust. , (August).

Sulaymon, A.H., Abid, B.A. & Al-najar, J.A. 2009. Removal of lead copper chromium and cobalt ions onto granular activated carbon in batch and fixed-bed adsorbers. , 155: 647–653.

Tofan, L., Teodosiu, C., Paduraru, C. & Wenkert, R. 2013. Cobalt (II) removal from aqueous solutions by natural hemp fibers: Batch and fixed-bed column studies. *Applied Surface Science*, 285(PARTA): 33–39. http://dx.doi.org/10.1016/j.apsusc.2013.06.151.

TOMUL, D.D.F., Kendüzler, E., Arslan, Y., Kabak, B. & Demir, K. 2017. Determination of Adsorption Characteristics of Orange Peel Activated with Potassium Carbonate for Chromium(III) Removal. *Journal of the Turkish Chemical Society, Section A: Chemistry*, 4(Iii): 1057–1070.

Town, C. Annexture A City of Cape Town Integrated Waste Management (IWM) Policy.

Trgo, M., Medvidović, N.V. & Perić, J. 2011. Application of mathematical empirical models to dynamic removal of lead on natural zeolite clinoptilolite in a fixed bed column. *Indian Journal of Chemical Technology*, 18(2): 123–131.

Yusuf, M., Elfghi, F.M. & Mallak, S.K. 2015. Iranica Journal of Energy & Environment Kinetic studies of Safranin-O removal from Aqueous Solutions using Pineapple Peels. , 6(3): 173–180.

9 Appendices

Appendix A : Data for batch studies

Table A 1: Data for effect of mass on biosorption of Co(II) on various biosorbents. (a) Experiment conducted with shaking 100 rpm, (b) experiment conducted without shaking.

Shaking	Weight	Ci Co (mg/L)	Co (ml)	Df*	Cf Co (mg/L)	Ci - Cf = C 24 hrs (mg/L)	% removal	Volume (L)	Q adsorbed
a	0,058	50	0,715	10	7,15	42,85	85,7	0,03	0,026
a	0,107	50	0,152	10	1,52	48,48	96,96	0,03	0,029
a	0,202	50	1,142	10	11,42	38,58	77,16	0,03	0,023
a	0,302	50	1,142	10	11,42	38,58	77,16	0,03	0,023
a	0,402	50	1,222	10	12,22	37,78	75,56	0,03	0,023
a	0,502	50	1,567	10	15,67	34,33	68,66	0,03	1,030
b	0,058	50	1,089	10	10,89	39,11	78,22	0,03	0,023
b	0,102	50	0	10	0	50	100	0,03	0,030
b	0,201	50	1,24	10	12,4	37,6	75,2	0,03	0,023
b	0,302	50	1,24	10	12,4	37,6	75,2	0,03	0,023
b	0,402	50	1,652	10	16,52	33,48	66,96	0,03	0,020
b	0,502	50	1,399	10	13,99	36,01	72,02	0,03	1,080

Table A 2: Data for effect of pH on biosorption of Co(II) on various biosorbents. Experimental conditions are given in table

Biosorbent	pH	Vol	Conc ppm Ci (mg/L)	Ce	dilution	Ce (mg/L)	Ci-Ce	Qe	Mass (g)	% absorbed	Ce/Qe	Log Ce	Log Qe
RPP	2	0,03	50	3,27	8	26,16	23,84	13,244	0,054	47,68	1,975	1,418	1,122
RPP	3	0,03	50	2,788	8	22,304	27,696	14,837	0,056	55,392	1,503	1,348	1,171
RPP	4	0,03	50	2,84	8	22,72	27,28	14,110	0,058	54,56	1,610	1,356	1,150
RPP	5	0,03	50	2,696	8	21,568	28,432	14,457	0,059	56,864	1,492	1,334	1,160
RPP	6	0,03	50	2,828	8	22,624	27,376	14,666	0,056	54,752	1,543	1,355	1,166
RPP	7	0,03	50	2,733	8	21,864	28,136	14,808	0,057	56,272	1,476	1,340	1,171
RPP	8	0,03	50	2,734	8	21,872	28,128	15,627	0,054	56,256	1,400	1,340	1,194
RPP	9	0,03	50	2,682	8	21,456	28,544	15,569	0,055	57,088	1,378	1,332	1,192
CTPP	2	0,03	50	3,437	12	41,244	8,756	4,529	0,058	17,512	9,107	1,615	0,656
CTPP	3	0,03	50	2,545	12	30,54	19,46	10,242	0,057	38,92	2,982	1,485	1,010
CTPP	4	0,03	50	2,123	12	25,476	24,524	13,624	0,054	49,048	1,870	1,406	1,134
CTPP	5	0,03	50	2,04	12	24,48	25,52	13,200	0,058	51,04	1,855	1,389	1,121
CTPP	6	0,03	50	2,065	12	24,78	25,22	14,011	0,054	50,44	1,769	1,394	1,146
CTPP	7	0,03	50	2,014	12	24,168	25,832	14,903	0,052	51,664	1,622	1,383	1,173
CTPP	8	0,03	50	1,978	12	23,736	26,264	13,585	0,058	52,528	1,747	1,375	1,133
CTPP	9	0,03	50	1,607	12	19,284	30,716	15,618	0,059	61,432	1,235	1,285	1,194
CPP	2	0,03	50	3,51	12	42,12	7,88	4,378	0,054	15,76	9,621	1,624	0,641
CPP	3	0,03	50	2,176	12	26,112	23,888	12,573	0,057	47,776	2,077	1,417	1,099
CPP	4	0,03	50	1,918	12	23,016	26,984	14,991	0,054	53,968	1,535	1,362	1,176
CPP	5	0,03	50	1,937	12	23,244	26,756	15,436	0,052	53,512	1,506	1,366	1,189
CPP	6	0,03	50	1,57	12	18,84	31,16	15,844	0,059	62,32	1,189	1,275	1,200
CPP	7	0,03	50	1,73	12	20,76	29,24	14,868	0,059	58,48	1,396	1,317	1,172
CPP	8	0,03	50	1,849	12	22,188	27,812	14,386	0,058	55,624	1,542	1,346	1,158
CPP	9	0,03	50	1,328	12	15,936	34,064	18,924	0,054	68,128	0,842	1,202	1,277
AC	2	0,03	50	3,827	12	45,924	4,076	2,264	0,054	8,152	20,280	1,662	0,355
AC	3	0,03	50	3,19	12	38,28	11,72	6,634	0,053	23,44	5,770	1,583	0,822

AC	4	0,03	50	3,007	12	36,084	13,916	7,731	0,054	27,832	4,667	1,557	0,888
AC	5	0,03	50	2,8	12	33,6	16,4	8,632	0,057	32,8	3,893	1,526	0,936
AC	6	0,03	50	2,305	12	27,66	22,34	11,359	0,059	44,68	2,435	1,442	1,055
AC	7	0,03	50	2,264	12	27,168	22,832	13,172	0,052	45,664	2,063	1,434	1,120
AC	8	0,03	50	3,104	12	37,248	12,752	6,596	0,058	25,504	5,647	1,571	0,819
AC	9	0,03	50	2,801	12	33,612	16,388	8,625	0,057	32,776	3,897	1,526	0,936

Table A 3: Data for effect of temperature on biosorption of Co(II) on various biosorbents. Experimental conditions are given in table

			Conc ppm									
Biosorbent	**Tempt (◦C)**	**Vol (L)**	**Ci (mg/L)**	**Ce**	**Ci/Ce**	**Ci/Ce - 1**	**Ln Ci/Ce**	**D factor**	**Ce (mg/L)**	**Ci-Ce**	**Qe**	**Mass (g)**	**%**
RPP	10	0,03	50	1,632	30,637	29,637	3,422	20	32,64	17,36	9,469	0,055	34,72
RPP	20	0,03	50	1,885	26,525	25,525	3,278	20	37,7	12,3	6,589	0,056	24,6
RPP	30	0,03	50	1,739	28,752	27,752	3,359	20	34,78	15,22	8,011	0,057	30,44
RPP	40	0,03	50	1,866	26,795	25,795	3,288	20	37,32	12,68	6,447	0,059	25,36
CTPP	10	0,03	50	0,892	56,054	55,054	4,026	20	17,84	32,16	17,542	0,055	64,32
CTPP	20	0,03	50	1,249	40,032	39,032	3,690	20	24,98	25,02	13,404	0,056	50,04
CTPP	30	0,03	50	0,477	104,822	103,822	4,652	20	9,54	40,46	22,069	0,055	80,92
CTPP	40	0,03	50	1,46	34,247	33,247	3,534	20	29,2	20,8	11,143	0,056	41,6
CTPP	10	0,03	50	1,287	38,850	37,850	3,660	20	25,74	24,26	12,548	0,058	48,52
CTPP	20	0,03	50	1,237	40,420	39,420	3,699	20	24,74	25,26	12,844	0,059	50,52
CTPP	30	0,03	50	1,325	37,736	36,736	3,631	20	26,5	23,5	12,155	0,058	47
CTPP	40	0,03	50	0,778	64,267	63,267	4,163	20	15,56	34,44	17,814	0,058	68,88
CPP	10	0,03	50	1,568	31,888	30,888	3,462	20	31,36	18,64	9,986	0,056	37,28
CPP	20	0,03	50	1,064	46,992	45,992	3,850	20	21,28	28,72	14,603	0,059	57,44
CPP	30	0,03	50	1,184	42,230	41,230	3,743	20	23,68	26,32	13,614	0,058	52,64
CPP	40	0,03	50	0,562	88,968	87,968	4,488	20	11,24	38,76	20,400	0,057	77,52
AC	10	0,03	50	2,275	21,978	20,978	3,090	20	45,5	4,5	2,328	0,058	9
AC	20	0,03	50	2,1	23,810	22,810	3,170	20	42	8	4,444	0,054	16

AC	30	0,03	50	2,213	22,594	21,594	3,118	20	44,26	5,74	3,075	0,056	11,48
AC	40	0,03	50	2,395	20,877	19,877	3,039	20	47,9	2,1	1,086	0,058	4,2

Table A 4: Data for effect of time (mins) on biosorption of Co(II) on RPP. Experimental conditions are given in table

Biosorbent	Volume	Time (min)	Ce (mg/L)	Co (mg/L)	Co-Ce (mg/L)	Mass	% Adsorbed
RPP	0,03	0,5	24,92	45,2	20,28	0,052	44,867
RPP	0,03	1	26,92	45,2	18,28	0,052	40,442
RPP	0,03	3	26,14	45,2	19,06	0,054	42,168
RPP	0,03	5	28,56	45,2	16,64	0,053	36,814
RPP	0,03	10	28,32	45,2	16,88	0,055	37,345
RPP	0,03	20	29,86	45,2	15,34	0,056	33,938
RPP	0,03	30	31,5	45,2	13,7	0,055	30,310
RPP	0,03	45	30,84	45,2	14,36	0,055	31,770
RPP	0,03	60	30,94	45,2	14,26	0,056	31,549
RPP	0,03	90	29,02	45,2	16,18	0,055	35,796
RPP	0,03	120	30,54	45,2	14,66	0,055	32,434
RPP	0,03	150	32,26	45,2	12,94	0,052	28,628
RPP	0,03	180	33,26	45,2	11,94	0,055	26,416

Table A 5: Data for effect of time (mins) on biosorption of Co(II) by CTPP. Experimental conditions are given in table

Biosorbent	Volume	Time	Ce (mg/L)	Co (mg/L)	Co-Ce (mg/L)	Mass	% biosorbed
CTPP	0,03	0,5	35,92	45,2	9,28	0,054	20,531
CTPP	0,03	1	34,98	45,2	10,22	0,057	22,611
CTPP	0,03	3	34,38	45,2	10,82	0,054	23,938
CTPP	0,03	5	33,02	45,2	12,18	0,056	26,947
CTPP	0,03	10	33,8	45,2	11,4	0,052	25,221
CTPP	0,03	20	33,38	45,2	11,82	0,053	26,150
CTPP	0,03	30	30,34	45,2	14,86	0,055	32,876
CTPP	0,03	40	29,96	45,2	15,24	0,056	33,717
CTPP	0,03	60	29,14	45,2	16,06	0,057	35,531
CTPP	0,03	90	26,62	45,2	18,58	0,058	41,106
CTPP	0,03	120	25,96	45,2	19,24	0,057	42,566
CTPP	0,03	150	25,34	45,2	19,86	0,058	43,938
CTPP	0,03	180	27,08	45,2	18,12	0,057	40,088

Table A 6: Data for effect of time (mins) on biosorption of Co(II) by CPP. Experimental conditions are given in table

Biosorbent	Volume	Time	Ct (mg/L)	Co (mg/L)	Co-Ce (mg/L)	Mass	% biosorbed
CPP	0,03	0,5	33,36	45,2	11,84	0,054	26,195
CPP	0,03	1	33,1	45,2	12,1	0,057	26,770
CPP	0,03	3	32,86	45,2	12,34	0,057	27,301
CPP	0,03	5	30,2	45,2	15	0,053	33,186
CPP	0,03	10	27,14	45,2	18,06	0,057	39,956
CPP	0,03	20	25,72	45,2	19,48	0,056	43,097
CPP	0,03	30	23,44	45,2	21,76	0,054	48,142
CPP	0,03	45	22,16	45,2	23,04	0,056	50,973
CPP	0,03	60	16,38	45,2	28,82	0,055	63,761
CPP	0,03	90	16,14	45,2	29,06	0,053	64,292
CPP	0,03	120	16,26	45,2	28,94	0,056	64,027
CPP	0,03	150	16,16	45,2	29,04	0,057	64,248
CPP	0,03	180	17,5	45,2	27,7	0,055	61,283

Table A 7: Data for effect of time (mins) on biosorption of Co(II) by AC. Experimental conditions are given in table

Adsorbent	Volume	Time (min)	Ce (mg/L)	Co (mg/L)	Co-Ce (mg/L)	Mass	% Biosorbed
AC	0,03	0,5	38,34	45,2	6,86	0,058	15,177
AC	0,03	1	37,84	45,2	7,36	0,053	16,283
AC	0,03	3	37,74	45,2	7,46	0,058	16,504
AC	0,03	5	37,66	45,2	7,54	0,057	16,681
AC	0,03	10	37,3	45,2	7,9	0,059	17,478
AC	0,03	20	37	45,2	8,2	0,058	18,142
AC	0,03	30	36,46	45,2	8,74	0,058	19,336
AC	0,03	45	36,48	45,2	8,72	0,053	19,292
AC	0,03	60	37,1	45,2	8,1	0,054	17,920
AC	0,03	90	36,66	45,2	8,54	0,054	18,894
AC	0,03	120	37,3	45,2	7,9	0,053	17,478
AC	0,03	150	35,68	45,2	9,52	0,057	21,062
AC	0,03	180	40,74	45,2	4,46	0,056	9,867

Appendix B : Kinetic modelling data

Table B 1: Kinetic modelling data for RPP

Biosorbent	Qt (mg/g)	Qe	Qe-Qt	Log Qe-Qt	Ce/Qe	Log Ce	Log Qe	t/Qe	t1/2
RPP	11,700	11,700	0,000	#NUM!	2,130	1,397	1,068	0,043	0,7071068
RPP	10,546	11,700	1,154	0,062	2,553	1,430	1,023	0,095	1
RPP	10,589	11,700	1,111	0,046	2,469	1,417	1,025	0,283	1,7320508
RPP	9,419	11,700	2,281	0,358	3,032	1,456	0,974	0,531	2,236068
RPP	9,207	11,700	2,493	0,397	3,076	1,452	0,964	1,086	3,1622777
RPP	8,218	11,700	3,482	0,542	3,634	1,475	0,915	2,434	4,472136
RPP	7,473	11,700	4,227	0,626	4,215	1,498	0,873	4,015	5,4772256
RPP	7,833	11,700	3,867	0,587	3,937	1,489	0,894	5,745	6,7082039
RPP	7,639	11,700	4,061	0,609	4,050	1,491	0,883	7,854	7,7459667
RPP	8,825	11,700	2,875	0,459	3,288	1,463	0,946	10,198	9,486833
RPP	7,996	11,700	3,704	0,569	3,819	1,485	0,903	15,007	10,954451
RPP	7,465	11,700	4,235	0,627	4,321	1,509	0,873	20,093	12,247449
RPP	6,513	11,700	5,187	0,715	5,107	1,522	0,814	27,638	13,416408

Table B 2: Kinetic modelling data for CTPP

Adsorbent	Qt (mg/g)	Qe	qe-qt	Log (qe-qt)	Ce/Qe	Log Ce	t/Qe	Log Qe	T1/2
CTPP	5,156	9,6103448	4,455	0,649	3,738	1,555	0,052	0,983	0,7071068
CTPP	5,379	9,6103448	4,231	0,626	3,640	1,544	0,104	0,983	1
CTPP	6,011	9,6103448	3,599	0,556	3,577	1,536	0,312	0,983	1,7320508
CTPP	6,525	9,6103448	3,085	0,489	3,436	1,519	0,520	0,983	2,236068
CTPP	6,577	9,6103448	3,033	0,482	3,517	1,529	1,041	0,983	3,1622777
CTPP	6,691	9,6103448	2,920	0,465	3,473	1,523	2,081	0,983	4,472136
CTPP	8,105	9,6103448	1,505	0,178	3,157	1,482	3,122	0,983	5,4772256
CTPP	8,164	9,6103448	1,446	0,160	3,117	1,477	4,162	0,983	6,3245553
CTPP	8,453	9,6103448	1,158	0,064	3,032	1,464	6,243	0,983	7,7459667
CTPP	9,610	9,6103448	0,000	#NUM!	2,770	1,425	9,365	0,983	9,486833
CTPP	10,126	9,6103448	-0,516	#NUM!	2,701	1,414	12,487	0,983	10,954451
CTPP	10,272	9,6103448	-0,662	#NUM!	2,637	1,404	15,608	0,983	12,247449
CTPP	9,537	9,6103448	0,074	-1,134	2,818	1,433	18,730	0,983	13,416408

Table B 3: Kinetic modelling data for CPP

Adsorbent	Qt (mg/g)	Qe	Qe-Qt	Log (qe-qt)	Log Ce	t/Qe	Log Qe	t1/2
CPP	6,578	15,720	9,142	0,961	1,418	0,076	0,818	0,7071068
CPP	6,368	15,720	9,352	0,971	1,428	0,157	0,804	1
CPP	6,495	15,720	9,225	0,965	1,436	0,462	0,813	1,7320508
CPP	8,491	15,720	7,229	0,859	1,521	0,589	0,929	2,236068
CPP	9,505	15,720	6,215	0,793	1,602	1,052	0,978	3,1622777
CPP	10,436	15,720	5,284	0,723	1,634	1,916	1,019	4,472136
CPP	12,089	15,720	3,631	0,560	1,683	2,482	1,082	5,4772256
CPP	12,343	15,720	3,377	0,529	1,707	3,646	1,091	6,7082039
CPP	15,720	15,720	0,000	#NUM!	1,805	3,817	1,196	7,7459667
CPP	16,449	15,720	-0,729	#NUM!	1,808	5,471	1,216	9,486833
CPP	15,504	15,720	0,216	-0,665	1,806	7,740	1,190	10,954451
CPP	15,284	15,720	0,436	-0,361	1,808	9,814	1,184	12,247449
CPP	15,109	15,720	0,611	-0,214	1,787	11,913	1,179	13,416408

Table B 4 Kinetic modelling data for AC

Adsorbent	Qt (mg/g)	Qe	Qe-Qt	Log Qe-Qt	Ce/Qe	Log Qe	Log Ce	t/Qe	t1/2
AC	3,548	5,011	1,462	0,165	10,805	0,550	1,584	0,141	0,707107
AC	4,166	5,011	0,844	-0,073	9,083	0,620	1,578	0,240	1
AC	3,859	5,011	1,152	0,061	9,781	0,586	1,577	0,777	1,732051
AC	3,968	5,011	1,042	0,018	9,490	0,599	1,576	1,260	2,236068
AC	4,017	5,011	0,994	-0,003	9,286	0,604	1,572	2,489	3,162278
AC	4,241	5,011	0,769	-0,114	8,724	0,628	1,568	4,715	4,472136
AC	4,521	5,011	0,490	-0,310	8,065	0,655	1,562	6,636	5,477226
AC	4,936	5,011	0,075	-1,127	7,391	0,693	1,562	9,117	6,708204
AC	4,500	5,011	0,511	-0,292	8,244	0,653	1,569	13,333	7,745967
AC	4,744	5,011	0,266	-0,575	7,727	0,676	1,564	18,970	9,486833
AC	4,472	5,011	0,539	-0,269	8,341	0,650	1,572	26,835	10,95445
AC	5,011	5,011	0,000	#NUM!	7,121	0,700	1,552	29,937	12,24745
AC	2,389	5,011	2,621	0,419	17,051	0,378	1,610	75,336	13,41641

Appendix C : Column Data

Table C 1: Data for effect of mass on column biosorption – mass 0.5 g. Conditions in table

Time	Volume	Mass	Ci	Ce	Ci-Ce	Qe	Ce/Qe	Log Ce	Log Qe	% Adsorbed	Ce/Ci
1	0,05	0,503	42,17	1,632	40,538	4,030	0,405	0,213	0,605	17,095	0,039
2	0,05	0,503	42,17	1,035	41,135	4,089	0,253	0,015	0,612	17,347	0,025
3	0,05	0,503	42,17	1,13	41,04	4,080	0,277	0,053	0,611	17,307	0,027
4	0,05	0,503	42,17	1,662	40,508	4,027	0,413	0,221	0,605	17,082	0,039
5	0,05	0,503	42,17	7,028	35,142	3,493	2,012	0,847	0,543	14,819	0,167
6	0,05	0,503	42,17	12,24	29,93	2,975	4,114	1,088	0,474	12,621	0,290
7	0,05	0,503	42,17	15,93	26,24	2,608	6,107	1,202	0,416	11,065	0,378
8	0,05	0,503	42,17	18,12	24,05	2,391	7,580	1,258	0,379	10,142	0,430
9	0,05	0,503	42,17	19,78	22,39	2,226	8,887	1,296	0,347	9,442	0,469
10	0,05	0,503	42,17	21,14	21,03	2,090	10,113	1,325	0,320	8,868	0,501
11	0,05	0,503	42,17	22,38	19,79	1,967	11,377	1,350	0,294	8,345	0,531
12	0,05	0,503	42,17	23,34	18,83	1,872	12,469	1,368	0,272	7,941	0,553
13	0,05	0,503	42,17	24,56	17,61	1,750	14,030	1,390	0,243	7,426	0,582
14	0,05	0,503	42,17	25,42	16,75	1,665	15,267	1,405	0,221	7,063	0,603
15	0,05	0,503	42,17	26,37	15,8	1,571	16,790	1,421	0,196	6,663	0,625
16	0,05	0,503	42,17	26,97	15,2	1,511	17,850	1,431	0,179	6,410	0,640
17	0,05	0,503	42,17	27,95	14,22	1,414	19,773	1,446	0,150	5,997	0,663
18	0,05	0,503	42,17	28,66	13,51	1,343	21,341	1,457	0,128	5,697	0,680
19	0,05	0,503	42,17	29,16	13,01	1,293	22,548	1,465	0,112	5,486	0,691
20	0,05	0,503	42,17	30,2	11,97	1,190	25,381	1,480	0,075	5,048	0,716
21	0,05	0,503	42,17	30,76	11,41	1,134	27,121	1,488	0,055	4,812	0,729
22	0,05	0,503	42,17	31,8	10,37	1,031	30,849	1,502	0,013	4,373	0,754
23	0,05	0,503	42,17	32,21	9,96	0,990	32,533	1,508	-0,004	4,200	0,764
24	0,05	0,503	42,17	33,25	8,92	0,887	37,499	1,522	-0,052	3,762	0,788
25	0,05	0,503	42,17	33,38	8,79	0,874	38,203	1,523	-0,059	3,707	0,792

26	0,05	0,503	42,17	34,37	7,8	0,775	44,328	1,536	-0,111	3,289	0,815
27	0,05	0,503	42,17	34,54	7,63	0,758	45,540	1,538	-0,120	3,218	0,819
28	0,05	0,503	42,17	34,84	7,33	0,729	47,816	1,542	-0,137	3,091	0,826
29	0,05	0,503	42,17	35,33	6,84	0,680	51,962	1,548	-0,168	2,884	0,838
30	0,05	0,503	42,17	35,91	6,26	0,622	57,708	1,555	-0,206	2,640	0,852
31	0,05	0,503	42,17	36,3	5,87	0,583	62,211	1,560	-0,234	2,475	0,861
32	0,05	0,503	42,17	36,17	6	0,596	60,645	1,558	-0,224	2,530	0,858
33	0,05	0,503	42,17	36,65	5,52	0,549	66,793	1,564	-0,261	2,328	0,869
34	0,05	0,503	42,17	36,69	5,48	0,545	67,354	1,565	-0,264	2,311	0,870
35	0,05	0,503	42,17	36,51	5,66	0,563	64,892	1,562	-0,250	2,387	0,866
36	0,05	0,503	42,17	37,22	4,95	0,492	75,643	1,571	-0,308	2,087	0,883
37	0,05	0,503	42,17	36,89	5,28	0,525	70,287	1,567	-0,280	2,227	0,875
38	0,05	0,503	42,17	37,32	4,85	0,482	77,410	1,572	-0,317	2,045	0,885
39	0,05	0,503	42,17	37,16	5,01	0,498	74,617	1,570	-0,303	2,113	0,881
40	0,05	0,503	42,17	37,29	4,88	0,485	76,872	1,572	-0,314	2,058	0,884
41	0,05	0,503	42,17	37,67	4,5	0,447	84,213	1,576	-0,349	1,898	0,893
42	0,05	0,503	42,17	37,62	4,55	0,452	83,177	1,575	-0,345	1,919	0,892
43	0,05	0,503	42,17	37,77	4,4	0,437	86,356	1,577	-0,359	1,855	0,896
44	0,05	0,503	42,17	38,1	4,07	0,405	94,173	1,581	-0,393	1,716	0,903
45	0,05	0,503	42,17	37,95	4,22	0,419	90,468	1,579	-0,377	1,780	0,900
46	0,05	0,503	42,17	38,06	4,11	0,409	93,159	1,580	-0,389	1,733	0,903
47	0,05	0,503	42,17	38,3	3,87	0,385	99,560	1,583	-0,415	1,632	0,908

Table C 2: Data for effect of mass on column biosorption – mass 1.0 g. Conditions in table

Time	Volume	Mass	Ci	Ce	Ci-Ce	Qe	Ce/Qe	Log Ce	Log Qe	% Adsorbed	Ce/Ci
2	0,01	1,006	40,05	0,931	39,069	0,388	2,397	0,380	-0,411	97,551	0,023
4	0,1	1,006	40,05	0,323	39,677	3,944	0,082	-1,087	0,596	99,069	0,008
6	0,1	1,006	40,05	0,103	39,897	3,966	0,026	-1,586	0,598	99,618	0,003
8	0,1	1,006	40,05	0,455	39,545	3,931	0,116	-0,936	0,594	98,739	0,011
10	0,1	1,006	40,05	1,601	38,399	3,817	0,419	-0,377	0,582	95,878	0,040
12	0,1	1,006	40,05	4,12	35,88	3,567	1,155	0,063	0,552	89,588	0,103
14	0,1	1,006	40,05	6,669	33,331	3,313	2,013	0,304	0,520	83,223	0,167
16	0,1	1,006	40,05	9,941	30,059	2,988	3,327	0,522	0,475	75,054	0,248
18	0,1	1,006	40,05	13,84	26,16	2,600	5,322	0,726	0,415	65,318	0,346
20	0,1	1,006	40,05	17,4	22,6	2,247	7,745	0,889	0,352	56,429	0,434
22	0,1	1,006	40,05	19,86	20,14	2,002	9,920	0,997	0,301	50,287	0,496
24	0,1	1,006	40,05	22,88	17,12	1,702	13,445	1,129	0,231	42,747	0,571
26	0,1	1,006	40,05	24,92	15,08	1,499	16,624	1,221	0,176	37,653	0,622
28	0,1	1,006	40,05	26,71	13,29	1,321	20,218	1,306	0,121	33,184	0,667
30	0,1	1,006	40,05	28,48	11,52	1,145	24,871	1,396	0,059	28,764	0,711
32	0,1	1,006	40,05	30,38	9,62	0,956	31,770	1,502	-0,019	24,020	0,759
34	0,1	1,006	40,05	30,81	9,19	0,914	33,727	1,528	-0,039	22,946	0,769
36	0,1	1,006	40,05	32,26	7,74	0,769	41,930	1,623	-0,114	19,326	0,805
38	0,1	1,006	40,05	33,28	6,72	0,668	49,821	1,697	-0,175	16,779	0,831
40	0,1	1,006	40,05	34,07	5,93	0,589	57,798	1,762	-0,230	14,806	0,851
42	0,1	1,006	40,05	34,57	5,43	0,540	64,047	1,806	-0,268	13,558	0,863
44	0,1	1,006	40,05	34,62	5,38	0,535	64,736	1,811	-0,272	13,433	0,864
46	0,1	1,006	40,05	35,28	4,72	0,469	75,194	1,876	-0,329	11,785	0,881
48	0,1	1,006	40,05	35,49	4,51	0,448	79,164	1,899	-0,348	11,261	0,886
50	0,1	1,006	40,05	35,92	4,08	0,406	88,567	1,947	-0,392	10,187	0,897
52	0,1	1,006	40,05	36,59	3,41	0,339	107,946	2,033	-0,470	8,514	0,914
54	0,1	1,006	40,05	36,46	3,54	0,352	103,612	2,015	-0,454	8,839	0,910
56	0,1	1,006	40,05	37,14	2,86	0,284	130,639	2,116	-0,546	7,141	0,927

58	0,1	1,006	40,05	36,77	3,23	0,321	114,522	2,059	-0,493	8,065	0,918
60	0,1	1,006	40,05	36,94	3,06	0,304	121,443	2,084	-0,517	7,640	0,922

Table C 3: Data for effect of mass on column biosorption – mass 1.5 g. Conditions in table

No.	Time (min)	Volume (L)	Mass (g)	Ci	Ce	Ci-Ce	Qe	Log Ce	Log Qe	Ce/Ci	% Biosorbed
1	3	0,015	1,503	40,62	0,932	39,688	0,396	-0,031	-0,402209	0,023	97,706
2	6	0,015	1,503	40,62	0,411	40,209	0,401	-0,386	-0,396544	0,010	98,988
3	9	0,015	1,503	40,62	0,342	40,278	0,402	-0,466	-0,3958	0,008	99,158
4	12	0,015	1,503	40,62	0,293	40,327	0,402	-0,533	-0,395272	0,007	99,279
5	15	0,015	1,503	40,62	0,704	39,916	0,398	-0,152	-0,399721	0,017	98,267
6	18	0,015	1,503	40,62	0,985	39,635	0,396	-0,007	-0,402789	0,024	97,575
7	21	0,015	1,503	40,62	1,862	38,758	0,387	0,270	-0,412506	0,046	95,416
8	24	0,015	1,503	40,62	4,708	35,912	0,358	0,673	-0,445628	0,116	88,410
9	27	0,015	1,503	40,62	8,813	31,807	0,317	0,945	-0,498345	0,217	78,304
10	30	0,015	1,503	40,62	13,36	27,26	0,272	1,126	-0,565342	0,329	67,110
11	33	0,015	1,503	40,62	16,52	24,1	0,241	1,218	-0,618851	0,407	59,330
12	36	0,015	1,503	40,62	21,21	19,41	0,194	1,327	-0,712842	0,522	47,784
13	39	0,015	1,503	40,62	24,59	16,03	0,160	1,391	-0,795934	0,605	39,463
14	42	0,015	1,503	40,62	27	13,62	0,136	1,431	-0,866691	0,665	33,530
15	45	0,015	1,503	40,62	28,96	11,66	0,116	1,462	-0,934169	0,713	28,705
16	48	0,015	1,503	40,62	30,74	9,88	0,099	1,488	-1,006111	0,757	24,323
17	51	0,015	1,503	40,62	31,85	8,77	0,088	1,503	-1,057868	0,784	21,590
18	54	0,015	1,503	40,62	32,73	7,89	0,079	1,515	-1,103791	0,806	19,424
19	57	0,015	1,503	40,62	33,62	7	0,070	1,527	-1,15577	0,828	17,233
20	60	0,015	1,503	40,62	34,17	6,45	0,064	1,534	-1,191308	0,841	15,879

21	63	0,015	1,503	40,62	34,72	5,9	0,059	1,541	-1,230016	0,855	14,525
22	66	0,015	1,503	40,62	35,39	5,23	0,052	1,549	-1,282366	0,871	12,875
23	69	0,015	1,503	40,62	35,79	4,83	0,048	1,554	-1,316921	0,881	11,891
24	72	0,015	1,503	40,62	35,65	4,97	0,050	1,552	-1,304511	0,878	12,235
25	75	0,015	1,503	40,62	36,38	4,24	0,042	1,561	-1,373502	0,896	10,438
26	78	0,015	1,503	40,62	36,61	4,01	0,040	1,564	-1,397723	0,901	9,872
27	81	0,015	1,503	40,62	36,92	3,7	0,037	1,567	-1,432666	0,909	9,109
28	84	0,015	1,503	40,62	36,77	3,85	0,038	1,565	-1,415407	0,905	9,478
29	87	0,015	1,503	40,62	37,09	3,53	0,035	1,569	-1,453093	0,913	8,690
30	90	0,015	1,503	40,62	37,39	3,23	0,032	1,573	-1,491665	0,920	7,952
31	93	0,015	1,503	40,62	37,58	3,04	0,030	1,575	-1,517994	0,925	7,484
32	96	0,015	1,503	40,62	37,41	3,21	0,032	1,573	-1,494363	0,921	7,903
33	99	0,015	1,503	40,62	38,08	2,54	0,025	1,581	-1,596034	0,937	6,253
34	102	0,015	1,503	40,62	37,91	2,71	0,027	1,579	-1,567898	0,933	6,672
35	105	0,015	1,503	40,62	38,33	2,29	0,023	1,584	-1,641032	0,944	5,638
36	108	0,015	1,503	40,62	38,51	2,11	0,021	1,586	-1,676585	0,948	5,194
37	111	0,015	1,503	40,62	38,73	1,89	0,019	1,588	-1,724406	0,953	4,653
38	114	0,015	1,503	40,62	38,39	2,23	0,022	1,584	-1,652563	0,945	5,490
39	117	0,015	1,503	40,62	38,72	1,9	0,019	1,588	-1,722114	0,953	4,677
40	120	0,015	1,503	40,62	38,69	1,93	0,019	1,588	-1,71531	0,952	4,751

Table C 4: Data on effect of flowrate on biosorption. Flowrate: 1 mL/min. Conditions in table

Time	Volume	Mass	Ci	Ce	Ci-Ce	Qe	Ce/Qe	Log Ce	Log Qe	Ce/Ci	% Biosorbed
10	0,015	1,005	41,57	0,34	41,23	0,615	0,553	-0,469	-0,211	0,008	99,182
20	0,015	1,005	41,57	0,038	41,532	0,620	0,061	-1,420	-0,208	0,001	99,909
30	0,015	1,005	41,57	0,434	41,136	0,614	0,707	-0,363	-0,212	0,010	98,956
40	0,015	1,005	41,57	2,147	39,423	0,588	3,649	0,332	-0,230	0,052	94,835
50	0,015	1,005	41,57	6,563	35,007	0,522	12,561	0,817	-0,282	0,158	84,212
60	0,015	1,005	41,57	13,03	28,54	0,426	30,589	1,115	-0,371	0,313	68,655
70	0,015	1,005	41,57	19,31	22,26	0,332	58,121	1,286	-0,479	0,465	53,548
80	0,015	1,005	41,57	24,51	17,06	0,255	96,258	1,389	-0,594	0,590	41,039
90	0,015	1,005	41,57	27,57	14	0,209	131,942	1,440	-0,680	0,663	33,678
100	0,015	1,005	41,57	30,26	11,31	0,169	179,259	1,481	-0,773	0,728	27,207
110	0,015	1,005	41,57	34,11	7,46	0,111	306,350	1,533	-0,953	0,821	17,946
120	0,015	1,005	41,57	31,79	9,78	0,146	217,784	1,502	-0,836	0,765	23,527
130	0,015	1,005	41,57	34,48	7,09	0,106	325,834	1,538	-0,975	0,829	17,056
140	0,015	1,005	41,57	35,82	5,75	0,086	417,381	1,554	-1,066	0,862	13,832
150	0,015	1,005	41,57	35,81	5,76	0,086	416,540	1,554	-1,066	0,861	13,856
160	0,015	1,005	41,57	36,29	5,28	0,079	460,498	1,560	-1,103	0,873	12,701
170	0,015	1,005	41,57	37,08	4,49	0,067	553,310	1,569	-1,174	0,892	10,801
180	0,015	1,005	41,57	36,87	4,7	0,070	525,594	1,567	-1,154	0,887	11,306
190	0,015	1,005	41,57	37,3	4,27	0,064	585,269	1,572	-1,196	0,897	10,272
200	0,015	1,005	41,57	37,8	3,77	0,056	671,777	1,577	-1,250	0,909	9,069
210	0,015	1,005	41,57	37,7	3,87	0,058	652,687	1,576	-1,238	0,907	9,310
220	0,015	1,005	41,57	37,84	3,73	0,056	679,700	1,578	-1,254	0,910	8,973
230	0,015	1,005	41,57	39,24	2,33	0,035	1128,361	1,594	-1,459	0,944	5,605
240	0,015	1,005	41,57	39,41	2,16	0,032	1222,440	1,596	-1,492	0,948	5,196

Table C 5: Data on effect of flowrate on biosorption. Flowrate: 3 mL/min. Conditions in table

Time	Volume	Mass	Ci	Ce	Ci-Ce	Qe	Ce/Qe	Log Ce	Log Qe	%Adsorbed	Ce/Ci
3	9	1,004	43,9	0,213	43,687	43,687	0,005	-0,672	1,640	99,515	0,005
6	9	1,004	43,9	0,213	43,687	43,687	0,005	-0,672	1,640	99,515	0,005
9	9	1,004	43,9	0,108	43,792	43,792	0,002	-0,967	1,641	99,754	0,002
15	9	1,004	43,9	0,277	43,623	43,623	0,006	-0,558	1,640	99,369	0,006
18	9	1,004	43,9	0,223	43,677	43,677	0,005	-0,652	1,640	99,492	0,005
21	9	1,004	43,9	0,309	43,591	43,591	0,007	-0,510	1,639	99,296	0,007
24	9	1,004	43,9	1,017	42,883	42,883	0,024	0,007	1,632	97,683	0,023
27	9	1,004	43,9	2,68	41,22	41,22	0,065	0,428	1,615	93,895	0,061
30	9	1,004	43,9	5,911	37,989	37,989	0,156	0,772	1,580	86,535	0,135
33	9	1,004	43,9	9,469	34,431	34,431	0,275	0,976	1,537	78,431	0,216
36	9	1,004	43,9	13,47	30,43	30,43	0,443	1,129	1,483	69,317	0,307
39	9	1,004	43,9	16,44	27,46	27,46	0,599	1,216	1,439	62,551	0,374
42	9	1,004	43,9	18,98	24,92	24,92	0,762	1,278	1,397	56,765	0,432
45	9	1,004	43,9	22,49	21,41	21,41	1,050	1,352	1,331	48,770	0,512
48	9	1,004	43,9	24,96	18,94	18,94	1,318	1,397	1,277	43,144	0,569
51	9	1,004	43,9	27,08	16,82	16,82	1,610	1,433	1,226	38,314	0,617
54	9	1,004	43,9	28,97	14,93	14,93	1,940	1,462	1,174	34,009	0,660
60	9	1,004	43,9	30,65	13,25	13,25	2,313	1,486	1,122	30,182	0,698
63	9	1,004	43,9	31,21	12,69	12,69	2,459	1,494	1,103	28,907	0,711
66	9	1,004	43,9	32,3	11,6	11,6	2,784	1,509	1,064	26,424	0,736
69	9	1,004	43,9	33,1	10,8	10,8	3,065	1,520	1,033	24,601	0,754
72	9	1,004	43,9	33,86	10,04	10,04	3,373	1,530	1,002	22,870	0,771
75	9	1,004	43,9	34,53	9,37	9,37	3,685	1,538	0,972	21,344	0,787
78	9	1,004	43,9	35,22	8,68	8,68	4,058	1,547	0,939	19,772	0,802
81	9	1,004	43,9	35,24	8,66	8,66	4,069	1,547	0,938	19,727	0,803
84	9	1,004	43,9	35,79	8,11	8,11	4,413	1,554	0,909	18,474	0,815
87	9	1,004	43,9	36,06	7,84	7,84	4,599	1,557	0,894	17,859	0,821
90	9	1,004	43,9	36,67	7,23	7,23	5,072	1,564	0,859	16,469	0,835

93	9	1,004	43,9	37,16	6,74	6,74	5,513	1,570	0,829	15,353	0,846
96	9	1,004	43,9	36,99	6,91	6,91	5,353	1,568	0,839	15,740	0,843
99	9	1,004	43,9	37,27	6,63	6,63	5,621	1,571	0,822	15,103	0,849
102	9	1,004	43,9	37,61	6,29	6,29	5,979	1,575	0,799	14,328	0,857
105	9	1,004	43,9	37,6	6,3	6,3	5,968	1,575	0,799	14,351	0,856
108	9	1,004	43,9	38,01	5,89	5,89	6,453	1,580	0,770	13,417	0,866
111	9	1,004	43,9	37,85	6,05	6,05	6,256	1,578	0,782	13,781	0,862
114	9	1,004	43,9	38,33	5,57	5,57	6,882	1,584	0,746	12,688	0,873
117	9	1,004	43,9	38,47	5,43	5,43	7,085	1,585	0,735	12,369	0,876
120	9	1,004	43,9	38,78	5,12	5,12	7,574	1,589	0,709	11,663	0,883
123	9	1,004	43,9	38,72	5,18	5,18	7,475	1,588	0,714	11,800	0,882
126	9	1,004	43,9	38,85	5,05	5,05	7,693	1,589	0,703	11,503	0,885
129	9	1,004	43,9	38,9	5	5	7,780	1,590	0,699	11,390	0,886
132	9	1,004	43,9	39,13	4,77	4,77	8,203	1,593	0,679	10,866	0,891
135	9	1,004	43,9	38,79	5,11	5,11	7,591	1,589	0,708	11,640	0,884
138	9	1,004	43,9	39,66	4,24	4,24	9,354	1,598	0,627	9,658	0,903
141	9	1,004	43,9	38,91	4,99	4,99	7,798	1,590	0,698	11,367	0,886
143	9	1,004	43,9	39,36	4,54	4,54	8,670	1,595	0,657	10,342	0,897

Table C 6: Data on effect of concentration on biosorption. Flowrate: 10 ppm. Conditions in table

Time	Volume	Mass	Ci	Ce	Ci-Ce	Qe	Ce/Qe	Log Ce	Log Qe	Ce/Ci	% adsorbed
10	0,01	1,001	10,15	-0,306	10,456	0,104	-2,929	#NUM!	-0,981	-0,030	103,015
20	0,01	1,001	10,15	-0,196	10,346	0,103	-1,896	#NUM!	-0,986	-0,019	101,931
30	0,01	1,001	10,15	0,401	9,749	0,097	4,117	-0,397	-1,011	0,040	96,049
40	0,01	1,001	10,15	1,245	8,905	0,089	13,995	0,095	-1,051	0,123	87,734
50	0,01	1,001	10,15	1,452	8,698	0,087	16,710	0,162	-1,061	0,143	85,695
60	0,01	1,001	10,15	1,923	8,227	0,082	23,398	0,284	-1,085	0,189	81,054
70	0,01	1,001	10,15	2,345	7,805	0,078	30,075	0,370	-1,108	0,231	76,897
80	0,01	1,001	10,15	2,877	7,273	0,073	39,597	0,459	-1,139	0,283	71,655
90	0,01	1,001	10,15	3,505	6,645	0,066	52,799	0,545	-1,178	0,345	65,468
100	0,01	1,001	10,15	3,599	6,551	0,065	54,993	0,556	-1,184	0,355	64,542
110	0,01	1,001	10,15	3,851	6,299	0,063	61,198	0,586	-1,201	0,379	62,059
120	0,01	1,001	10,15	4,335	5,815	0,058	74,623	0,637	-1,236	0,427	57,291
130	0,01	1,001	10,15	4,503	5,647	0,056	79,821	0,654	-1,249	0,444	55,635
140	0,01	1,001	10,15	4,674	5,476	0,055	85,440	0,670	-1,262	0,460	53,951
150	0,01	1,001	10,15	4,828	5,322	0,053	90,808	0,684	-1,274	0,476	52,433
160	0,01	1,001	10,15	4,838	5,312	0,053	91,168	0,685	-1,275	0,477	52,335
170	0,01	1,001	10,15	4,839	5,311	0,053	91,204	0,685	-1,275	0,477	52,325
180	0,01	1,001	10,15	5,048	5,102	0,051	99,041	0,703	-1,293	0,497	50,266
190	0,01	1,001	10,15	5,224	4,926	0,049	106,156	0,718	-1,308	0,515	48,532
200	0,01	1,001	10,15	5,383	4,767	0,048	113,035	0,731	-1,322	0,530	46,966
210	0,01	1,001	10,15	6,089	4,061	0,041	150,088	0,785	-1,392	0,600	40,010
220	0,01	1,001	10,15	6,151	3,999	0,040	153,96727	0,789	-1,398483	0,606	39,399
230	0,01	1,001	10,15	6,306	3,844	0,038	164,21191	0,800	-1,415651	0,621	37,872
240	0,01	1,001	10,15	6,604	3,546	0,035	186,42425	0,820	-1,450695	0,651	34,936
250	0,01	1,001	10,15	6,978	3,172	0,032	220,20738	0,844	-1,499	0,687	31,251
260	0,01	1,001	10,15	7,097	3,053	0,030	232,69234	0,851	-1,516	0,699	30,079

270	0,01	1,001	10,15	7,267	2,883	0,029	252,31589	0,861	-1,541	0,716	28,404
280	0,01	1,001	10,15	7,637	2,513	0,025	304,20362	0,883	-1,600	0,752	24,759
290	0,01	1,001	10,15	7,64	2,51	0,025	304,68685	0,883	-1,601	0,753	24,729
300	0,01	1,001	10,15	7,879	2,271	0,023	347,28661	0,896	-1,644	0,776	22,374
310	0,01	1,001	10,15	8,089	2,061	0,021	392,87186	0,908	-1,686	0,797	20,305
320	0,01	1,001	10,15	8,212	1,938	0,019	424,15955	0,914	-1,713	0,809	19,094
330	0,01	1,001	10,15	8,419	1,731	0,017	486,85263	0,925	-1,762	0,829	17,054

Table C 6: Data on effect of concentration on biosorption. Flowrate: 25 ppm. Conditions in table

Time	Volume	Mass	Ci	Ce	Ci-Ce	Qe	Ce/Qe	Log Ce	Log Qe	Ce/Ci	%adsorbed
5	0,01	1,009	24,41	0,486	23,924	0,237	2,050	-0,313	-0,625	0,020	98,01
10	0,01	1,009	24,41	0,645	23,765	0,236	2,739	-0,190	-0,628	0,026	97,36
15	0,01	1,009	24,41	0,872	23,538	0,233	3,738	-0,059	-0,632	0,036	96,43
20	0,01	1,009	24,41	3,083	21,327	0,211	14,586	0,489	-0,675	0,126	87,37
25	0,01	1,009	24,41	5,476	18,934	0,188	29,182	0,738	-0,727	0,224	77,57
30	0,01	1,009	24,41	7,212	17,198	0,170	42,313	0,858	-0,768	0,295	70,45
35	0,01	1,009	24,41	8,898	15,512	0,154	57,878	0,949	-0,813	0,365	63,55
40	0,01	1,009	24,41	10,17	14,24	0,141	72,061	1,007	-0,850	0,417	58,34
45	0,01	1,009	24,41	10,7	13,71	0,136	78,748	1,029	-0,867	0,438	56,17
50	0,01	1,009	24,41	12,22	12,19	0,121	101,148	1,087	-0,918	0,501	49,94
55	0,01	1,009	24,41	13,03	11,38	0,113	115,530	1,115	-0,948	0,534	46,62
60	0,01	1,009	24,41	13,7	10,71	0,106	129,069	1,137	-0,974	0,561	43,88
65	0,01	1,009	24,41	14,88	9,53	0,094	157,544	1,173	-1,025	0,610	39,04
70	0,01	1,009	24,41	15,85	8,56	0,085	186,830	1,200	-1,071	0,649	35,07
75	0,01	1,009	24,41	16,25	8,16	0,081	200,934	1,211	-1,092	0,666	33,43
80	0,01	1,009	24,41	17,04	7,37	0,073	233,288	1,231	-1,136	0,698	30,19
85	0,01	1,009	24,41	17,59	6,82	0,068	260,239	1,245	-1,170	0,721	27,94
90	0,01	1,009	24,41	17,51	6,9	0,068	256,052	1,243	-1,165	0,717	28,27
95	0,01	1,009	24,41	17,8	6,61	0,066	271,713	1,250	-1,184	0,729	27,08
100	0,01	1,009	23,3	18,79	4,51	0,045	420,379	1,274	-1,350	0,806	19,36
105	0,01	1,009	23,3	19,23	4,07	0,040	476,734	1,284	-1,394	0,825	17,47
110	0,01	1,009	23,3	19,95	3,35	0,033	600,882	1,300	-1,479	0,856	14,38
115	0,01	1,009	23,3	20,41	2,89	0,029	712,584	1,310	-1,543	0,876	12,40
120	0,01	1,009	23,3	20,73	2,57	0,025	813,874	1,317	-1,594	0,890	11,03
125	0,01	1,009	23,3	20,67	2,63	0,026	793,005	1,315	-1,584	0,887	11,29
130	0,01	1,009	23,3	20,7	2,6	0,026	803,319	1,316	-1,589	0,888	11,16
135	0,01	1,009	23,3	21,02	2,28	0,023	930,227	1,323	-1,646	0,902	9,79

140	0,01	1,009	23,3	21,09	2,21	0,022	962,887	1,324	-1,659	0,905	9,48
145	0,01	1,009	23,3	21,12	2,18	0,022	977,527	1,325	-1,665	0,906	9,36
150	0,01	1,009	23,3	21,27	2,03	0,020	1057,213	1,328	-1,696	0,913	8,71
155	0,01	1,009	23,3	21,62	1,68	0,017	1298,487	1,335	-1,779	0,928	7,21
160	0,01	1,009	23,3	21,39	1,91	0,019	1129,974	1,330	-1,723	0,918	8,20
165	0,01	1,009	23,3	21,47	1,83	0,018	1183,783	1,332	-1,741	0,921	7,85
170	0,01	1,009	23,3	21,81	1,49	0,015	1476,932	1,339	-1,831	0,936	6,39
175	0,01	1,009	23,3	21,89	1,41	0,014	1566,455	1,340	-1,855	0,939	6,05

Appendix D : Laboratory images

Figure D 1: (a) Raw pineapple peels (b) Oven dried pineapple peels (c) 200 ppm cobalt solution

Figure D 2: The pineapple grinding process in the miller

Figure D 3: The sieving process

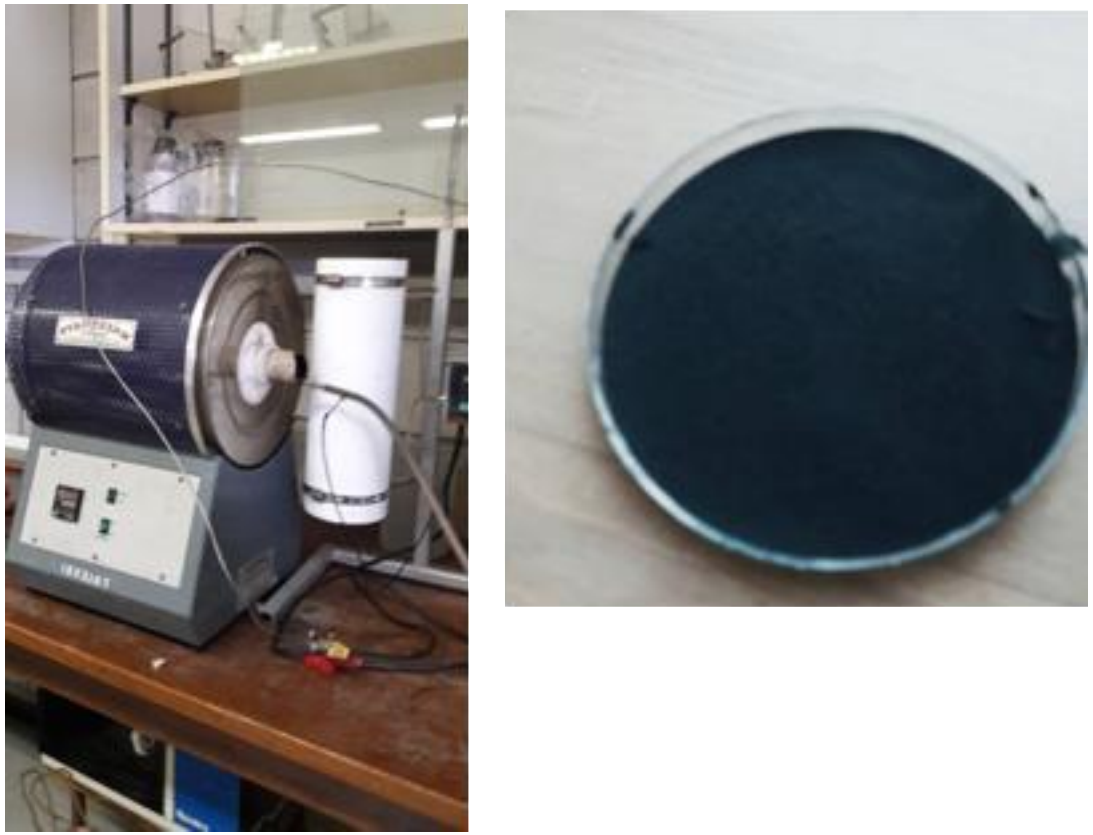

Figure D 4: Pyrotherm tube furnace and carbonised pineapple peel

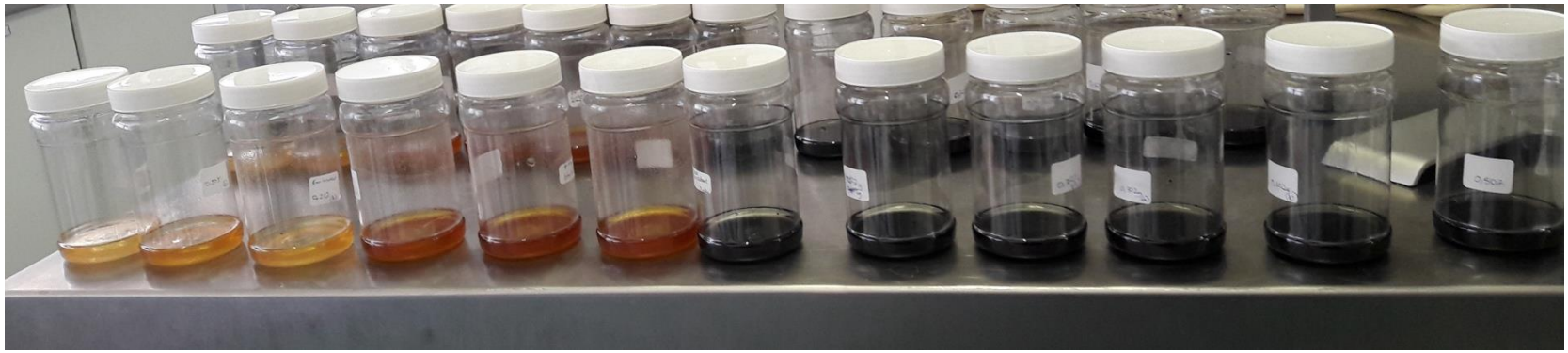

Figure D 5: Adsorption of biosorbents in cobalt solution

Figure D 6: Filtering of solutions and water-bath shaking